The Labor Market Incidence of New Technologies

Tianyu Fan
Yale University

September 28, 2025
(Click here for the most recent version)

This paper develops a framework for evaluating how technological shocks reshape labor markets through their interaction with occupational substitution structure. Central to our theory is the distance-dependent elasticity of substitution (DIDES), where worker mobility declines with skill distance between occupations. We show that both automation and artificial intelligence cluster within skill-adjacent occupations, constraining employment adjustment and amplifying wage effects. Mapping 306 occupations into cognitive, manual, and interpersonal skill dimensions, we estimate a low-dimensional latent skill model that preserves granular substitution patterns. This clustering generates unequal outcomes: 25-45% of demand shocks translate to wages (versus 30% under standard models), while mobility recovers only 20% of losses (versus 30% from standard estimates).

Keywords. technological change, occupational mobility, labor market adjustment, distance-dependent elasticity of substitution, automation, artificial intelligence

JEL Classification. J24, O33, J31, J62

Tianyu Fan: Yale University. Email: tianyu.fan@yale.edu. Website: `https://tianyu-fan.com`.
I am deeply grateful to Michael Peters, Pascual Restrepo, and Fabrizio Zilibotti for their invaluable guidance and unwavering support throughout this project. I thank Serdar Birinci, Lorenzo Caliendo, Yu-Ting Chiang, Maxim Dvorkin, Ana Cecilia Fieler, Mayara Felix, Joel Flynn, David Hémous, Zhen Huo, Sam Kortum, Julian Kozlowski, Danial Lashkari, Ricardo Marto, Kjetil Storesletten, Michael Song, Kailan Tian, Sharon Traiberman, Laura Veldkamp, and Anton Yang for insightful discussions and constructive feedback. I also benefited from helpful comments from participants at the CCER Summer Institute, CUFE Workshop, Dissertation Fellow Workshop (Federal Reserve Bank of St. Louis), Growth and Development Conference (Federal Reserve Bank of Minneapolis), Growth and Institution Workshop (Tsinghua University), TRAIN Conference, Yale Macro Lunch Workshop, and Yale Trade Lunch Workshop. Financial support from the Stripe Economics of AI Fellowship is gratefully acknowledged.

1. Introduction

Recent technological advances in automation and artificial intelligence have transformed labor markets, spurring productivity gains while deepening inequality.[1] These technologies share a defining characteristic that fundamentally shapes their labor market impact: they cluster within specific skill domains rather than dispersing across occupations. Automation concentrates in routine manual tasks—manufacturing, assembly, transportation—while AI targets cognitive work—data analysis, research, decision-making. This clustering creates a mobility trap for displaced workers: they can easily transition to skill-similar occupations, but these alternatives face similar technological threats and offer no economic refuge. An assembly worker displaced by automation could shift to construction or welding—occupations where their manual skills transfer—but finds these jobs similarly automated. A data analyst threatened by AI discovers that financial analysis and market research, their most accessible alternatives, face equivalent AI exposure. Workers are most mobile precisely where mobility provides the least benefits.

This paper develops a new framework to understand how technological clustering interacts with occupational substitution structure to determine labor market incidence. Our central contribution demonstrates that the distributional consequences of technological change depend not on average labor market flexibility but on the alignment between shock distributions and the underlying substitution structure. When technologies cluster in skill space, workers have limited outside options, generating severe and persistent inequality that conventional models systematically understate. We make this argument through three interconnected contributions: a theoretical framework revealing the mechanism, an empirical implementation estimating flexible and granular substitution structure, and applications demonstrating the consequences for both historical automation and prospective AI adoption.

We build our theoretical analysis on a Roy model of occupational choice augmented with distance-dependent elasticity of substitution (DIDES). Workers draw correlated productivity across occupations, where correlation declines with skill distance. This correlation structure directly generates substitution patterns: high correlation between skill-similar occupations creates strong substitutability, while low correlation between skill-distant occupations limits substitution. The framework transforms these productivity correlations into a flexible substitution structure, naturally generating realistic elasticities from a parsimonious skill-based foundation. A key innovation is achieving dimensionality reduction while preserving granular substitution patterns. Rather than estimating hundreds of thousands of bilateral elasticities among occupations, we parameterize the entire substitution structure through a low-dimensional skill space. The correlation function

[1] We follow Acemoglu and Restrepo (2022); Restrepo (2024) in defining automation technologies as industrial robots, machinery, and software without AI capability.

governing productivity draws depends on just $S + 1$ parameters for S skill dimensions: one cross-skill elasticity θ and S within-skill correlation parameters $\{\rho_s\}_{s=1}^{S}$. This parsimony makes estimation feasible from standard aggregate data while maintaining the flexibility to capture how technological clustering constrains adjustment.

Our empirical implementation proceeds in three integrated steps that connect measurement to theory to quantification. First, we map 306 detailed occupations into a three-dimensional skill space using O*NET data, extracting cognitive, manual, and interpersonal skill requirements through principal component analysis. These skill measures operationalize the theoretical framework: they position occupations in skill space and determine substitution distances between them. Second, we construct technological exposure measures by having ChatGPT evaluate the automation and AI feasibility of 19,200 tasks across 862 occupations. This reveals the clustering patterns central to our analysis—automation concentrates in manual-intensive occupations while AI targets cognitive-intensive roles, with both technologies showing systematic concentration within skill-adjacent occupations rather than random dispersion. Third, we estimate the structural parameters governing substitution by exploiting how occupational employment and average wage responded to automation between 1980 and 2010.

The estimation reveals striking departures from standard models that fundamentally alter our understanding of labor market adjustment. Under conventional CES assumptions, we estimate an average elasticity of 3.12, suggesting substantial worker mobility across all occupations. But allowing for skill-based correlation through our DIDES framework changes this picture dramatically. The cross-skill elasticity plummets to 1.10, implying that moving across skill boundaries is far more difficult than standard models assume. Within-skill elasticities show substantial heterogeneity: 4.8 for cognitive occupations, 4.4 for interpersonal occupations, but only 2.1 for manual occupations. The correlation parameters driving these differences reveal that cognitive skills prove most transferable ($\rho_{\text{cog}} = 0.77$), while manual skills exhibit limited transferability ($\rho_{\text{man}} = 0.48$). These estimates reveal that two-thirds of observed occupational substitution occurs within skill clusters rather than across them—a pattern that becomes crucial when technological shocks themselves cluster.

With the substitution structure estimated, we quantify how automation and AI reshape labor market outcomes. The clustering of technological shocks within skill domains fundamentally constrains adjustment: when entire skill clusters face negative shocks simultaneously, workers have limited escape routes. This manifests in heterogeneous wage pass-through across occupations. While standard models predict uniform 30% pass-through from demand shocks to wages, we find rates ranging from 25% to 45%. Production workers facing automation experience 40–45% pass-through—nearly half their demand losses translate directly to wage declines. The variation directly reflects how

clustering eliminates escape routes: when skill-similar occupations face simultaneous threats, the effective elasticity of substitution collapses, forcing wage absorption rather than employment reallocation.

Mobility provides limited insurance against these wage losses. Workers recover only 20% of automation-induced wage declines through occupational transitions, compared to 30% predicted by standard models. This constraint emerges from technological shocks concentrating precisely where skill transferability is weakest. Automation targets manual occupations where workers have the lowest transferability ($\rho_{man} = 0.48$), creating large losses with minimal recovery options. AI affects cognitive occupations where higher transferability ($\rho_{cog} = 0.77$) offers better prospects, yet clustering still constrains escape because natural transition targets face similar AI threats. The interaction between shock distribution and heterogeneous transferability—absent from models assuming uniform elasticity—drives the severe distributional consequences we document.

We extend this static analysis to examine dynamic adjustment by embedding DIDES into a discrete choice framework with forward-looking workers facing transition costs. Using CPS data aggregated to occupation clusters, we estimate a short-run elasticity of 0.07, confirming sluggish adjustment that amplifies the constraints identified in our static analysis. Our examination of historical automation reveals remarkably persistent effects: gradual adoption since 1985 generated wage gaps up to 50% between high and low exposure occupations. Employment shifts absorbed two-thirds of demand changes over this period, but mobility gains offset only half of wage losses, leaving substantial permanent inequality. Under a counterfactual scenario where AI rapidly reaches automation's scale by 2030, adjustment proves even more constrained. The labor market initially absorbs less than one-third of shocks, generating sharp wage declines with mobility recovering only one-third of losses during the transition. The clustering that constrains static adjustment also slows dynamic transitions, with forward-looking behavior providing limited relief because improved outside options are offset by similar threats to alternative occupations.

These findings reshape our understanding of how technological progress affects workers and carry immediate policy implications. The conventional estimates indicate that labor market flexibility mitigates technological disruption proves dangerously incomplete. When technical changes cluster in skill space—as our evidence definitively establishes for both automation and AI—they systematically target the rigidities in occupational substitution. Workers cannot escape to unaffected occupations because skill requirements create barriers, and the occupations they can reach face similar technological threats. This interaction between clustering and substitution structure, completely invisible to standard frameworks, explains why technological change generates such pronounced and persistent inequality. Standard policy prescriptions for worker retraining miss this fundamental constraint: displaced workers' natural transition targets face similar technological

risks. As AI deployment accelerates, understanding these mechanisms becomes essential for designing policies that facilitate necessary economic transitions while protecting vulnerable workers from concentrated disruption.

Related Literature. Our paper contributes to four interconnected literatures: skill-biased technical change, labor reallocation dynamics, the Roy model tradition, and assignment theory.

Skill-biased Technical Change: Our work builds on the extensive literature examining labor market consequences of technological change. Early research by Katz and Murphy (1992) and Autor, Katz, and Krueger (1998) introduced the concept of skill-biased technical change (SBTC), later refined by Acemoglu (2002) and Autor and Dorn (2013) to show how technological advances disproportionately benefit skilled workers, thereby widening wage inequality. Recent task-based frameworks provide a more granular understanding of how automation technologies generate unequal labor demand shifts across occupations (Acemoglu and Restrepo 2018, 2020, 2022). Our contribution complements this demand-side focus by modeling supply-side adjustment—developing a framework that captures how workers reallocate across occupations and how the interaction between supply constraints and demand shocks determines equilibrium incidence.

In parallel, emerging research explores AI's distinct disruptive potential. Webb (2019) and Acemoglu et al. (2022) demonstrate that AI affects both routine and non-routine cognitive tasks, while experimental studies by Noy and Zhang (2023) and Brynjolfsson, Li, and Raymond (2025) document how generative AI transforms knowledge-based and creative work. Although recent analyses primarily examine AI's demand-side impact through task frameworks (Eloundou et al. 2024; Brynjolfsson, Chandar, and Chen 2025; Hampole et al. 2025; Freund and Mann 2025), we provide the first systematic assessment of worker mobility constraints under AI exposure.

Labor Reallocation and Mobility Frictions: A growing literature emphasizes how reallocation frictions shape responses to demand shocks.[2] Recent work documents how occupational mobility constraints amplify wage inequality during transitions (Lee and Wolpin 2006; Dvorkin and Monge-Naranjo 2019; Traiberman 2019), with dynamic models studying the regulation policies (Guerreiro, Rebelo, and Teles 2022; Lehr and Restrepo 2022; Beraja and Zorzi 2024). Regarding the source of slow adjustment, Bocquet (2024) examines adjustment through job transition networks, while Adão, Beraja, and Pandalai-Nayar (2024) highlights skill specialization as a constraint on reallocation. We extend this literature by introducing a flexible substitution structure that captures how technological clustering—not just average mobility frictions—determines incidence.[3]

[2] Foundational contributions include Matsuyama (1992) on sectoral shifts and skill acquisition, and Heckman, Lochner, and Taber (1998) on general equilibrium effects of skill formation.

[3] While Böhm, Etheridge, and Irastorza-Fadrique (2025) also highlights the importance of heterogeneous

Roy Models and Multidimensional Skills: Following the Roy tradition of selection on comparative advantage (Heckman and Sedlacek 1985), recent work incorporates multidimensional skills to study business cycle dynamics (Grigsby 2022), discrimination (Hurst, Rubinstein, and Shimizu 2024), and household sorting (Lise and Postel-Vinay 2020). We build on Lise and Postel-Vinay (2020)'s insight about multidimensional skill structure but extend it to aggregate labor supply across granular occupations. Our innovation is mapping 300+ occupations into three-dimensional skill space while preserving rich substitution patterns—all estimable from standard employment and wage data. By adopting a Roy-Fréchet structure with copula-based correlation, we focus directly on substitution patterns while circumventing the well-known identification challenges of unobserved heterogeneity that plague selection models (Heckman and Honore 1990; French and Taber 2011; Erosa et al. 2025). This approach yields a tractable framework that uses occupational skill requirements to parameterize substitution structure and aggregate employment shares as sufficient statistics, enabling estimation without relying on individual-level data.

Assignment Theory and DIDES: The distance-dependent elasticity of substitution emerges naturally from assignment models where workers sort based on comparative advantage (Sattinger 1993; Teulings 1995, 2005). These models establish that substitutability declines with skill distance—a theoretical result we operationalize empirically. While Lindenlaub (2017) explores multidimensional assignment theoretically, we provide the first empirical implementation that quantifies DIDES using occupational data, estimates its parameters from observed labor market responses, and demonstrates its crucial role in technological incidence.

Our contribution synthesizes these literatures: we embed assignment-theoretic insights into a Roy framework, estimate the resulting substitution structure, and show how its interaction with clustered technological shocks fundamentally reshapes our understanding of labor market adjustment and inequality.

Road Map. The paper proceeds as follows. Section 2 develops a static model featuring distance-dependent elasticity of substitution (DIDES). Section 3 implements the framework empirically, estimating a flexible and granular substitution structure. Section 4 quantifies the incidence of automation and AI, revealing how technological clustering results in unequal outcomes. Section 5 extends to dynamic adjustment, embedding DIDES into a discrete choice framework to examine gradual transitions. Section 6 concludes.

labor supply elasticities, their heterogeneity stems solely from differences in employment shares across occupations, not from underlying variation in substitution structure.

2. Theoretical Framework

This section develops a framework for analyzing how labor market incidence depends on the interaction between technological shocks and occupational substitution patterns. The key innovation is a low-dimensional representation that collapses O^2 bilateral elasticities between occupations into a parsimonious skill-based structure. Through correlated productivity draws across skill-similar occupations, the framework embeds distance-dependent elasticity of substitution (DIDES) into a Roy model of occupational choice.

2.1. Static Model

Production and Labor Demand. Labor demand derives from a task-based production framework following Acemoglu and Restrepo (2018, 2022). In the underlying model (detailed in Appendix A.1), occupations perform distinct task sets that can be produced using either labor or capital, with technological change shifting task allocation between these inputs. This yields the reduced-form representation:

$$y = \mathcal{A}\left(\sum_{o=1}^{O} \alpha_o^{\frac{1}{\sigma}} L_o^{\frac{\sigma-1}{\sigma}}\right)^{\frac{\sigma}{\sigma-1}} \tag{1}$$

where L_o denotes employment in occupation o, σ is the elasticity of substitution between occupations, $\mathcal{A}$ captures aggregate productivity, and α_o represents the share of tasks performed by labor in occupation o after technology adoption.

The parameter α_o serves as a sufficient statistic for technological displacement. When automation or AI replaces labor in specific tasks, the corresponding α_o declines: $d\ln \alpha_o < 0$ for occupations whose tasks become automated. This parsimonious representation captures technology's distributional effects without explicitly tracking task assignments, as the demand shifters $\{\alpha_o\}$ fully summarize technological impacts across occupations.[4]

From profit maximization, occupational wages equal marginal products:

$$w_o = \frac{\partial y}{\partial L_o} = y^{\frac{1}{\sigma}} \alpha_o^{\frac{1}{\sigma}} L_o^{-\frac{1}{\sigma}}$$

This labor demand equation, combined with the labor supply framework developed below, determines equilibrium wage and employment responses to technological change.

Workers and Labor Supply. The economy consists of a continuum of workers indexed by i. Each worker draws a productivity vector $\boldsymbol{\epsilon}(i) = \{\epsilon_o(i)\}_{o=1}^{O}$ across occupations from a

[4]The aggregate productivity effect $d\ln \mathcal{A}$ represents a level shift that affects all occupations proportionally. Since our focus is on distributional incidence across occupations, this term cancels out in relative wage analysis and is omitted from subsequent analysis.

generalized multivariate Fréchet distribution:

$$\Pr[\epsilon_1(i) \leq \epsilon_1, \ldots, \epsilon_O(i) \leq \epsilon_O] = \exp\left[-F(A_1\epsilon_1^{-\theta}, \ldots, A_O\epsilon_O^{-\theta})\right] \tag{2}$$

where $A_o > 0$ captures average productivity in occupation o and $\theta > 0$ governs productivity dispersion across workers. The marginal distributions are Fréchet: $\Pr[\epsilon_o(i) \leq \epsilon_o] = \exp(-A_o\epsilon_o^{-\theta})$, standard in Roy models with extreme value distributions. The correlation function F governs productivity similarity across occupations, serving as the primitive that determines substitution patterns.[5]

Workers choose occupations to maximize utility. Worker i receives utility $u_o(i) = w_o\epsilon_o(i)$ from occupation o, where w_o is the wage and $\epsilon_o(i)$ represents both productivity and inverse effort cost.[6] The optimal occupational choice is:

$$o^*(i) = \arg\max_{o \in \{1,\ldots,O\}} \{w_o\epsilon_o(i)\}$$

The correlation function $F : \mathbb{R}_+^O \to \mathbb{R}_+$ determines substitution patterns between occupations. This function is homogeneous of degree one and satisfies the sign-switching property, ensuring occupations are gross substitutes.[7] We normalize $F(1, 0, \ldots, 0) = 1$ to separate scale from correlation effects.

PROPOSITION 1 (Occupational Employment Shares). *Given the multivariate Fréchet productivity distribution in equation* (2) *and optimal worker choices, the share of workers selecting occupation o is:*

$$\pi_o = \frac{A_o w_o^\theta F_o(A_1 w_1^\theta, \ldots, A_O w_O^\theta)}{F(A_1 w_1^\theta, \ldots, A_O w_O^\theta)}$$

where $F_o = \partial F/\partial x_o$ denotes the partial derivative with respect to the o-th argument.

PROOF. The employment share equals the probability that occupation o yields the highest utility: $\pi_o = \Pr[w_o\epsilon_o(i) = \max_{o'} w_{o'}\epsilon_{o'}(i)]$. This probability derives from the principle of maximum stability for multivariate extreme value distributions. See Appendix C.1 for the complete derivation. □

The employment share expression reveals that occupation o's share depends on three factors: average productivity A_o, wage raised to the dispersion parameter (w_o^θ), and how

[5] The correlation function F is related to the copula of the productivity distribution. See Appendix A.2.1 for formal properties.

[6] Formally, workers consume $c_o = w_o$ and supply effort $\ell_o(i) = 1/\epsilon_o(i)$, yielding utility $u_o(i) = \ln(c_o/\ell_o(i)) = \ln(w_o\epsilon_o(i))$. The baseline analysis assumes idiosyncratic productivity does not enter firm production. In an extension, we extend to incorporate efficiency effects.

[7] The sign-switching property requires that mixed partial derivatives alternate in sign, guaranteeing negative cross-wage elasticities. For detailed properties of F and its connection to max-stable distributions, see Appendix A.2.1 and Lind and Ramondo (2023).

the correlation function responds to changes in that occupation's attractiveness (F_o/F). This last term breaks the independence of irrelevant alternatives (IIA) property, allowing realistic substitution patterns where wage changes in one occupation affect employment shares differently across other occupations.[8]

Total labor supply to occupation o is $L_o = \pi_o \bar{L}$, where $\bar{L}$ is the total workforce. The correlation function F fully characterizes substitution patterns through its effect on employment share responses to wage changes. Section 2.4 parameterizes F to capture distance-dependent elasticity of substitution (DIDES), where substitutability declines with skill distance between occupations—the key mechanism explaining why technological clustering generates inequality.

Market Equilibrium. A competitive equilibrium consists of a wage vector $\boldsymbol{w}^* = \{w_o^*\}_{o=1}^O$ and allocation $\boldsymbol{L}^* = \{L_o^*\}_{o=1}^O$ such that:

a. **Profit maximization:** Firms choose labor to maximize profits, yielding demand:

$$L_o^d(\boldsymbol{w}) = \left(\frac{\alpha_o}{w_o}\right)^\sigma y(\boldsymbol{L})^{1-\frac{1}{\sigma}}$$

b. **Utility maximization:** Workers choose occupations optimally, yielding supply:

$$L_o^s(\boldsymbol{w}) = \pi_o(\boldsymbol{w})\bar{L} = \frac{A_o w_o^\theta F_o(A_1 w_1^\theta, \ldots, A_O w_O^\theta)}{F(A_1 w_1^\theta, \ldots, A_O w_O^\theta)} \bar{L}$$

c. **Market clearing:** Labor markets clear in all occupations:

$$L_o^d(\boldsymbol{w}^*) = L_o^s(\boldsymbol{w}^*) = L_o^* \quad \forall o$$

PROOF. Existence follows from continuity and Brouwer's fixed point theorem. Uniqueness follows from the gross substitutes property: the correlation function F ensures negative cross-wage elasticities in labor supply, ruling out multiple equilibria. See Appendix A.3 for details. □

2.2. Technological Shocks and Labor Market Incidence

We model automation and AI as technologies that reduce the share of tasks performed by labor in affected occupations. For technology $j \in \{\text{Automation}, \text{AI}\}$, let $d\ln \alpha_o^j < 0$ denote the proportional reduction in occupation o's task share, equal to the fraction of tasks newly automated relative to tasks initially performed by labor.[9] While these technologies displace

[8] When $F(x_1, \ldots, x_O) = \sum_o x_o$ (independent productivity draws), $F_o/F = 1/\sum_j x_j$ for all o, restoring IIA and reducing to standard CES with uniform elasticity θ.

[9] Formally, $d\ln \alpha_o^j = -M_{\mathcal{D}_o^j}/M_{\mathcal{T}_o^\ell}$, where $M_{\mathcal{D}_o^j}$ measures newly automated tasks and $M_{\mathcal{T}_o^\ell}$ measures tasks initially performed by labor. See Appendix A.1 for derivation.

labor from specific tasks, they simultaneously increase aggregate output by reducing production costs—a key source of productivity growth. The distributional question is how aggregate gains and occupation-specific losses are shared across workers.

As demonstrated in Section 3, automation predominantly affects manual-intensive occupations, while AI targets cognitive-intensive ones. Both technologies cluster within skill-adjacent occupations. This clustering raises a fundamental question: how do concentrated technological shocks propagate through the labor market when affected workers' natural alternatives face similar threats?

PROPOSITION 2 (Equilibrium Responses to Technology). *Consider a technological shock characterized by task share changes* $\{d\ln \alpha_o\}_{o=1}^{O}$. *To first order:*
(i) Wage and employment responses satisfy:

$$d\ln \boldsymbol{w} = \frac{1}{\sigma} d\ln y \cdot \mathbf{1} - \frac{1}{\sigma} d\ln \boldsymbol{\alpha} - \frac{1}{\sigma} d\ln \boldsymbol{L}$$
$$d\ln \boldsymbol{L} = \Theta \cdot d\ln \boldsymbol{w}$$

(ii) Equilibrium wage incidence is:

$$d\ln \boldsymbol{w} = \frac{1}{\sigma} d\ln y \cdot \mathbf{1} - \Delta \cdot \frac{d\ln \boldsymbol{\alpha}}{\sigma} \tag{3}$$

where $\Delta = (\mathbf{I} + \Theta/\sigma)^{-1}$ *is the pass-through matrix and* Θ *is the matrix of labor supply elasticities:*

$$\Theta_{oo'} = \begin{cases} \theta \left[\left. \frac{x_{o'} F_{oo'}}{F_o} \right|_{x_j = A_j w_j^{\theta}} - \pi_{o'} \right] & \text{if } o \neq o' \\ \theta \left[\left. \frac{x_o F_{oo}}{F_o} \right|_{x_j = A_j w_j^{\theta}} + 1 - \pi_o \right] & \text{if } o = o' \end{cases} \tag{4}$$

PROOF. Part (i) follows from log-differentiating first-order conditions and employment shares. Part (ii) combines wage and employment responses. See Appendix C.2. □

This proposition reveals how technological incidence depends on the interaction between shock distribution and substitution structure. The aggregate productivity gain ($d\ln y/\sigma$) raises all wages uniformly. The distributional effect, captured by pass-through matrix Δ, depends on both demand elasticity σ and substitution matrix Θ. This matrix embeds distance-dependent substitution through two components: the correlation term $\theta x_{o'} F_{oo'}/F_o$ reflects productivity correlation between skill-similar occupations, while the share term $-\theta\pi_{o'}$ represents baseline substitution. When productivities are independent ($F = \sum_o x_o$), only the share term remains, reducing to the standard CES.[10]

[10] Rows of Θ sum to zero, confirming that only relative wage changes induce reallocation. This property

Pass-through matrix Δ embodies a fundamental trade-off: greater worker mobility (larger $\|\Theta\|$) enables employment adjustment that dampens wage effects, while limited mobility (smaller $\|\Theta\|$) translates shocks directly into wage disparities. In the limit where $\|\Theta\| \to 0$ (no mobility) or $\sigma \to \infty$ (perfectly inelastic demand), the pass-through matrix approaches identity, yielding complete wage incidence. When automation or AI clusters in skill-adjacent occupations, affected workers' natural alternatives face similar threats, reducing effective substitutability and amplifying wage inequality—a mechanism we formalize through spectral analysis in the next section.

Mobility Gains and Welfare Recovery. While equation (3) captures wage effects for workers remaining in their occupations, some workers benefit from transitions.

PROPOSITION 3 (Mobility Gains from Reallocation). *The expected welfare gain for workers initially in occupation o from occupational transitions is:*

$$\text{Mobility Gain}_o = \sum_{o' : d\ln w_{o'} > d\ln w_o} \mu_{oo'} (d\ln w_{o'} - d\ln w_o) \tag{5}$$

where $\mu_{oo'} = -\Theta_{oo'}(d\ln w_{o'} - d\ln w_o)$ is the fraction of workers reallocating from o to o'.

PROOF. Marginal workers are indifferent between occupations before the shock. Their welfare gain equals the differential wage changes upon switching. See Appendix A.5 for the complete derivation. □

These gains decompose into average and correlation effects:

$$\text{Mobility Gain}_o = \underbrace{\bar{\mu}_o \cdot \overline{\Delta w^+}}_{\text{Average effect}} + \underbrace{\text{Cov}(\mu_{oo'}, d\ln w_{o'} - d\ln w_o)}_{\text{Correlation effect}} \tag{6}$$

where $\bar{\mu}_o$ is the average transition rate to better-off occupations and $\overline{\Delta w^+}$ is the mean wage gain conditional on moving.

The correlation effect reveals why clustering undermines welfare recovery. Workers have high transition probabilities precisely to occupations facing similar negative shocks—a data analyst threatened by AI can easily transition to financial analysis, but that occupation faces comparable AI exposure. This negative correlation implies that standard models with uniform elasticities overstate welfare recovery through reallocation while understating persistent inequality.

follows from the homogeneity of F. See Appendix C.3.

2.3. Spectral Analysis of Technological Incidence

We employ spectral analysis to understand how the distribution of technological shocks shapes their labor market incidence. This approach reveals why the clustering of shocks in skill space—a pattern we document for both automation and AI—amplifies wage inequality while limiting worker reallocation. Before parameterizing the specific correlation structure underlying distance-dependent substitution in the next section, we first establish general principles through eigendecomposition.

2.3.1. Eigendecomposition and Pass-Through

The wage incidence equation (3) can be reformulated using the eigenstructure of the labor supply elasticity matrix Θ. While Θ is not generally symmetric due to heterogeneous occupational scales and skill requirements, it admits an eigendecomposition $\Theta = U\Lambda U^{-1}$ where $\Lambda = \text{diag}(\lambda_1, \ldots, \lambda_O)$ contains eigenvalues in ascending order and $U = [\boldsymbol{u}_1, \ldots, \boldsymbol{u}_O]$ contains corresponding eigenvectors.[11]

Each eigenvalue λ_n represents the labor supply elasticity along its corresponding eigenvector $\boldsymbol{u}_n$—that is, how readily workers reallocate when relative wages change according to pattern $\boldsymbol{u}_n$. This transforms the complex $O \times O$ substitution matrix into O independent dimensions, each with its own elasticity.

LEMMA 1 (Eigenvalue Properties). *The labor supply elasticity matrix Θ satisfies:*

a. *All eigenvalues are non-negative: $\lambda_n \geq 0$ for all n*
b. *Exactly one zero eigenvalue: $\lambda_1 = 0$ with eigenvector $\boldsymbol{u}_1 \propto \mathbf{1}$*
c. *Remaining eigenvalues are strictly positive: $\lambda_n > 0$ for $n > 1$*

PROOF. The zero eigenvalue follows from the row sum property $\sum_{o'} \Theta_{oo'} = 0$. Non-negativity follows from gross substitutes. See Appendix C.4. □

The zero eigenvalue $\lambda_1 = 0$ reflects a fundamental constraint: uniform wage changes (pattern $\boldsymbol{u}_1 \propto \mathbf{1}$) induce no reallocation since only relative wages matter for occupational choice. Positive eigenvalues $\lambda_n > 0$ measure labor supply elasticities for different patterns of relative wage changes. Large eigenvalues indicate shock patterns enabling extensive reallocation—workers have many unaffected alternatives. Small eigenvalues signal limited mobility options—affected occupations and their natural alternatives face similar shocks.

[11] The non-symmetry of Θ requires distinguishing between right eigenvectors (columns of U) and left eigenvectors (rows of U^{-1}). Empirically, all eigenvalues are distinct with O linearly independent eigenvectors, ensuring: (i) diagonalizability, (ii) a complete basis spanning $\mathbb{R}^O$, and (iii) unique projection of shocks onto this basis given our normalization $\|\boldsymbol{u}_n\| = 1$.

PROPOSITION 4 (Spectral Decomposition of Incidence). *Any technological shock decomposes uniquely into eigenshocks:*

$$\frac{d\ln \boldsymbol{\alpha}}{\sigma} = \sum_{n=1}^{O} b_n \boldsymbol{u}_n$$

where weights b_n can be recovered as the coefficients in a linear projection of the shocks onto basis $\boldsymbol{b} = \left(U'U\right)^{-1} U' \cdot (d\ln \boldsymbol{\alpha}/\sigma)$. The wage response is:

$$d\ln \boldsymbol{w} = \frac{d\ln y}{\sigma}\mathbf{1} - \sum_{n=1}^{O} \underbrace{\frac{\sigma}{\sigma+\lambda_n}}_{\textit{pass-through}} b_n \boldsymbol{u}_n$$

PROOF. Apply eigendecomposition to $\Delta = (\mathbf{I} + \Theta/\sigma)^{-1} = U(\mathbf{I} + \Lambda/\sigma)^{-1}U^{-1}$. See Appendix A.6. □

The pass-through factor $\sigma/(\sigma+\lambda_n)$ generalizes the classic one-dimensional incidence formula to a multi-dimensional occupational setting. Our spectral decomposition reveals that each shock pattern has its own effective elasticity λ_n, generating heterogeneous incidence across different shock distributions. When technological shocks align with low-elasticity dimensions (small λ_n), workers cannot escape through reallocation, generating near-complete pass-through to wages. When shocks align with high-elasticity dimensions (large λ_n), extensive worker mobility dissipates the impact through employment adjustment. This decomposition shows why shock distribution matters: technological changes loading heavily on low-elasticity eigenvectors—those affecting clusters of skill-similar occupations—create maximal wage inequality with minimal offsetting mobility. The multi-dimensional structure thus reveals incidence patterns invisible to single-elasticity frameworks.

2.3.2. Illustration: Clustered versus Dispersed Shocks

To illustrate these results, consider four occupations organized in two skill clusters: cognitive (c_1, c_2) and manual (m_1, m_2). Workers' productivity follows a nested structure with within-cluster correlation $\rho \in [0, 1)$:

$$\Pr[\boldsymbol{\epsilon}(i) \leq \boldsymbol{\epsilon}] = \exp\left[-\left(\epsilon_{c_1}^{\frac{-\theta}{1-\rho}} + \epsilon_{c_2}^{\frac{-\theta}{1-\rho}}\right)^{1-\rho} - \left(\epsilon_{m_1}^{\frac{-\theta}{1-\rho}} + \epsilon_{m_2}^{\frac{-\theta}{1-\rho}}\right)^{1-\rho}\right]$$

This structure generates high substitutability within clusters but limited substitution

across them. With equal initial employment shares, the eigendecomposition yields:

$$\boldsymbol{\lambda} = \begin{pmatrix} 0 \\ \theta \\ \theta/(1-\rho) \\ \theta/(1-\rho) \end{pmatrix}, \quad U = \frac{1}{2}\begin{pmatrix} 1 & 1 & 1 & 1 \\ 1 & 1 & -1 & -1 \\ 1 & -1 & 1 & -1 \\ 1 & -1 & -1 & 1 \end{pmatrix}$$

Three distinct shock patterns emerge:

- $\boldsymbol{u}_1 = (1, 1, 1, 1)'$: Uniform shocks ($\lambda_1 = 0$) with complete pass-through
- $\boldsymbol{u}_2 = (1, 1, -1, -1)'$: Cross-cluster shocks ($\lambda_2 = \theta$) affecting cognitive and manual occupations oppositely
- $\boldsymbol{u}_3, \boldsymbol{u}_4$: Within-cluster shocks ($\lambda = \theta/(1-\rho)$) with differential effects within each cluster

The cross-cluster shock $\boldsymbol{u}_2$ has the smallest positive eigenvalue, yielding pass-through $\sigma/(\sigma + \theta)$. When θ is small (limited overall mobility) or σ is large (rigid demand), this approaches complete pass-through. Crucially, workers displaced from cognitive occupations find their natural alternatives—other cognitive occupations—similarly affected, constraining mobility and amplifying wage disparity.

Within-cluster shocks achieve better adjustment. With eigenvalue $\theta/(1-\rho)$, pass-through becomes $\sigma(1-\rho)/[\sigma(1-\rho) + \theta]$. Higher within-cluster correlation ρ increases the eigenvalue, enabling more reallocation because workers can transition to unaffected occupations in the same cluster. When one cognitive occupation faces a negative shock while another remains stable, high correlation within the cognitive cluster facilitates movement between them.

This example crystallizes why technological clustering matters. When automation or AI concentrates in skill-adjacent occupations—aligning with low-eigenvalue eigenvectors—it generates maximal wage inequality with minimal offsetting mobility. The next section parameterizes this intuition through a cross-nested CES structure that captures distance-dependent substitution in high-dimensional occupational space.

2.4. Distance-Dependent Elasticity of Substitution

The spectral analysis revealed why technological shocks clustered in skill space generate severe wage inequality. We now move from the illustrative 2×2 example to the full complexity of real labor markets with hundreds of occupations and multiple skill dimensions. The key challenge is maintaining tractability while capturing realistic substitution patterns. We achieve this through a cross-nested CES framework (Lind and Ramondo 2023) that embeds distance-dependent substitution via a low-dimensional latent skill structure.

2.4.1. Latent Skill Formulation

Microfoundation: Skills and Occupational Productivity. Workers possess a vector of latent skills $s \in \mathcal{S}$. For each skill, they draw productivity across occupations from a correlated Fréchet distribution:

$$\Pr[\epsilon_1^s(i) \leq \epsilon_1^s, \ldots, \epsilon_O^s(i) \leq \epsilon_O^s] = \exp\left[-\left(\sum_{o=1}^{O}(\epsilon_o^s)^{\frac{-\theta}{1-\rho_s}}\right)^{1-\rho_s}\right]$$

where skill-specific correlation coefficient $\rho_s \in [0, 1)$ governs skill transferability. This parameter captures a fundamental aspect of human capital: some skills transfer seamlessly across occupations while others are context-specific. General cognitive abilities—problem-solving, analytical thinking—typically exhibit high transferability (large ρ_s), while occupation-specific manual techniques—operating particular machinery, specialized surgical procedures—show low transferability (small ρ_s).

Occupations differ in their skill utilization. Let A_o^s denote occupation o's productivity when employing skill s. Workers optimally deploy their skills, achieving productivity:

$$\epsilon_o(i) = \max_{s \in \mathcal{S}} A_o^s \cdot \epsilon_o^s(i)$$

This max operator captures how workers sort into occupations based on comparative advantage. Different occupations require different skill combinations: data analysis demands strong cognitive skills, construction requires manual dexterity, and sales positions need interpersonal abilities. The parameters $\{A_o^s\}$ encode these occupation-specific skill productivity. Workers with exceptional manual dexterity but modest cognitive skills achieve the highest productivity in manual-intensive occupations where A_o^{manual} is large. Conversely, cognitively gifted workers maximize productivity in occupations with high $A_o^{\text{cognitive}}$. This generates endogenous sorting: workers self-select into occupations that best utilize their skill endowments, with the occupation-skill match determining productivity.

Cross-Nested CES Structure. The microfoundation yields a tractable aggregate structure:

PROPOSITION 5 (DIDES through Cross-Nested CES). *The joint productivity distribution across occupations follows:*

$$\Pr[\epsilon_1(i) \leq \epsilon_1, \ldots, \epsilon_O(i) \leq \epsilon_O] = \exp[-F(A_1\epsilon_1^{-\theta}, \ldots, A_O\epsilon_O^{-\theta})]$$

with correlation function:

$$F(x_1, \ldots, x_O) = \sum_{s \in \mathcal{S}} \left[\sum_{o=1}^{O} (\omega_o^s x_o)^{\frac{1}{1-\rho_s}} \right]^{1-\rho_s} \tag{7}$$

where $A_o = \sum_s (A_o^s)^\theta$ *is aggregate productivity and* $\omega_o^s = (A_o^s)^\theta / A_o$ *represents occupation o's skill intensity.*

PROOF. See Appendix A.7. □

The skill intensities $\{\omega_o^s\}$ map occupations into skill space, creating a geography of occupational skill content. Each ω_o^s measures how intensively occupation o relies on skill s. Data analysts and financial analysts locate near each other in this space (both cognitive-intensive), while construction workers occupy distant regions (manual-intensive). This geography determines substitution patterns through two mechanisms:

- **Proximity effect:** Occupations with similar skill intensities (nearby in skill space) are natural substitutes
- **Transferability effect:** High ρ_s amplifies substitution between occupations sharing transferable skills

The cross-nested structure achieves remarkable dimensionality reduction. The full substitution matrix requires O^2 parameters—with 300 occupations, this means 90,000 bilateral elasticities. Our framework collapses this to $S + 1$ parameters: S transferability parameters and one productivity dispersion parameter θ, with skill intensities $\{\omega_o^s\}$ measured directly from occupational data. For three skills (cognitive, manual, interpersonal), we estimate just four structural parameters while capturing rich substitution patterns across hundreds of occupations.

2.4.2. Employment and Substitution Structure

The cross-nested CES framework generates explicit expressions for employment shares and substitution elasticities, revealing how distance in skill space governs labor market outcomes.

PROPOSITION 6 (CNCES Employment and Elasticities). *Under CNCES, occupational employment shares decompose as:*

$$\pi_o = \sum_{s \in \mathcal{S}} \pi_o^s = \sum_{s \in \mathcal{S}} \underbrace{\pi_o^{s,W}}_{\text{within-skill share}} \cdot \underbrace{\pi^{s,B}}_{\text{skill share}} \tag{8}$$

where:

$$\pi_o^{s,W} = \frac{(\omega_o^s A_o w_o^\theta)^{\frac{1}{1-\rho_s}}}{\sum_{o'}(\omega_{o'}^s A_{o'} w_{o'}^\theta)^{\frac{1}{1-\rho_s}}} \quad \textit{(occupation o's share among skill-s users)}$$

$$\pi^{s,B} = \frac{\left[\sum_{o'}(\omega_{o'}^s A_{o'} w_{o'}^\theta)^{\frac{1}{1-\rho_s}}\right]^{1-\rho_s}}{\sum_{s'}\left[\sum_{o'}(\omega_{o'}^{s'} A_{o'} w_{o'}^\theta)^{\frac{1}{1-\rho_{s'}}}\right]^{1-\rho_{s'}}} \quad \textit{(skill s's share of workforce)}$$

The correlated substitution elasticities are:

$$\theta \frac{x_{o'} F_{oo'}}{F_o}\bigg|_{x_j = A_j w_j^\theta} = -\theta \sum_{s \in \mathcal{S}} \frac{\rho_s}{1-\rho_s} \cdot \pi_o^{s,W} \pi_{o'}^{s,W} \cdot \frac{\pi^{s,B}}{\pi_o} \tag{9}$$

PROOF. See Appendix A.8. □

The employment decomposition in equation (8) shows that occupational employment π_o aggregates skill-specific contributions π_o^s, each equaling the product of within-skill share $\pi_o^{s,W}$ (occupation o's share among skill-s users) and between-skill share $\pi^{s,B}$ (skill s's workforce share). This multiplicative structure embeds employment patterns into distance-dependent substitution.

The elasticity formula (9) reveals how skill distance determines substitutability. The product $\pi_o^{s,W}\pi_{o'}^{s,W}$ measures skill overlap between occupations, while $\rho_s/(1-\rho_s)$ scales this overlap by transferability—high ρ_s amplifies substitution even with modest overlap, while low ρ_s limits substitution despite substantial overlap. Two data analysts at different firms (high overlap, high transferability) are strong substitutes; a data analyst and welder (low overlap, low transferability) are not.

This structure explains why technological clustering amplifies inequality. When automation concentrates in manual-intensive occupations, displaced workers face a mobility trap: their high within-skill shares ($\pi_o^{\text{manual},W}$ large) indicate concentration in manual occupations, while clustering ensures their natural alternatives—other manual occupations—face similar negative shocks.

The framework nests standard models as special cases. When $\rho_s = 0$ for all skills (no transferability), the correlation term vanishes and the model reduces to CES with uniform elasticity θ. Our framework generalizes nested CES models where each occupation belongs exclusively to one nest. Traditional nested CES requires pre-specifying rigid occupation groups—manufacturing versus services, routine versus non-routine. In contrast, CNCES allows occupations to draw from multiple skills with varying intensities $\{\omega_o^s\}$, measured directly from occupational data. This flexibility proves crucial: data reveal that most occupations blend multiple skills, and these continuous skill intensities—not discrete

categories—determine substitution patterns.

2.5. Heterogeneous Workers

Our baseline model assumes workers are ex-ante identical, differing only in their idiosyncratic productivity draws. We now extend the framework to incorporate systematic heterogeneity across demographic groups, providing additional identifying variation for our empirical analysis.

Consider demographic groups $g \in G$ (e.g., race × gender combinations) that differ in their occupational productivity distributions. Each group draws productivity from:

$$\Pr[\boldsymbol{\epsilon}^g(i) \leq \boldsymbol{\epsilon}] = \exp\left[-F\left(A_1^g \epsilon_1^{-\theta}, \ldots, A_O^g \epsilon_O^{-\theta}\right)\right]$$

where A_o^g represents group g's average productivity in occupation o. While comparative advantages $\{A_o^g\}$ vary across groups, the correlation function F and dispersion parameter θ remain common, preserving the underlying substitution structure.[12]

The productivity differences $\{A_o^g\}$ can arise from multiple sources—labor market discrimination, differences in skill endowments, or heterogeneous preferences for job amenities. The source of these differences does not affect our estimation strategy: given observed employment distributions, groups with identical employment shares $\{\pi_o^g\}$ exhibit identical substitution elasticities, regardless of whether these shares arise from discrimination or preferences. The elasticity matrix Θ^g depends only on the equilibrium employment distribution, not on its underlying causes.

This group heterogeneity serves two purposes in our analysis. First, it provides crucial identifying variation: different groups exhibit distinct substitution patterns based on their initial occupational distributions. A group concentrated in manual occupations shows different reallocation responses than one concentrated in cognitive occupations when faced with identical wage changes, helping to separately identify correlation parameters $\{\rho_s\}$ from average elasticity θ. Second, it enables us to study heterogeneous impacts of technological change across demographic groups in an extension, revealing how automation and AI affect different segments of the workforce.

3. Measurement and Estimation

This section implements the theoretical framework empirically in two steps. First, we measure key model inputs: occupational skill requirements (ω_o^s) from O*NET descriptors and technological exposure through task-level evaluations of automation and AI feasibility. These measurements reveal that both technologies cluster within skill-adjacent occupa-

[12] Group-specific employment shares are denoted π_o^g, yielding group-specific elasticity matrices Θ^g.

tions—automation in manual-intensive jobs and AI in cognitive-intensive ones. Second, we estimate structural parameters $\{\theta, \{\rho_s\}_{s\in\mathcal{S}}\}$ by exploiting occupational employment responses to automation-induced wage changes between 1980 and 2010.

3.1. Data and Measurement

The primary data source for measuring both skill requirements and occupational exposure is O*NET (the Occupational Information Network).[13] O*NET provides two key elements: (i) skill requirements, which define an occupation's location in the skill space of labor supply, and (ii) task descriptions, which allow measurement of exposure to automation and AI.

Occupational Skill Requirements. The theoretical framework requires measures of skill requirements $\{\omega_o^s\}$ that map occupations into a low-dimensional skill space where proximity determines substitutability. To operationalize this concept, we follow Lise and Postel-Vinay (2020) and extract skill requirements directly from O*NET data rather than estimating them, ensuring consistency with the DIDES structure.

We apply Principal Component Analysis (PCA) to approximately 200 O*NET descriptors covering skills, abilities, knowledge, work activities, and work context. Following Lise and Postel-Vinay (2020), we reduce these to three interpretable dimensions through exclusion restrictions: (i) mathematics scores load exclusively onto cognitive requirements, (ii) mechanical knowledge onto manual requirements, and (iii) social perceptiveness onto interpersonal requirements.[14] These orthogonal dimensions align with the model's assumption of independent skill-specific productivity distributions.

To construct skill requirement parameters ω_o^s that enter correlation function F, we first rescale principal component loadings to $r_o^s \in [0, 1]$ using linear transformations that preserve relative distances between occupations.[15] The final skill requirements are computed as variance-weighted shares:

$$\omega_o^s = \frac{r_o^s \times \text{Var}_s}{\sum_{s'\in\mathcal{S}} r_o^{s'} \times \text{Var}_{s'}}$$

where Var_s is the variance explained by skill s. This formulation ensures $\sum_s \omega_o^s = 1$ for each

[13] The O*NET database, maintained by the U.S. Department of Labor, provides comprehensive data on occupational characteristics, worker skills, and job requirements across a wide range of professions. (Link: `https://www.onetonline.org/`)

[14] The three principal components explain 58% of total variation, with cognitive skills accounting for 35.6%, manual skills 15.2%, and interpersonal skills 6.9%. This concentration of explanatory power in cognitive and manual dimensions aligns with their dominance in determining substitution patterns, as shown in Section 2.

[15] Linear transformations are crucial here as they maintain the distance metric in skill space—a key feature for DIDES. Converting to ranks would impose uniform spacing between adjacent occupations, eliminating meaningful variation in skill proximity.

occupation, consistent with the theoretical requirement that $\omega_o^s = (A_o^s)^\theta / A_o$ represents relative skill intensity. Table 1 provides illustrative examples, with detailed methodology in Appendix B.2.

TABLE 1. Skill Requirements and Technological Exposures for Selected Occupations

	Skill Requirements			Technological Exposure	
Occupation	Cognitive	Manual	Interpersonal	AI	Automation
Chief Executives	0.71	0.11	0.18	0.28	0.03
Electrical Engineers	0.73	0.19	0.08	0.71	0.19
Economists	0.79	0.07	0.14	0.86	0.31
Licensed Practical Nurses	0.52	0.26	0.22	0.08	0.47
Textile Machine Operators	0.52	0.47	0.01	0.02	0.51

Notes: Skill requirements (ω_o^s) represent the relative importance of cognitive, manual, and interpersonal skills for each occupation, with values summing to 1.0 across the three dimensions. Technological exposure measures indicate the share of tasks within each occupation that can potentially be performed by AI (generative models) or automation (robots, machines, and rule-based software) without human intervention.

Occupational Exposure to Technologies. Several measures exist for occupational exposure to automation (Acemoglu and Restrepo 2022; Autor et al. 2024). In contrast, measuring occupational exposure to AI presents unique challenges, as its full labor market impact has yet to materialize. To construct forward-looking measures, we follow Eloundou et al. (2024) and leverage ChatGPT to evaluate task-level automation and AI feasibility.[16]

Specifically, we query ChatGPT on whether each task in O*NET's database (covering 19,200 tasks across 862 occupations) can be performed without human intervention by: (i) industrial robots, machines, and computers without AI capabilities (representing traditional automation exposure) or (ii) generative AI models like ChatGPT (representing AI exposure). ChatGPT estimates that approximately 6,000 tasks—one-third of the total—can potentially be performed by AI, a magnitude comparable to automation technologies.

Table 2 provides examples of task evaluations for two occupations: economists and sewing machine operators. This classification distinguishes automation-exposed tasks, which involve well-defined, rule-based processes susceptible to mechanization, from AI-exposed tasks, which primarily involve inductive reasoning, complex decision-making, and non-physical cognitive work. The latter aligns with Polanyi's Paradox—many cognitive tasks resist codification into explicit rules, making them more amenable to AI than traditional automation (Autor 2015).

[16]This LLM-based approach has been validated by subsequent studies. Bick, Blandin, and Deming (2024) and Tomlinson et al. (2025) demonstrate high correlations between LLM task evaluations and ex-post real-world generative AI adoption patterns. Most notably, Brynjolfsson, Chandar, and Chen (2025) find that LLM exposure measures predict actual employment declines: early-career workers (ages 22-25) in the most AI-exposed occupations have experienced a 13% relative decline in employment since widespread AI adoption.

TABLE 2. Task-Level Evaluation of Automation and AI Exposure

Task Description	Automation	AI
Economists, Market and Survey Researchers		
Explain economic impact of policies to the public	No	Yes
Supervise research projects and students' study projects	No	No
Teach theories, principles, and methods of economics	No	Yes
Textile Sewing Machine Operators		
Remove holding devices and finished items from machines	Yes	No
Cut materials according to specifications, using tools	Yes	No
Record quantities of materials processed	Yes	Yes

This table presents examples of task-level evaluations using ChatGPT. Automation exposure is assessed by asking: "Can industrial robots, machines, and computers (no AI capability) perform this task without human intervention?" AI exposure is determined by querying: "Can generative AI (e.g., large language models like ChatGPT) potentially perform this task without human intervention?" Each task receives a binary classification.

Using these task-level evaluations, we compute the share of tasks within each occupation that are either automatable or AI-exposed, forming our occupational exposure measures. Table 1 reports automation and AI exposure levels for selected occupations. Additional methodological details and validation against existing measures are provided in Appendix B.3.

Technological Exposure in Skill Space. We now examine how technological exposure maps onto occupational skill requirements, revealing the clustering patterns central to our analysis. Consistent with existing research showing that manual-intensive occupations are more susceptible to automation (Autor, Levy, and Murnane 2003), our ChatGPT evaluations confirm this relationship. Panel (a) of Figure 1 demonstrates that automation exposure increases with manual skill requirements and decreases with cognitive requirements. Conversely, Panel (b) reveals that AI exposure follows the opposite pattern: cognitive-intensive occupations face greater vulnerability to AI, as these technologies increasingly perform complex analytical and decision-making tasks.

While automation and AI target distinct occupational segments, they share a critical feature: both technologies cluster within skill-adjacent occupations. Panels (c) and (d) of Figure 1 visualize this clustering in cognitive-manual skill space, where darker shading indicates higher exposure. Automation concentrates in the lower-right region (high manual, low cognitive requirements), while AI clusters in the upper-left region (high cognitive, low manual requirements). This spatial concentration has profound implications for labor market adjustment: as established in Section 2.3, clustering restricts worker mobility because displaced workers' natural alternatives—occupations requiring similar skills—face

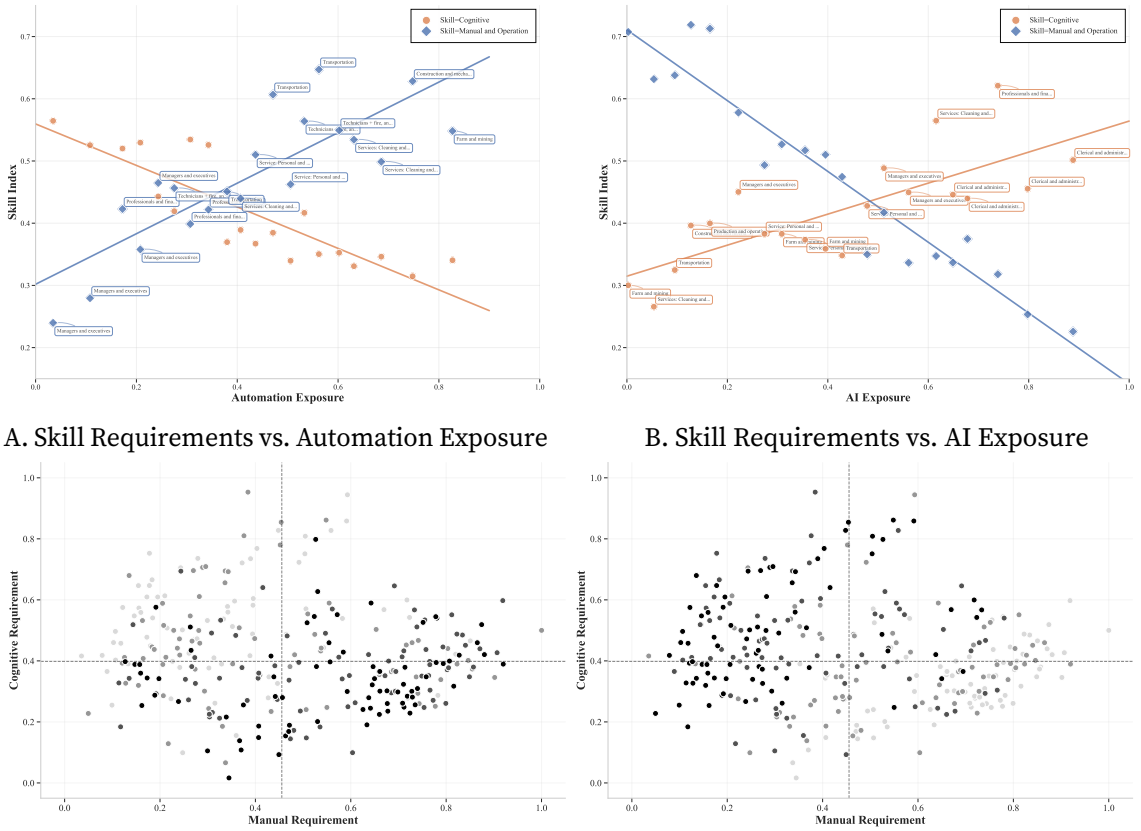

A. Skill Requirements vs. Automation Exposure

B. Skill Requirements vs. AI Exposure

C. Automation Exposure in Skill Space

D. AI Exposure in Skill Space

FIGURE 1. Technological Exposure in Skill Space

This figure illustrates the distribution of automation and AI exposure across occupational skill space. Panels (a) and (b) present binscatter plots of occupational skill indices against technological exposure. Panels (c) and (d) visualize the same exposure patterns in two-dimensional cognitive-manual skill space, where darker shading indicates higher exposure levels.

similar technological threats.

The choice of cognitive and manual dimensions in our analysis reflects their empirical importance: together they account for 88% of total skill requirements across occupations.[17] Given this dominance, our descriptive analysis focuses on these two dimensions, while Appendix B.4 examines technological exposure along the interpersonal dimension.

3.2. Estimation of Structural Parameters

Having established technological exposure patterns across skill space, we now estimate the labor supply elasticities $\{\theta, \{\rho_s\}_{s\in\mathcal{S}}\}$ that govern occupational substitution. Our estimation strategy exploits long-run employment responses to automation-induced wage changes

[17] Since cognitive and manual skills dominate occupational differentiation, they largely determine substitution patterns and mobility constraints.

across demographic groups.

3.2.1. Linear Representation and Identification

While the full model is nonlinear, first-order approximation clarifies our identification strategy. Log-linearizing the labor supply system yields:

$$\hat{\mathbf{L}}^g = \Theta^g(\theta, \boldsymbol{\rho}, \boldsymbol{\omega}, \mathbf{L}^g) \cdot \hat{\mathbf{w}} + \boldsymbol{\varepsilon}^g$$

where the elasticity matrix Θ^g depends on structural parameters $\{\theta, \boldsymbol{\rho}\}$ and group-specific employment shares $\mathbf{L}^g$. As shown in equation (4), elements of Θ^g decompose into two components: a baseline term capturing average substitutability and a correlation term reflecting skill-based proximity.

ASSUMPTION 1 (Exclusion Restriction). *Automation exposure* $\mathbf{z}$ *affects employment only through wages:*

$$\mathbb{E}[\boldsymbol{\varepsilon}^g | \mathbf{z}] = 0$$

where $\boldsymbol{\varepsilon}^g$ *represents unobserved labor supply shocks for group* g*.*

This orthogonality condition is plausible because automation feasibility is determined by technological capabilities—whether tasks can be codified into rules—rather than by worker preferences or labor supply shifts.

Cross-skill elasticity θ is identified from employment responses along clustering shocks, while correlation parameters $\{\rho_s\}$ are identified from differential responses along dispersed shocks. Consider the 2×2 example from Section 2.3: the clustering shock $\boldsymbol{u}_2 = (1, 1, -1, -1)'$ with eigenvalue $\lambda_2 = \theta$ affects cognitive and manual clusters oppositely, directly identifying θ from between-cluster reallocation. Within-cluster shocks $\boldsymbol{u}_3, \boldsymbol{u}_4$ with eigenvalue $\theta/(1-\rho)$ create dispersed effects, identifying ρ from differential responses of groups with varying within-cluster distributions.

In our empirical setting with hundreds of occupations, automation provides the clustering shock (concentrated in manual occupations), while variation in exposure within skill clusters provides dispersed shocks. Cross-group variation strengthens identification: groups concentrated in different clusters identify θ, while groups with different within-cluster distributions identify $\{\rho_s\}$.

3.2.2. Wage Effects from PSID

We first estimate automation-induced wage changes using the Panel Study of Income Dynamics (PSID) from 1985-2019. Following Cortes (2016), we exploit within-individual job

spell variation to address selection concerns that plague cross-sectional wage comparisons:[18]

$$\ln w_{i(o),t} = \beta_t \cdot \text{Automation}_o + \mathbf{X}'_{it}\gamma + \delta_{i,o} + u_{i,o,t}$$

where $\delta_{i,o}$ represents individual-occupation spell fixed effects and $\mathbf{X}_{it}$ includes year effects and time-varying individual characteristics.

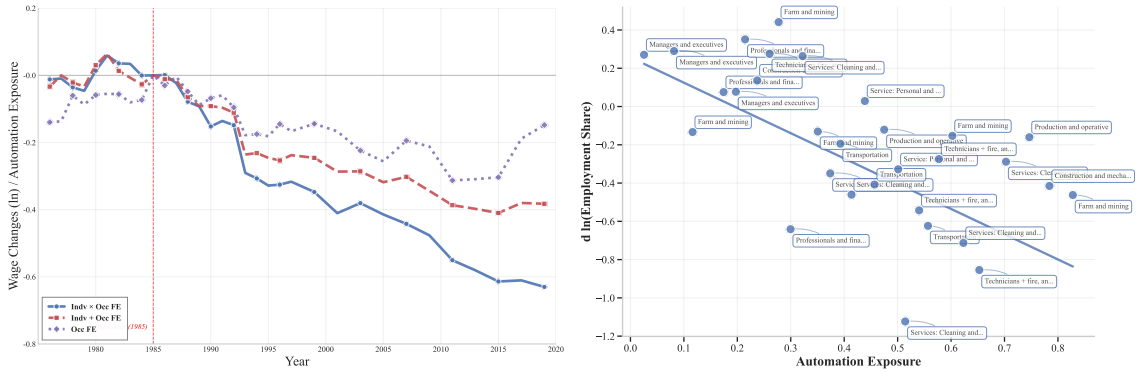

A. Wage Effects from PSID

B. Employment Effects from Census

FIGURE 2. Effects of Automation on Wages and Employment

Panel (a) shows estimated wage effects of automation exposure using PSID data. The solid line uses individual-occupation spell fixed effects to control for selection, while dashed lines show alternative specifications that yield attenuated estimates. Panel (b) presents employment share changes from Census (1980-2000) and ACS (2010-2018) data, showing a 1.2 log point decline for maximally exposed occupations. The simultaneous decline in both wages and employment confirms that automation represents a negative labor demand shock rather than a supply shift.

The importance of controlling for selection is evident in Figure 2. Panel (a) compares three specifications: (i) our preferred specification with job spell fixed effects (solid blue line), (ii) occupation fixed effects only (dashed purple), and (iii) both individual and occupation fixed effects (dashed red). The cross-sectional specification without individual controls yields only a 30 log point wage decline for maximally exposed occupations, while our preferred specification shows a 60 log point decline by 2019. This difference reflects both composition changes and selection of workers in cross-sectional wage comparisons. Wage effects of automation for men and women are remarkably similar, as shown in Appendix B.5.

Panel (b) shows corresponding employment effects using Census and ACS data. Occupations with maximum automation exposure experienced a 100 log point decline in employment share relative to unexposed occupations. Crucially, the simultaneous decline in both wages and employment—rather than opposing movements—confirms that automation operates as a negative labor demand shock. If automation were a supply

[18] Cortes (2016) classifies occupations into discrete groups. We instead use continuous automation exposure for 306 occupations, providing richer variation for identification.

phenomenon (workers leaving certain occupations), we would observe rising wages in exposed occupations due to reduced labor supply. Instead, the parallel declines in wages and employment unambiguously identify automation as reducing firms' demand for labor in affected occupations. These wage and employment responses provide the key moments for structural estimation.

3.2.3. Structural Estimation via Exact Hat Algebra

Given estimated wage changes $\{\hat{w}_o\}$ from automation, we now estimate structural parameters $\{\theta, \boldsymbol{\rho}\}$ using the exact hat algebra approach.

PROPOSITION 7 (Hat Algebra). *Given relative wage changes $\hat{\mathbf{w}}$, correlation function F, and parameters $\{\theta, \boldsymbol{\rho}\}$, observed employment shares $\{\boldsymbol{\pi}_t^g\}_{g\in G}$ serve as sufficient statistics for predicting counterfactual shares $\{\boldsymbol{\pi}_{t+1}^g\}_{g\in G}$ without requiring levels of wages or productivities.*

PROOF. See Appendix A.9 for proof and algorithm. □

This result allows us to express equilibrium conditions in terms of ratios. For each demographic group g, model-implied employment changes are:

$$\hat{\pi}_o^g = \hat{\pi}_o^g\left(\theta, \boldsymbol{\rho}, \{\omega_o^s\}, \{\pi_{o,t}^g\}, \{\hat{w}_o\}\right)$$

where the function applies the hat transformation. We estimate parameters using pseudo-Poisson maximum likelihood:

$$\{\hat{\theta}, \hat{\boldsymbol{\rho}}\} = \arg\min_{\theta,\boldsymbol{\rho}} \sum_{o,g} \kappa\left(\pi_{o,t+1}^g, \pi_{o,t}^g \cdot \hat{\pi}_o^g(\theta, \boldsymbol{\rho})\right)$$

where $\kappa(x, \hat{x}) = 2[x\ln(x/\hat{x}) - (x - \hat{x})]$. The estimation embeds the exclusion restriction:

$$\mathbb{E}\left[\nu_{o,t}^g \mid \hat{\mathbf{w}}_t, \{\boldsymbol{\pi}_t^g\}_{g\in G}\right] = 0$$

where $\nu_{o,t}^g = \pi_{o,t+1}^g / \hat{\pi}_{o,t}^{g,\text{Auto}} - 1$.

Table 3 presents PPML estimation results. The CES benchmark in column 1 imposes $\rho_s = 0$, yielding $\hat{\theta} = 3.12$ (s.e. = 0.20). This represents average elasticity under independent productivity draws across occupations. Column 2 shows our main CNCES specification using all demographic groups, which dramatically alters the results.

Three key findings emerge. First, cross-skill elasticity falls to $\hat{\theta} = 1.10$ (s.e. = 0.23), implying that approximately two-thirds of observed substitution occurs within skill clusters rather than across them. Second, skill transferability varies substantially: cognitive skills show the highest correlation parameter ($\hat{\rho}_{\text{Cog}} = 0.77$, s.e. = 0.13), followed by interpersonal skills ($\hat{\rho}_{\text{Int}} = 0.75$, s.e. = 0.13), while manual skills exhibit the lowest transferability

TABLE 3. PPML Estimation Results of Labor Supply Elasticities across Demographic Groups

	1980–2000				1980–2010			
	CES All	CNCES All	CNCES White Men & Women	CNCES White Women	CES All	CNCES All	CNCES White Men & Women	CNCES White Women
θ	3.12	1.10	1.07	2.29	2.85	1.02	1.06	1.97
	(0.20)	(0.23)	(0.47)	(2.08)	(0.20)	(0.50)	(0.46)	(0.80)
ρ_{Cog}	0	0.77	0.78	0.65	0	0.76	0.75	0.65
	–	(0.13)	(0.09)	(0.36)	–	(0.17)	(0.22)	(0.67)
ρ_{Man}	0	0.48	0.50	0.39	0	0.44	0.45	0.38
	–	(0.18)	(0.15)	(0.44)	–	(0.23)	(0.19)	(0.52)
ρ_{Int}	0	0.75	0.77	0.62	0	0.72	0.74	0.62
	–	(0.13)	(0.14)	(0.41)	–	(0.19)	(0.14)	(0.27)

Standard errors in parentheses. Following the literature, we scale the Poisson deviance by the mean-variance ratio of the data to obtain standard errors. While scaling does not affect the estimates, it aligns the deviance with the data variance. The CES specification imposes $\rho = 0$ across all occupation groups, while the CNCES specification allows for heterogeneous distance-dependent elasticities. Columns 1 and 5 report CES estimates for the full sample. Columns 2 and 6 report CNCES estimates for the full sample. Columns 3 and 7 restrict the sample to white men and women, while columns 4 and 8 further restrict to white women only. The estimates for the CES specification are close to those from a simple OLS regression with predicted wage effect as a regressor.

($\hat{\rho}_{\text{Man}} = 0.48$, s.e. = 0.18). Third, these parameters imply heterogeneous within-skill elasticities: $\theta/(1-\rho_s)$ equals 4.8 for cognitive occupations, 4.4 for interpersonal occupations, but only 2.1 for manual occupations.

The remaining columns demonstrate robustness. Columns 3-4 show that estimates remain stable when restricting to white workers, though standard errors increase with smaller samples.[19] Columns 5-8 replicate the analysis using 1980-2010 employment changes, yielding nearly identical point estimates with slightly larger standard errors. Consistency across time periods and demographic subsamples validates our identification strategy: technological clustering within skill domains fundamentally constrains worker mobility, with manual workers facing the most severe limitations due to lower skill transferability.

To assess our CNCES approach, we compare it with standard Nested CES specifications that partition occupations into mutually exclusive categories. Using the same estimation procedure, we test two nesting structures: occupation categories (low-skill service,

[19]The larger but imprecise estimate for white women alone ($\hat{\theta} = 2.29$, s.e. = 2.08) likely reflects both identification and compositional effects. First, cross-skill identification comes primarily from men, whose employment concentrates in manual occupations, providing clearer variation in response to clustering shocks. Second, rising female labor force participation during our sample period means cross-sectional variation partly captures new entrants who are inherently more flexible in their occupational choices, inflating the estimated elasticity. Women's more dispersed employment across skill clusters, however, provides valuable identifying variation for correlation parameters $\{\rho_s\}$. This complementarity in identification across demographic groups strengthens our overall estimates.

high-skill service, manufacturing) and skill intensity groupings (cognitive, manual, interpersonal). Results detailed in Appendix B.6 reveal that most within-nest correlation parameters are statistically insignificant, while cross-nest elasticities (2.05–2.67) converge toward our CES benchmark of 3.12, effectively reducing nested CES to standard CES. The contrast with our CNCES estimates—where $\theta = 1.10$ and substantial skill-specific correlations emerge—demonstrates that continuous skill intensities rather than discrete categorical boundaries are empirically critical.

3.3. The Topology of Occupational Substitution

Our estimated parameters reveal the fundamental structure of labor market substitution. Using 1980–2000 estimates, Figure 3 visualizes the substitution network among 306 occupations based on estimated cross-wage elasticities from our CNCES model.

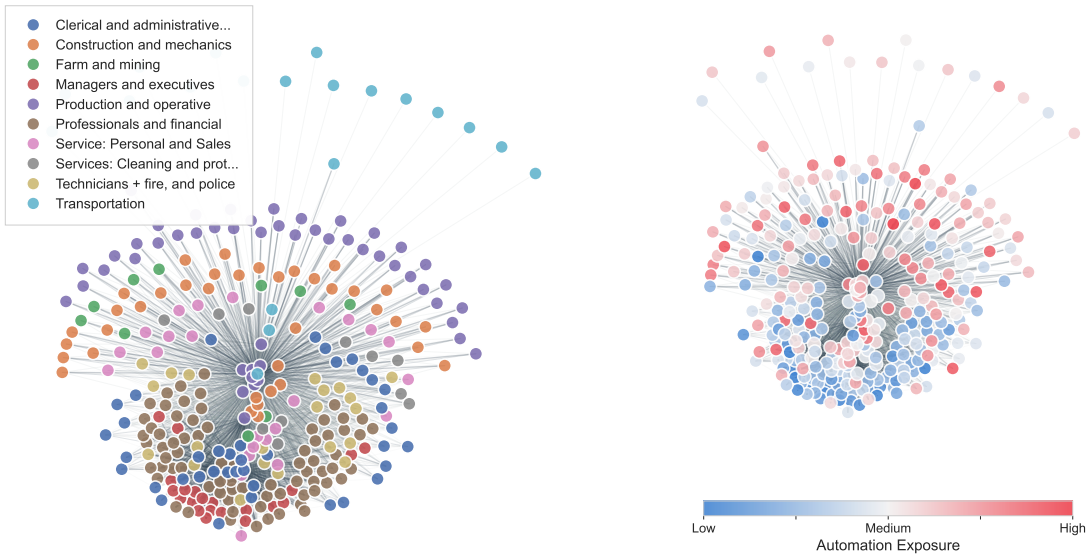

FIGURE 3. The Network Structure of Occupational Substitutability and Automation Exposure, 1980

This figure visualizes the substitution structure among 306 occupations based on estimated cross-wage elasticities from the CNCES model. Edges represent substitutability between occupation pairs, with darker and thicker lines indicating stronger substitution relationships (top 20% of elasticities shown). Node positions are determined using a force-directed layout algorithm that places more substitutable occupations closer together. The left panel colors nodes by broad occupational categories, revealing natural clustering of similar occupations. The right panel maps automation exposure onto the same network structure, with colors ranging from blue (low exposure) to red (high exposure), demonstrating the concentration of technological shocks within skill-adjacent occupations.

The left panel demonstrates how our three-skill framework organizes occupations into economically meaningful clusters. Production and operative occupations form dense interconnections through shared manual skills; professional and financial occupations

create even tighter clusters around cognitive requirements; service occupations fragment based on specific skill combinations. The cognitive cluster exhibits the highest density of connections, directly reflecting our estimated correlation parameters: $\rho_{\text{cog}} = 0.77$ versus $\rho_{\text{man}} = 0.48$. This differential density validates our model's ability to capture both occupational position in skill space (through ω_o^s) and varying strength of within-skill connections (through ρ_s). This structure emerges from estimated elasticities rather than imposed assumptions, confirming that our framework captures both the geography of occupations and heterogeneous mobility constraints governing transitions between them.

The network topology directly illustrates distance-dependent elasticity of substitution (DIDES). Within-cluster connections are dense (high substitutability for similar ω_o^s), while cross-cluster edges remain sparse (limited substitution across skill boundaries). This contrasts sharply with nested CES specifications, which impose rigid categorical boundaries. Our empirical tests of nested CES reveal why such approaches fail: within-nest correlations are statistically insignificant and cross-nest elasticities converge to the CES benchmark.[20] The CNCES framework's flexibility—with $\theta = 1.10$ for cross-skill substitution but within-skill elasticities ranging from 2.1 to 4.8—captures heterogeneous mobility constraints that discrete nesting misses.

The right panel overlays automation exposure, revealing how technological clustering constrains adjustment. Automation concentrates in the production-operative cluster, creating a mobility trap: workers' most natural alternatives face similar threats. Dense within-cluster connections that normally facilitate adjustment instead propagate shocks. High within-cluster substitutability amplifies rather than dissipates wage effects when entire skill clusters face negative shocks.[21] This visualization crystallizes our theoretical insight: when automation hits manufacturing workers, they can easily move to construction or transportation jobs—but those jobs are also being automated.

4. The Incidence of Automation and AI

Having estimated the labor supply elasticities that govern occupational substitution, we now evaluate the labor market incidence of automation and AI. For labor demand elasticity, we use the estimate from Caunedo, Jaume, and Keller (2023) of $\sigma = 1.34$, based on occupational input responses to labor productivity changes. Our analysis proceeds in three complementary steps: we first decompose technological shocks using spectral analysis

[20] Standard nesting forces dissimilar occupations together while separating similar ones across arbitrary boundaries. For instance, nested CES might group all "service" occupations despite heterogeneous skill requirements. Our CNCES allows occupations to draw from multiple skills—a economist requires primarily cognitive skills ($\omega_o^{\text{cog}} = 0.79$) but also interpersonal abilities ($\omega_o^{\text{int}} = 0.14$)—letting data determine relative distances rather than imposing discrete categories. See Appendix B.6 for detailed comparisons.

[21] Appendix B.7 shows AI exhibits identical clustering in cognitive-intensive occupations, suggesting this pattern characterizes skill-biased technological change generally.

to understand their fundamental structure, then examine resulting heterogeneous wage pass-through across occupations, and finally quantify welfare recovery achieved through occupational mobility. Throughout, we use 1980–2000 elasticity estimates, which provide the most robust identification.

4.1. Spectral Decomposition of Technological Shocks

We apply the spectral framework from Section 2.3 to decompose automation and AI shocks into eigenshocks—fundamental patterns revealing the labor market's absorption capacity. Each eigenshock's eigenvalue determines reallocation possibilities: smaller eigenvalues indicate rigid adjustment channels and larger wage effects.[22]

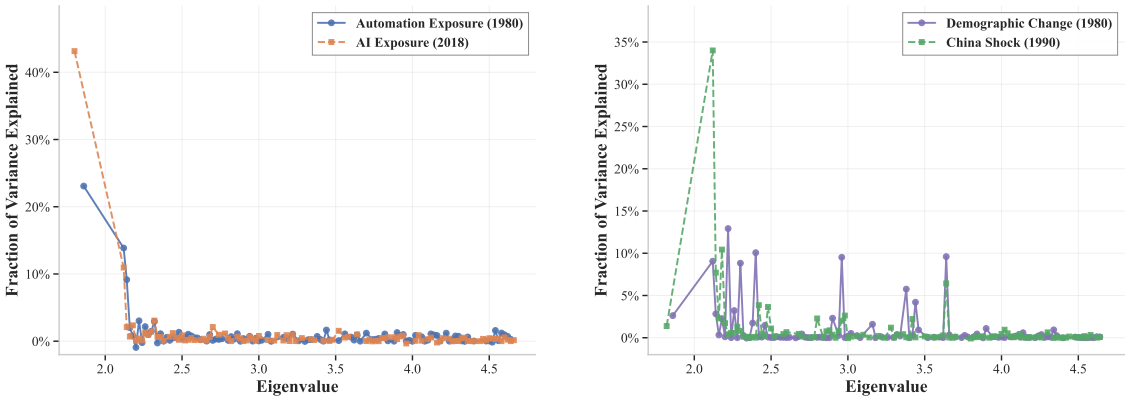

A. Automation and AI Exposures

B. Trade and Demographic Shocks

FIGURE 4. Variance Decomposition of Labor Demand Shocks

Decomposition of labor demand shocks into eigenshocks ordered by eigenvalue magnitude. Smaller eigenvalues indicate limited employment reallocation. Panel A: Automation and AI concentrate on low-eigenvalue eigenshocks. Panel B: Trade and demographic shocks distribute across higher eigenvalues, enabling better adjustment.

Figure 4 reveals why technological shocks generate severe distributional consequences. Panel A shows both automation and AI load disproportionately onto eigenshocks with the smallest eigenvalues (1.8–2.0). Automation concentrates 23% of its variance on the smallest eigenvalue; AI shows 44%—dwarfing other contributions. These small eigenvalues represent shock patterns affecting clusters of similar occupations simultaneously, leaving workers with minimal escape routes. When technological shocks concentrate on such rigid adjustment channels, the labor market cannot dissipate them through employment reallocation.

Clustering patterns vary across demographic groups, reflecting heterogeneous employment distributions across skill space. Appendix B.8 demonstrates that automation

[22] We compute the substitution matrix by inverting employment shares to obtain implied productivity levels $A_{o,t}w_{o,t}^{\theta}$. Eigenshocks are eigenvectors of this matrix, with eigenvalues measuring absorption capacity.

constrains male workers more severely—loading 31% of variance on the smallest eigenvalue versus women's 10%—due to men's concentration in manual-intensive occupations. This gender difference disappears for AI, where both groups face similar extreme concentration on low eigenvalues, suggesting cognitive task clustering affects all workers regardless of occupational segregation patterns.[23]

Panel B contrasts this with trade and demographic shocks, which distribute variance across eigenshocks with moderate-to-high eigenvalues. The China shock's largest loading (34%) occurs at eigenvalue 2.1, while demographic changes load substantially on eigenvalues above 2.5.[24] These patterns create multiple adjustment pathways—workers displaced from declining industries or occupations can transition to expanding ones, a mechanism that technological clustering eliminates.

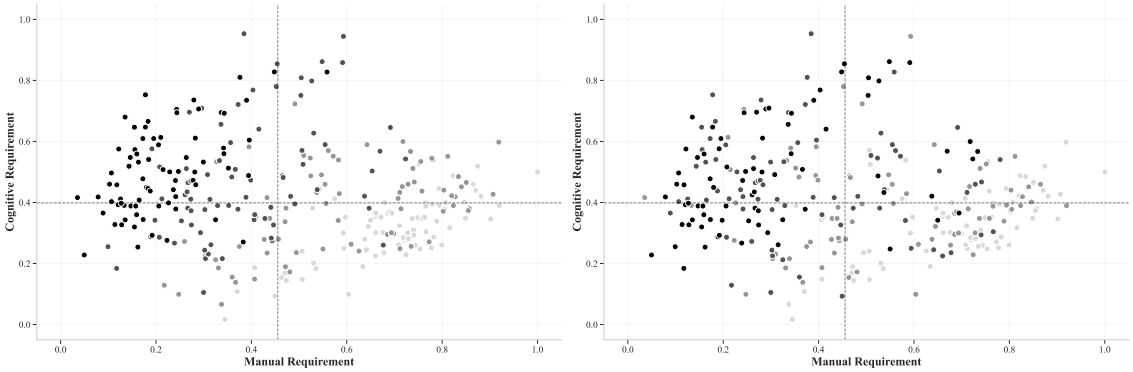

A. Eigenshock with Smallest Eigenvalue B. AI Exposure in Skill Space

FIGURE 5. Spatial Structure of Technological Constraints

Panel A: Eigenshock with smallest eigenvalue (2018) in cognitive-manual skill space. Panel B: AI exposure distribution. Darker shading indicates higher loading/exposure. Dashed lines mark median skill requirements. The correspondence shows AI aligns with the shock pattern least absorbable through reallocation.

Figure 5 maps why technological shocks resist adjustment. Panel A visualizes the eigenshock with the smallest eigenvalue across cognitive-manual skill space. The pattern bifurcates: high-manual/low-cognitive occupations (lower right) and high-cognitive/low-manual occupations (upper left) load strongly but oppositely. Panel B reveals AI exposure concentrates precisely in the high-cognitive region identified by the eigenshock—not coincidence but mathematical necessity.

The grayscale gradient exposes the trap: occupations with highest eigenshock loading (darkest quartile) form tight clusters. A financial analyst facing AI exposure cannot escape

[23]The convergence in AI's gender impact contrasts with automation's differentiated effects, implying future technological shocks may generate more uniform demographic impacts while maintaining severe absolute clustering effects.

[24]We obtain occupation-level demand changes from the China shock and population aging (demographic shock) from Autor et al. (2024), who estimate these effects based on trade exposure and demographic composition across U.S. commuting zones.

to data analysis or market research—these skill-similar alternatives face comparable threats. The correlation enabling natural transitions becomes the mechanism preventing escape.[25]

The spectral decomposition establishes two key insights: (i) Technological concentration on low-eigenvalue eigenshocks drives distributional consequences—not a technical detail but the fundamental mechanism; (ii) The labor market's limited capacity to absorb skill-clustered shocks represents a structural constraint, not temporary friction, shaping how technological progress creates persistent wage disparities.

4.2. The Structure of Wage Incidence

The spectral analysis revealed aggregate patterns; we now document their heterogeneous manifestation across occupations. Our central finding: technological incidence depends not on average substitutability but on the structure of substitution—specifically, how clustering interacts with skill-based mobility constraints.

Figure 6 reveals systematic heterogeneity in how demand shocks split between employment and wage adjustments.[26] Panel A shows automation's pass-through ranging from 25% to 45%—far exceeding the 30% CES benchmark for most exposed occupations. This variation directly reflects our theoretical prediction: when shocks cluster in skill space, affected workers cannot escape through reallocation, forcing adjustment through wages.

Production and transportation workers (purple/cyan points) exemplify this trap. Facing the largest negative shocks with 40-45% pass-through, nearly half their demand destruction becomes wage losses—not the 30% standard models predict. Automation clusters in manual-intensive occupations, eliminating natural transition pathways. The effective elasticity falls from 3.12 to 2.38, yielding an average pass-through of 0.36. This reveals that ignoring substitution structure and clustering overstates labor supply elasticity by 31%, systematically understating wage inequality from technological change.

Panel B reveals AI's distinctive pattern compared to automation. While highly exposed occupations (right side) show modestly elevated pass-through around 35%, the larger pass-through emerges for AI-complementary occupations (left side), which exhibit pass-through rates of 40-45%. This asymmetry reveals that AI generates larger wage gains for beneficiaries than wage losses for those displaced. Workers in AI-complementary occupations—those with minimal AI exposure—capture substantial wage increases because displaced cognitive workers cannot easily transition into these roles, which often require different skill combinations like manual or interpersonal expertise. This creates a pro-

[25] Dashed median lines divide the space into quadrants. Occupations in the upper-left quadrant face double jeopardy: direct AI exposure plus surrounding by similarly threatened occupations.

[26] We invert the model using automation wage effects to recover demand changes. For AI, we normalize shocks to match automation's aggregate effect, enabling distributional comparison.

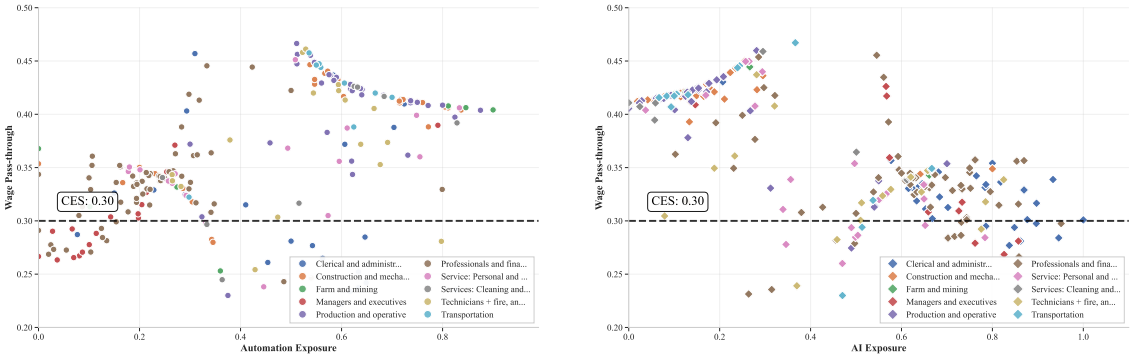

A. Automation Pass-Through

B. AI Pass-Through

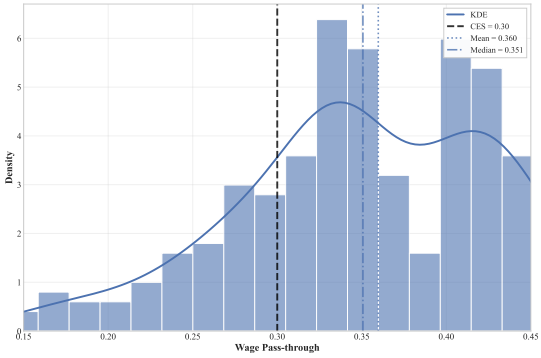

C. Distribution of Automation Pass-Through

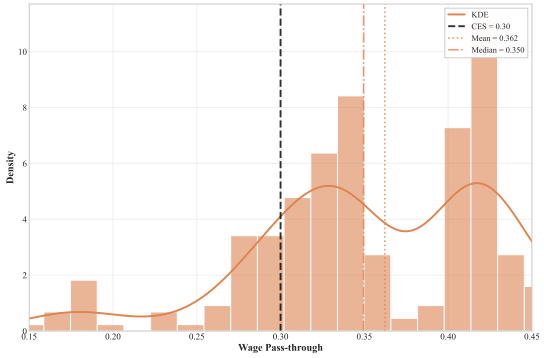

D. Distribution of AI Pass-Through

FIGURE 6. Heterogeneous Wage Pass-Through of Technological Shocks

Panels A-B: Pass-through rates versus exposure, with points colored by occupation category. Horizontal line marks CES benchmark (0.30). Panels C-D: Pass-through distributions with CES benchmark (dashed), mean (dotted), and median (dash-dotted) lines.

nounced winner-take-all than automation: those who benefit from AI experience larger relative gains, amplifying inequality through a different mechanism than the symmetric displacement effects of automation.

Economic Magnitudes. Panels C and D translate occupation-specific effects into workforce distributions. Three features challenge conventional models. First, mean pass-through (0.362 for automation, 0.360 for AI) exceeds the CES benchmark by 20%, implying that CES overstates average labor supply elasticity by 31% and systematically understates wage inequality. Second, pronounced bimodality—with modes at 0.32 (peripheral occupations) and 0.42 (core exposure)—contradicts uniform incidence assumptions. Third, the three-fold range (0.15-0.45) reflects fundamental heterogeneity in substitution structure, not measurement error. These patterns have substantial consequences. For a 30% demand shock, heavily exposed manual occupations experience 13.5% wage declines (30% × 0.45)

versus 9% under CES—a 50% larger effect.[27]

The key insight connecting to our theory: technological clustering transforms the fundamental trade-off between employment and wage adjustment. In equation (3), pass-through matrix $\Delta = (\mathbf{I} + \Theta/\sigma)^{-1}$ depends on the full structure of Θ, not just its average. When technology clusters (concentrating on low-eigenvalue eigenshocks), workers cannot escape through employment reallocation—the mechanism that typically dissipates shocks—forcing adjustment through wages. This structural constraint, not average rigidity, drives the severe and persistent inequality we document.

4.3. Welfare Recovery Through Occupational Mobility

While wage pass-through captures static losses, workers partially recover through occupational transitions. These mobility gains, however, depend crucially on the interaction between exposure patterns and skill transferability—revealing why average elasticities mislead.

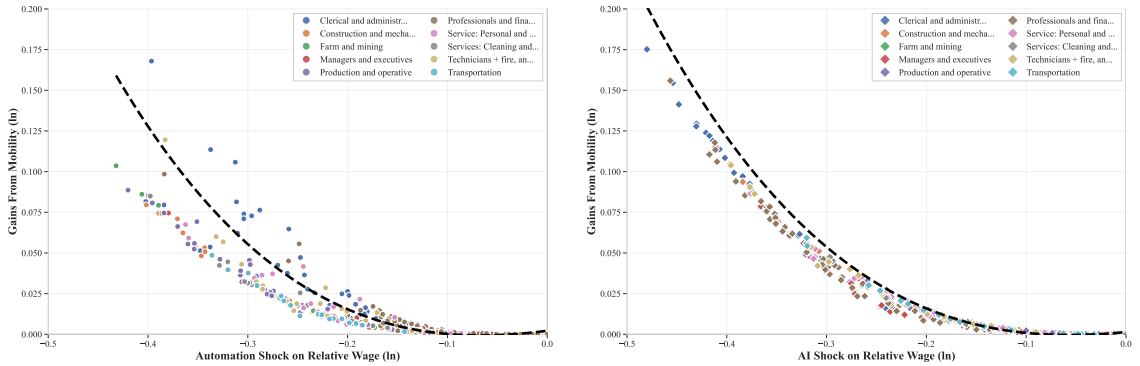

A. Automation: Mobility Gains

B. AI: Mobility Gains

FIGURE 7. Welfare Recovery Through Occupational Mobility

Welfare gains from transitions (equivalent variation) versus wage shocks. Points represent occupations (CNCES model); black dashed curves show CES predictions. The convex relationship reflects stronger transition incentives for larger shocks, but recovery remains partial and heterogeneous.

Figure 7 quantifies mobility gains as equivalent variation: $\text{EV}_o = \sum_{o'} \mu_{oo'} \cdot d\ln(w_{o'}/w_o)$. The convex relationship confirms that larger shocks induce more transitions. Yet the systematic gap between our estimates and CES predictions reveals how clustering constrains recovery.

Panel A exposes automation's mobility trap: workers experiencing 40 log point wage declines recover only 20% of losses through transitions, versus 30% under CES—a 50% overstatement. This gap emerges from a cruel interaction: automation concentrates in

[27] Persistence matters for policy: high pass-through reflects structural mobility constraints requiring sustained intervention, not temporary frictions that markets arbitrage away.

manual occupations where workers have the lowest skill transferability ($\rho_{man} = 0.48$). Production workers cannot escape to construction or transportation—their most productive alternatives—because these face similar threats. The clustering that drives wage losses simultaneously blocks escape routes. Standard models using average elasticity $\theta = 3.12$ miss this interaction, falsely implying that manual workers enjoy the same mobility options as others.

Panel B reveals AI's contrasting pattern: cognitive workers experiencing 40 log point wage declines recover approximately 27% of losses, still below CES predictions but notably higher than automation's impact. This improvement directly reflects our estimated $\rho_{cog} = 0.77$—cognitive skills transfer more readily across occupations. A threatened data analyst has more viable alternatives than a displaced welder, even when many cognitive occupations face AI exposure. Yet recovery remains limited: even with higher transferability, clustering ensures that workers' best alternatives are often similarly threatened.

4.4. Summary: The Complete Incidence Picture

Our three-pronged analysis reveals how technological clustering fundamentally reshapes labor market adjustment, generating more severe and persistent inequality than standard frameworks predict.

The spectral decomposition established that automation and AI concentrate on eigenshocks with the smallest eigenvalues (1.8–2.0), channeling disruption through the labor market's most rigid adjustment channels. While other shocks—trade, demographics—distribute across multiple eigenvalues enabling reallocation, technology loads 23–44% of variance onto patterns that mathematically minimize escape possibilities.

This concentration manifests in heterogeneous wage pass-through. Our estimates reveal 25-45% of demand shifts for both automation and AI translate to wages—substantially exceeding the 30% CES benchmark. Heavily automation-exposed occupations face pass-through rates reaching 45%, implying 50% larger wage effects than standard models predict.

Mobility provides limited insurance against these losses. Workers largely exposed to automation recover only 20% of wage declines through occupational transitions, compared to 30% under conventional assumptions. This constraint emerges from a cruel interaction: technological shocks cluster precisely where skill transferability is weakest. Automation targets manual occupations with $\rho_{man} = 0.48$, creating a double bind—large losses with minimal recovery options. AI focuses on cognitive occupations where $\rho_{cog} = 0.77$ offers better prospects, yet clustering still constrains escape routes.

The crucial insight connecting theory to empirics: incidence depends not on average substitutability but on the interaction between shock distribution and substitution structure. In our framework, pass-through matrix $\Delta = (\mathbf{I} + \Theta/\sigma)^{-1}$ captures this interac-

tion—when shocks align with low-eigenvalue eigenshocks (clustering), the labor market cannot dissipate shocks through reallocation, forcing adjustment through wages. This structural mechanism, absent from models assuming uniform elasticity, explains why technological change generates such pronounced and persistent distributional consequences.

5. Dynamic Extension with Transition

Our model retains the Roy structure, enabling a seamless integration of DIDES into related frameworks while incorporating a richer substitution structure — essential for counterfactual analysis. In this quantitative section, we extend our static model into a dynamic discrete choice framework (Artuç, Chaudhuri, and McLaren 2010; Caliendo, Dvorkin, and Parro 2019) to capture gradual labor market transitions. This extension allows us to examine the dynamic labor market incidence of technological adoption in the transition and the long run (Lehr and Restrepo 2022; Adão, Beraja, and Pandalai-Nayar 2024).[28]

5.1. Dynamic Discrete Choice with DIDES

Our focus is on studying the dynamic labor market incidence of technological adoption rather than modeling firms' endogenous technology adoption decisions. The production side remains identical to the static framework, while workers make rational, forward-looking occupational choices in response to automation and AI shocks. To model these choices, we adopt a structure similar to Caliendo, Dvorkin, and Parro (2019) with a correlated productivity distribution among jobs.

Workers' Dynamic Decision. In each period, we denote the vector of occupational employment by $\boldsymbol{L}_t$. Workers are assumed to be hand-to-mouth, taking the wage path $\{\boldsymbol{w}_t\}_{t=0}^{\infty}$ as given, and derive utility from consumption and labor supply according to:

$$U\left(\{c_t(i), \ell_t(i)\}_{t=0}^{\infty}\right) = \sum_{t=0}^{\infty} \beta^t \left(\ln c_t(i) - \ln \ell_t(i)\right)$$

At the beginning of each period, workers draw labor productivity across all occupations from the same distribution as in the static model:[29]

$$\Pr\left[\epsilon_1(i) \leq \epsilon_1, \ldots, \epsilon_O(i) \leq \epsilon_O\right] = \exp\left[-F\left(A_1\epsilon_1^{-\theta}, \ldots, A_O\epsilon_O^{-\theta}\right)\right]$$

[28] Different from Dvorkin and Monge-Naranjo (2019) and Seo and Oh (2024), we abstract from persistent worker heterogeneity while allowing for the flexible substitution structure to focus on the incidence.

[29] The correlation function in both transition and steady state corresponds to the same empirical elasticities. If transition probabilities are identical across all origins, these probabilities correspond to the stationary distribution, implying they share the same substitution structure.

After observing their labor productivity, workers choose an occupation, with consumption equal to occupational income, $c_t = w_{o,t}$, and labor supply given by:

$$\ln\left(\ell_t\left(i\right)\right) = -\kappa \ln\left(\epsilon_{o,t}\left(i\right)\right)$$

In contrast to the static model, productivity enters the labor supply function with short-run discounting factor κ, which governs short-run labor supply elasticity. While we could allow workers to redraw labor productivity with a short-run probability, doing so yields the same sufficient statistics for counterfactual welfare and similar dynamics.[30] Additionally, workers incur job transition cost $\tau_{oo'}$ when switching occupations.

ASSUMPTION 2. *Job transition cost is constant over time $\tau_{oo'}$ and measured in terms of utility.*

Given this economic environment, we formulate workers' decisions recursively via the following Hamilton-Jacobi-Bellman (HJB) equation:

$$v_{o,t}\left(\boldsymbol{\epsilon}_t\right) = \max_{o'}\left\{\ln w_{o',t} + \kappa \ln \epsilon_{o',t} + \beta V_{o,t+1} - \tau_{oo'}\right\}$$

where $V_{o,t+1} = \mathrm{E}_{\boldsymbol{\epsilon}}\left[v_{o,t+1}\left(\boldsymbol{\epsilon}\right)\right]$ and $v_{o,t}\left(\boldsymbol{\epsilon}_t\right)$ denote a worker's lifetime utility in occupation o after observing their productivity. This utility comprises current-period benefits $\ln w_{o',t} + \kappa \ln \epsilon_{o',t}$ and discounted expected future utility $V_{o,t+1}$, net of job transition cost $\tau_{oo'}$. Workers choose occupation o' to maximize lifetime utility.

Consequently, we can recursively express occupational expected utility as:

$$V_{o,t} = \ln\left(F\left(A_{1,t}Z_{o1,t}{}^{\frac{\theta}{\kappa}}, \ldots, A_{O,t}Z_{oO,t}^{\frac{\theta}{\kappa}}\right)^{\frac{\kappa}{\theta}}\right) + \bar{\gamma}\frac{\kappa}{\theta}$$

$$\text{where } Z_{oo',t} = \exp\left(\beta V_{o',t+1} + \ln w_{o',t} - \tau_{oo'}\right)$$

Additionally, job transition probability can be derived as shown in Appendix A.11:

$$\mu_{oo',t} = \frac{A_{o',t}Z_{oo',t}{}^{\frac{\theta}{\kappa}} \times F_{o'}\left(A_{1,t}Z_{o1,t}{}^{\frac{\theta}{\kappa}}, \ldots, A_{O,t}Z_{oO,t}^{\frac{\theta}{\kappa}}\right)}{F\left(A_{1,t}Z_{o1,t}{}^{\frac{\theta}{\kappa}}, \ldots, A_{O,t}Z_{oO,t}^{\frac{\theta}{\kappa}}\right)}$$

The interplay of job transition costs and idiosyncratic productivity shocks generates slow labor market adjustments in our model. A key distinction of our approach is that it allows for rich substitution patterns between jobs, as embedded in the correlation function F. When F is additive, our framework reduces to the standard model.

[30] Allowing for short-run probability of redrawing productivity can also be interpreted as an overlapping generations (OLG) framework. However, permitting productivity redraws would imply larger gains from reallocation under the same transition dynamics.

Dynamic Equilibrium. As discussed in the static model, the share of tasks performed by labor, denoted by $\left\{\boldsymbol{s}_t^{\ell}\right\}_{t=0}^{\infty}$, characterizes distributional effects of technological adoption, while aggregate capital productivity, $\left\{a_t^k\right\}_{t=0}^{\infty}$, is Hicks-neutral (see Appendix A.13). All other occupational labor productivity is represented by $\{\boldsymbol{A}_t\}_{t=0}^{\infty}$.

Given time-varying fundamentals $\{\Psi_t\}_{t=0}^{\infty} = \left\{\boldsymbol{s}_t^{\ell}, a_t^k, \boldsymbol{A}_t\right\}_{t=0}^{\infty}$, we define a dynamic equilibrium under rational expectations. In this equilibrium, there exists a time path of wages $\{\boldsymbol{w}_t\}_{t=0}^{\infty}$, occupational allocations $\{\boldsymbol{L}_t\}_{t=0}^{\infty}$, and job transition probabilities $\{\mu_t\}_{t=0}^{\infty}$ such that:

a. Wage vector $\boldsymbol{w}_t = \boldsymbol{w}\left(\boldsymbol{s}_t^{\ell}, a_t^k, \boldsymbol{L}_t\right)$ solves the static production equilibrium.
b. Workers' optimal occupational choices yield job transitions $\mu_t = \left\{\mu_{oo',t}\right\}_{o=1,o'=1}^{O,O}$.
c. Labor allocation evolves according to $L_{o,t} = \sum_{o'} \mu_{oo',t} L_{o,t-1}$.[31]

5.2. Dynamic Hat Algebra with Correlation

In this section, we extend the dynamic hat algebra to incorporate correlated productivity distributions, enabling richer substitution patterns. The model addresses key counterfactual questions: What would have happened to the wage distribution if automation technologies had not been adopted? How much can the labor market absorb unequal demand shocks caused by AI if AI technologies are adopted to the same extent as automation, but at a much more rapid pace by 2030?

Formally, our counterfactual analysis studies how equilibrium allocations across occupations and over time change relative to a baseline economy when faced with an alternative sequence of fundamentals, denoted by $\left\{\Psi_t'\right\}_{t=1}^{\infty}$. We examine how changes in these counterfactual fundamentals affect equilibrium outcomes of interest.

To facilitate characterization of the dynamic equilibrium, we introduce additional notation. For any scalar or vector x, we denote its proportional change between periods t and $t+1$ as $\dot{x}_{t+1} = x_{t+1}/x_t$. Additionally, x_t' denotes the corresponding variable in the counterfactual economy. Finally, we define $\hat{x}_{t+1} = \dot{x}_{t+1}'/\dot{x}_{t+1}$, which represents the ratio of the time change in the counterfactual equilibrium to that in the initial equilibrium.

Before characterizing counterfactual outcomes, we introduce the correlation-adjusted transition probability:

$$\tilde{\mu}_{oo',t} = A_{o',t} Z_{oo',t}^{\frac{\theta}{\kappa}} / F\left(A_{1,t} Z_{o1,t}^{\frac{\theta}{\kappa}}, \ldots, A_{O,t} Z_{oO,t}^{\frac{\theta}{\kappa}}\right)$$

which serves as a sufficient statistic. Note that when F is additive, $\tilde{\mu}_t$ coincides with μ_t since $\tilde{\mu}_{oo',t} = \mu_{oo',t}/F_{o'}$.

[31] We construct job flows from retrospective responses in the March CPS; consequently, aggregate flows derived from these responses do not directly match observed occupational employment levels. To account for this discrepancy, we adjust the evolution of occupational employment as $L_{o,t} = \sum_{o'} \mu_{oo',t} L_{o,t-1} + \Delta L_{o,t}$.

LEMMA 2. *Given correlation function F, there exists a unique mapping between occupation transition probability μ_t and correlation-adjusted transition probability $\tilde{\mu}_t$:*

$$\left\{\mu_{oo',t} = \tilde{\mu}_{oo',t} F_{o'}\left(\tilde{\mu}_{o1,t}, \ldots, \tilde{\mu}_{oO,t}\right)\right\}_{o'=1}^{O}, \quad \forall\, o$$

With this correlation-adjusted transition probability, we introduce the dynamic hat algebra with correlation to analyze how economic outcomes change counterfactually. Specifically, we study how allocations and wages across occupations evolve over time in response to alternative sequences of fundamentals, denoted by $\left\{\hat{\Psi}_t\right\}_{t=1}^{\infty}$.

PROPOSITION 8 (Dynamic Hat Algebra with Correlation). *For time-varying counterfactual changes in fundamentals $\left\{\hat{\Psi}_t\right\}_{t=1}^{\infty} = \left\{\hat{\boldsymbol{s}}_t^{\ell}, \hat{a}_t^{k}, \hat{\boldsymbol{A}}_t\right\}_{t=1}^{\infty}$ with $\lim_{t\to\infty} \hat{\Psi}_t = 1$, observed allocations and transition probability $\{\boldsymbol{L}_t, \mu_t\}_{t=0}^{\infty}$ are sufficient to characterize counterfactual changes in allocations, wages, and expected utility ($u_{o,t} = \exp\left(V_{o,t}\right)$). Formally:*

- *Counterfactual changes in wages $\hat{\boldsymbol{w}}_t = \hat{\boldsymbol{w}}\left(\hat{\boldsymbol{s}}_t^{\ell}, \hat{a}_t^{k}, \hat{L}_t\right)$ solve the static production equilibrium.*
- *Counterfactual correlation-adjusted transition probability is:*

$$\tilde{\mu}'_{oo',t} = \frac{\tilde{\mu}'_{oo',t-1}\dot{\tilde{\mu}}_{oo',t}\hat{A}_{o',t}\hat{u}_{o',t+1}^{\beta\frac{\theta}{\kappa}}\hat{w}_{o',t}^{\frac{\theta}{\kappa}}}{F\left(\left\{\tilde{\mu}'_{oo'',t-1}\dot{\tilde{\mu}}_{oo'',t}\hat{A}_{o'',t}\hat{u}_{o'',t+1}^{\beta\frac{\theta}{\kappa}}\hat{w}_{o'',t}^{\frac{\theta}{\kappa}}\right\}_{o''=1}^{O}\right)}$$

- *Counterfactual change in utility is characterized by:*

$$\hat{u}_{o,t+1} = F\left(\left\{\tilde{\mu}'_{oo'',t}\dot{\tilde{\mu}}_{oo'',t+1}\hat{A}_{o'',t+1}\hat{u}_{o'',t+2}^{\beta\frac{\theta}{\kappa}}\hat{w}_{o'',t+1}^{\frac{\theta}{\kappa}}\right\}_{o''=1}^{O}\right)^{\frac{\kappa}{\theta}}$$

  with terminal condition $\lim_{t\to\infty} \hat{u}_{o,t} = 1$.
- *Counterfactual occupational allocation evolves according to $L'_{o',t} = \sum_o \mu'_{oo',t} L'_{o,t-1}$.*

PROOF. See Appendix A.16 for proof and for the different expression for time 0 that accounts for unexpected changes in fundamentals. □

Proposition 8 demonstrates the sufficient statistic property of the dynamic hat algebra: observed allocations and transition probabilities fully characterize counterfactual outcomes under a new sequence of fundamentals. Moreover, it underscores the critical role of the substitution structure—captured by function F—which governs counterfactual implications. While observed allocations serve as sufficient statistics, the specific form of F determines how changes in fundamentals translate into counterfactual wages and allocations.[32] Our static results, showing that clustering of technological changes combined

[32]When F is additive, we return to the standard dynamic hat algebra approach with independent productivity distribution.

with DIDES leads to unequal labor market incidence, persist in the dynamic framework.

Finally, as derived in Appendix A.17, welfare change resulting from a shift in fundamentals—measured in terms of consumption equivalent variation—can be expressed as:

$$\mathrm{EV}_{o,t} = \sum_{s=t}^{\infty} \beta^{s-t} \ln\left(\hat{w}_{o,s} / \hat{\tilde{\mu}}_{oo,s}^{\frac{\kappa}{\theta}}\right)$$

Moreover, changes in occupation-specific adjusted staying probabilities capture gains from mobility, echoing results in Arkolakis, Costinot, and Rodríguez-Clare (2012), once the substitution structure is taken into account.

5.3. Data and Estimation

The Euler-Equation Approach. Based on the Euler-equation approach introduced by Artuç, Chaudhuri, and McLaren (2010), we account for correlation in the productivity distribution and corresponding substitution structure. Specifically, we derive the following analogous estimating equation:

$$\ln \frac{\tilde{\mu}_{oo',t}}{\tilde{\mu}_{oo,t}} = \frac{\theta}{\kappa} \ln \frac{w_{o',t}}{w_{o,t}} + \beta \ln \frac{\tilde{\mu}_{oo',t+1}}{\tilde{\mu}_{o'o',t+1}} + (\beta - 1)\,\tau_{oo'} + \nu_t$$

where ν_t is an error term. This expression parallels ACM's formulation but with correlation-adjusted job transitions. Intuitively, cross-sectional adjusted job transition flows incorporate information on expected future wages and the option value of job mobility, with adjusted future job transition flows serving as sufficient statistics for these option values (see Appendix A.17 for details). The key insight is that, after conditioning on adjusted future values, coefficient $\frac{\theta}{\kappa}$ represents the elasticity of relative adjusted job transitions with respect to changes in relative wages.[33] As in ACM, the theory implies that lagged values of wages and adjusted job transitions are valid instruments.[34]

Data and Estimation Results. Our estimation strategy requires aggregate job flows across occupations and average wages—data readily available from standard sources. We construct these measures using individual-level data from the US Census Bureau's March Current Population Survey (CPS). While our approach requires only aggregate transitions and wages, the limited sample size of CPS necessitates grouping occupations. We therefore cluster occupations into 15 groups based on their skill requirements using a k-means algorithm. This procedure is intuitive, as occupations with similar skill requirements naturally group together in skill space. We then compute annualized job transition probabilities

[33] We cannot separately estimate θ and κ, nor is it necessary, as they enter equilibrium dynamics and welfare metrics jointly, as demonstrated in Proposition 8.

[34] The exclusion condition requires that error term ν_t is not correlated over time. See ACM for detailed discussion.

among these 15 clusters, μ_t, for the period 1976–2019. Appendix B.10 provides detailed discussion of data construction.

TABLE 4. Estimation of Short-Run Elasticity θ/κ

	(1) OLS	(2) IV	(3) IV + Dest. FE	(4) IV + Origin FE
θ/κ	0.063***	0.071***	0.068**	0.080**
	(0.018)	(0.018)	(0.025)	(0.025)
Observations	630	630	630	630
Destination FE	No	No	Yes	No
Origin FE	No	No	No	Yes
IV	No	Yes	Yes	Yes

Notes: This table reports estimates of the short-run elasticity θ/κ from the Euler equation specification. Column (1) presents the baseline OLS estimate. Column (2) employs IV estimation using lagged adjusted job transition probabilities and wages as instruments. Columns (3) and (4) add destination and origin fixed effects, respectively, both with IV. Standard errors in parentheses. Significance levels: *** $p < 0.01$, ** $p < 0.05$, * $p < 0.1$.

We use $\beta = 0.96$ as the annual discount factor. Table 4 reports estimation results for short-run elasticity $\frac{\theta}{\kappa}$. Column (1) presents the OLS estimate, yielding a short-run elasticity of 0.063. Column (2) implements an IV approach using lagged adjusted job transition probabilities and wages as instruments, resulting in an estimate of 0.071. Columns (3) and (4) incorporate destination and origin fixed effects, respectively, yielding estimates of 0.068 and 0.080. While these estimates are broadly consistent, they are lower than those reported in ACM, primarily due to our use of correlation-adjusted job transition probabilities. As discussed in the static model, this adjustment nets out within-skill substitutability—a major source of variation in the response of job transitions to relative wage changes. Moreover, grouping occupations by similar skill requirements further reduces across-cluster job transition responses, contributing to smaller elasticity estimates.

5.4. The Dynamic Incidence of Automation and AI

We now assess the distributional effects of automation and AI within a slow-adjustment labor market framework. In our quantitative evaluation, we employ 15 occupation clusters with transition probabilities constructed from CPS data. For counterfactual applications, we use elasticities from our static estimation, augmented by short-run labor supply elasticity $\theta/\kappa = 0.07$ estimated via the Euler-equation approach. To maintain clarity, we focus on average effects over time, as cross-sectional heterogeneity closely mirrors results from the static model.

For automation technologies, we obtain ex-post estimates of their dynamic wage effects, as shown in Panel A of Figure 2. Occupations with higher automation exposure have experienced gradual relative wage decline since 1985, resulting in up to 50% difference between occupations where all tasks are exposed and those where none are. To match this

observed wage trend, we calibrate the share of tasks performed by labor, $\{s_t^\ell\}$. We then implement the following counterfactual: what would have occurred if task labor shares $\{s_t^\ell\}$ had remained unchanged since 1985?[35]

Panel A of Figure 8 illustrates the relative decline in occupational labor demand due to automation exposure (dashed line) alongside the share of demand changes absorbed by employment shifts (green line). Employment adjustments mitigate roughly two-thirds of relative demand changes, with the remaining one-third materializing as relative wage changes (blue line in Panel B). In Panel B, the orange line represents cumulative mobility-adjusted wage changes, given by $\sum_{s=1985}^{t} \ln\left(\hat{w}_{o,s}/\hat{\tilde{\mu}}_{oo,s}^{\kappa/\theta}\right)$, which accounts for worker mobility gains. These gains offset approximately half of wage losses. Compared to the static model, mobility gains are higher because we allow workers to redraw productivity—a more realistic setting when occupational productivity is not permanent.[36] Furthermore, because workers are forward-looking, mobility gains occur early in the adjustment process, as outside options improve immediately for negatively affected jobs, while wage effects accumulate gradually.

The gradual wage impact of automation suggests progressive adoption over the past four decades, allowing the labor market to absorb roughly two-thirds of associated labor demand shifts. This gradual adoption makes labor market adjustment in transition similar to that in the long run. However, if AI advances rapidly—as many practitioners advocate—the labor market may face greater adjustment challenges. To explore this scenario, we consider a counterfactual in which AI adoption reaches automation's scale by 2030, allowing us to evaluate labor market responses to rapid technological transition.

Panels C and D of Figure 8 illustrate the dynamic incidence of accelerated AI adoption. Panel C shows that the labor market adjusts sluggishly, absorbing less than one-third of relative demand shifts initially, with another third absorbed over subsequent decades. In Panel D, occupations highly exposed to AI experience sharp wage decline as full adoption materializes by 2030, followed by gradual recovery. Mobility gains offset approximately one-third of relative wage losses during transition. These findings suggest that slow labor market adjustment severely limits its ability to absorb rapid AI advancement impacts.

These findings underscore a key insight extending beyond the static model: clustering of both automation and AI exposure constrains worker mobility, limiting the labor market's capacity to absorb shocks through occupational transitions in both the short and long run. For automation, this rigidity is most pronounced in the long run, as gradual adoption has contributed to persistent wage disparities across occupations. For rapid AI expansion,

[35] Since we focus on unequal effects of additional automation exposure, we omit discussion of aggregate gains.

[36] Workers in current jobs typically have higher occupation-specific productivity due to selection; if productivity were permanent, they would face greater losses when transitioning. Allowing new productivity draws each period provides the same sufficient statistics for mobility gains as an overlapping generations (OLG) model.

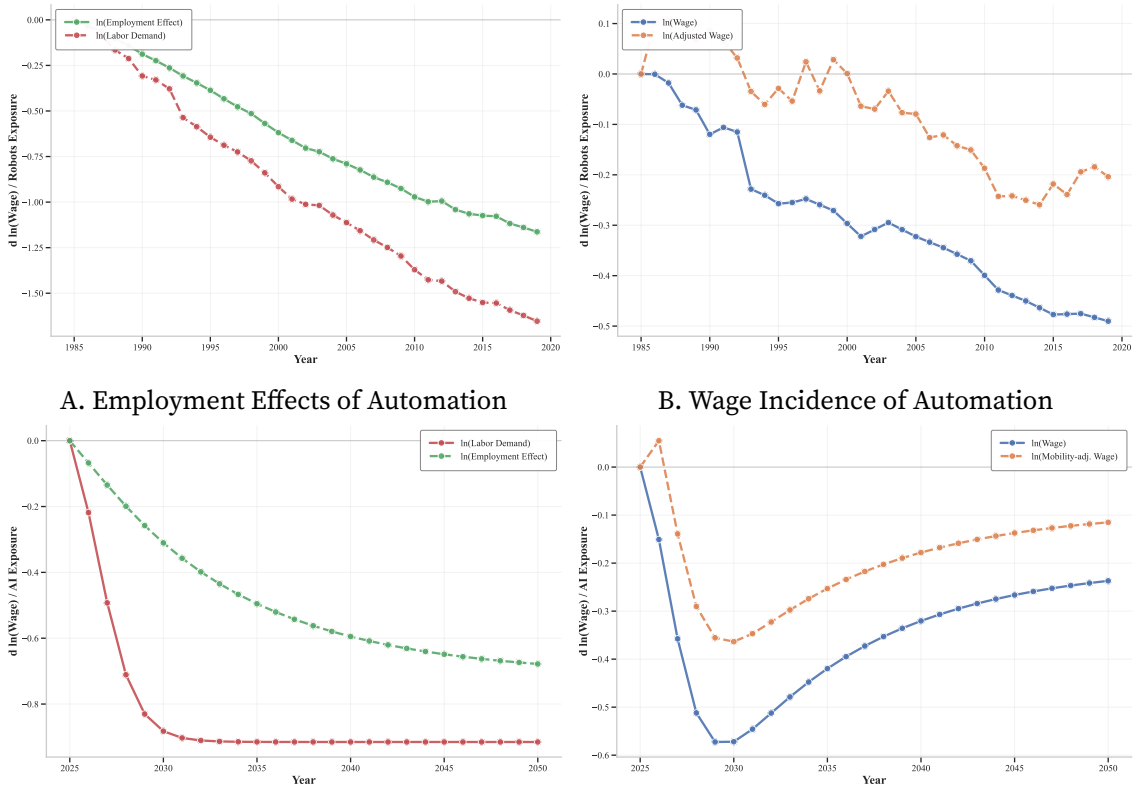

A. Employment Effects of Automation

B. Wage Incidence of Automation

C. Employment Effects of AI

D. Wage Incidence of AI

FIGURE 8. The Dynamic Incidence of Automation and AI

Panels A and B show employment and wage effects of automation exposure, while Panels C and D depict projected effects of rapid AI adoption. Dashed lines represent changes in labor demand, green lines indicate employment shifts, and blue lines capture wage incidence. Orange lines in Panels B and D account for mobility-adjusted wage changes.

however, mobility constraints operate in both the short and long run, amplifying labor market inequality and resulting in highly uneven economic incidence.

6. Conclusion

This paper establishes that the labor market incidence of technological change depends fundamentally on the interaction between shock distribution and substitution structure—not on average labor market rigidity. By developing and implementing a framework with distance-dependent elasticity of substitution (DIDES), we reveal how automation and AI generate severe inequality through technological clustering in skill-adjacent occupations.

Our theoretical contribution embeds DIDES into a Roy model through correlated productivity draws that decline with skill distance. This achieves crucial dimensionality reduction—transforming hundreds of thousands of bilateral elasticities into four parame-

ters in three-dimensional skill space. When shocks cluster, they align with low-eigenvalue eigenvectors of the substitution matrix, forcing wage adjustment rather than employment reallocation.

Empirically, we map 306 occupations into cognitive, manual, and interpersonal skill dimensions and estimate that two-thirds of substitution occurs within skill clusters. Cognitive skills prove most transferable ($\rho_{cog} = 0.77$) while manual skills show limited portability ($\rho_{man} = 0.48$). These heterogeneous elasticities interact with technological clustering to generate striking patterns: on average, 36% of demand shocks from both automation and AI translate to wages (versus 30% under CES)—implying standard models overstate labor supply elasticity by 31%. For most automation-exposed occupations, pass-through rates reach 45%, generating wage effects 50% larger than CES predictions. Workers recover only 20% of wage losses through mobility, compared to 35% predicted by standard models.

The dynamic analysis reveals persistent constraints. Gradual automation since 1985 generated wage gaps of up to 50% between high and low exposure occupations. Rapid AI adoption shows starker patterns: less than one-third of shocks absorbed initially, with mobility offsetting only one-third of wage losses. This sluggish adjustment reflects clustered shocks eliminating transition pathways precisely where workers need them most.

Three key insights emerge. First, technological clustering is the fundamental driver of distributional consequences, not an ancillary detail. Second, heterogeneous skill transferability creates asymmetric vulnerability—manual workers face high automation exposure with low transferability, while cognitive workers under AI threat benefit only partially from higher transferability. Third, conventional frameworks underestimate wage effects by 20% on average and 50% for heavily exposed occupations. These findings reshape policy prescriptions. Standard retraining programs miss the fundamental constraint: displaced workers' natural transition targets face similar technological threats. Effective interventions must either help workers cross skill boundaries—costly given our estimated elasticities—or slow adoption in clustered domains. As AI deployment accelerates, the concentration in cognitive occupations threatens adjustment challenges exceeding historical automation.

Future research should explore endogenous skill acquisition under clustered risks, firm-level adoption decisions driving clustering patterns, and international dimensions of technological disruption. The DIDES framework extends beyond technology to any clustered shock—pandemics, climate change, or demographic shifts. The central message is clear: technological progress need not generate severe inequality, but clustering combined with skill-based mobility constraints ensures that it does. Recognizing this mechanism—invisible to frameworks assuming uniform substitution—is essential for policies that protect workers while facilitating adjustment in an increasingly automated economy.

References

Acemoglu, Daron. 2002. "Directed Technical Change." *The Review of Economic Studies* 69 (4): 781–809.

Acemoglu, Daron, David Autor, Jonathon Hazell, and Pascual Restrepo. 2022. "Artificial intelligence and jobs: Evidence from online vacancies." *Journal of Labor Economics* 40 (S1): S293–S340.

Acemoglu, Daron and Pascual Restrepo. 2018. "The race between man and machine: Implications of technology for growth, factor shares, and employment." *American Economic Review* 108 (6): 1488–1542.

Acemoglu, Daron and Pascual Restrepo. 2020. "Robots and jobs: Evidence from US labor markets." *Journal of Political Economy* 128 (6): 2188–2244.

Acemoglu, Daron and Pascual Restrepo. 2022. "Tasks, automation, and the rise in U.s. wage inequality." *Econometrica* 90 (5): 1973–2016.

Adão, Rodrigo, Martin Beraja, and Nitya Pandalai-Nayar. 2024. "Fast and slow technological transitions." *Journal of Political Economy Macroeconomics* 2 (2): 183–227.

Arkolakis, Costas, Arnaud Costinot, and Andrés Rodríguez-Clare. 2012. "New trade models, same old gains?" *American Economic Review* 102 (1): 94–130.

Artuç, Erhan, Shubham Chaudhuri, and John McLaren. 2010. "Trade shocks and labor adjustment: A structural empirical approach." *American Economic Review* 100 (3): 1008–1045.

Autor, D H, L F Katz, and A B Krueger. 1998. "Computing inequality: Have computers changed the labor market?" *The Quarterly Journal of Economics* 113 (4): 1169–1213.

Autor, D H, F Levy, and R J Murnane. 2003. "The skill content of recent technological change: An empirical exploration." *The Quarterly Journal of Economics* 118 (4): 1279–1333.

Autor, David, Caroline Chin, Anna Salomons, and Bryan Seegmiller. 2024. "New frontiers: The origins and content of new work, 1940–2018." *The Quarterly Journal of Economics* 139 (3): 1399–1465.

Autor, David H. 2015. "Why are there still so many jobs? The history and future of workplace automation." *Journal of Economic Perspectives* 29 (3): 3–30.

Autor, David H and David Dorn. 2013. "The growth of low-skill service jobs and the polarization of the US labor market." *American Economic Review* 103 (5): 1553–1597.

Beraja, Martin and Nathan Zorzi. 2024. "Inefficient Automation." *The Review of Economic Studies* p. rdae019.

Bick, Alexander, Adam Blandin, and David J Deming. 2024. "The Rapid Adoption of Generative AI." Working Paper 32966, National Bureau of Economic Research.

Bocquet, Leonard. 2024. "The network origin of slow labor reallocation."

Brynjolfsson, Erik, Bharat Chandar, and Ruyu Chen. 2025. "Canaries in the coal mine? six facts about the recent employment effects of artificial intelligence." Tech. rep., Working paper. Latest version available at https://digitaleconomy.

Brynjolfsson, Erik, Danielle Li, and Lindsey Raymond. 2025. "Generative AI at work." *The Quarterly Journal of Economics* p. qjae044.

Böhm, Michael J., Ben Etheridge, and Aitor Irastorza-Fadrique. 2025. "The impact of labour demand shocks when occupational labour supplies are heterogeneous." Tech. Rep. W25/15, Institute for Fiscal Studies.

Caliendo, Lorenzo, Maximiliano Dvorkin, and Fernando Parro. 2019. "Trade and labor market dynamics: General equilibrium analysis of the China trade shock." *Econometrica* 87 (3): 741–835.

Caunedo, Julieta, David Jaume, and Elisa Keller. 2023. "Occupational exposure to capital-embodied technical change." *American Economic Review* 113 (6): 1642–1685.

Cortes, Guido Matias. 2016. "Where have the middle-wage workers gone? A study of polarization using panel data." *Journal of Labor Economics* 34 (1): 63–105.

Dvorkin, Maximiliano and Alexander Monge-Naranjo. 2019. "Occupation mobility, human capital and the aggregate consequences of task-biased innovations." *FRB St. Louis Working Paper* 13.

Eloundou, Tyna, Sam Manning, Pamela Mishkin, and Daniel Rock. 2024. "GPTs are GPTs: Labor market impact potential of LLMs." *Science* 384 (6702): 1306–1308.

Erosa, Andrés, Luisa Fuster, Gueorgui Kambourov, and Richard Rogerson. 2025. "Labor market polarization and inequality: a roy model perspective." Tech. rep., National Bureau of Economic Research.

French, Eric and Christopher Taber. 2011. "Identification of models of the labor market." In *Handbook of Labor Economics*, vol. 4 of *Handbook of labour economics*, edited by Orley Ashenfelter and David Card, pp. 537–617. Elsevier.

Freund, Lukas and Lukas Mann. 2025. "Job Transformation, Specialization, and the Labor Market Effects of AI."

Grigsby, John R. 2022. "Skill Heterogeneity and Aggregate Labor Market Dynamics." Tech. rep., National Bureau of Economic Research.

Guerreiro, Joao, Sergio Rebelo, and Pedro Teles. 2022. "Should robots be taxed?" *The Review of Economic Studies* 89 (1): 279–311.

Hampole, Menaka, Dimitris Papanikolaou, Lawrence DW Schmidt, and Bryan Seegmiller. 2025. "Artificial intelligence and the labor market." Tech. rep., National Bureau of Economic Research.

Heckman, James J and Bo E Honore. 1990. "The empirical content of the Roy model." *Econometrica: journal of the Econometric Society* 58 (5): 1121.

Heckman, James J, Lance Lochner, and Christopher Taber. 1998. "Explaining rising wage inequality: Explorations with a dynamic general equilibrium model of labor earnings with heterogeneous agents." *Review of Economic Dynamics* 1 (1): 1–58.

Heckman, James J and Guilherme Sedlacek. 1985. "Heterogeneity, aggregation, and market wage functions: An empirical model of self-selection in the labor market." *Journal of Political Economy* 93 (6): 1077–1125.

Hurst, Erik, Yona Rubinstein, and Kazuatsu Shimizu. 2024. "Task-based discrimination." *American Economic Review* 114 (6): 1723–1768.

Katz, L F and K M Murphy. 1992. "Changes in relative wages, 1963-1987: Supply and demand factors." *The Quarterly Journal of Economics* 107 (1): 35–78.

Lee, Donghoon and Kenneth I Wolpin. 2006. "Intersectoral labor mobility and the growth of the service sector." *Econometrica* 74 (1): 1–46.

Lehr, Nils Haakon and Pascual Restrepo. 2022. "Optimal Gradualism." Tech. rep., National Bureau of Economic Research.

Lind, Nelson and Natalia Ramondo. 2023. "Trade with correlation." *American Economic Review* 113 (2): 317–353.

Lindenlaub, Ilse. 2017. "Sorting multidimensional types: Theory and application." *The Review of Economic Studies* 84 (2): rdw063.

Lise, Jeremy and Fabien Postel-Vinay. 2020. "Multidimensional skills, sorting, and human capital

accumulation." *American Economic Review* 110 (8): 2328–2376.

Matsuyama, Kiminori. 1992. "A simple model of sectoral adjustment." *The Review of Economic Studies* 59: 375–387.

Noy, Shakked and Whitney Zhang. 2023. "Experimental evidence on the productivity effects of generative artificial intelligence." *Science* 381 (6654): 187–192.

Restrepo, Pascual. 2024. "Automation: Theory, evidence, and outlook." *Annual review of economics* 16 (1): 1–25.

Sattinger, M. 1993. "Assignment models of the distribution of earnings." *Journal of Economic Literature* 31 (2): 831–880.

Seo, Jaeeun and Ryungha Oh. 2024. "Sectoral Shocks and Labor Market Dynamics: A Sufficient Statistics Approach."

Teulings, Coen N. 1995. "The wage distribution in a model of the assignment of skills to jobs." *Journal of Political Economy* 103 (2): 280–315.

Teulings, Coen N. 2005. "Comparative advantage, relative wages, and the accumulation of human capital." *Journal of Political Economy* 113 (2): 425–461.

Tomlinson, Kiran, Sonia Jaffe, Will Wang, Scott Counts, and Siddharth Suri. 2025. "Working with AI: Measuring the Occupational Implications of Generative AI."

Traiberman, Sharon. 2019. "Occupations and import competition: Evidence from Denmark." *American Economic Review* 109 (12): 4260–4301.

Webb, Michael. 2019. "The impact of artificial intelligence on the labor market."

Appendix A. Proof of Results in Main Text

A.1. Production and Labor Demand

A.1.1. Task Framework

Following Acemoglu and Restrepo (2022), we begin with a task-based production framework where final output aggregates a continuum of tasks $\mathcal{T}$ through a constant elasticity of substitution technology:

$$y = \left(\int_{\mathcal{T}} y(x)^{\frac{\sigma-1}{\sigma}} dx \right)^{\frac{\sigma}{\sigma-1}}$$

where $y(x)$ denotes the input of task x and $\sigma > 1$ is the elasticity of substitution between tasks.

The task space is partitioned across O occupations, $\mathcal{O} = \{\mathcal{T}_1, \mathcal{T}_2, \ldots, \mathcal{T}_O\}$, where each task belongs exclusively to one occupation:

$$\mathcal{T} = \bigcup_{o=1}^{O} \mathcal{T}_o \quad \text{with} \quad \mathcal{T}_i \cap \mathcal{T}_j = \varnothing \text{ for } i \neq j$$

Each task can be produced using either labor or capital under perfect substitution:

$$y(x) = \ell_o(x) + a(x)k(x), \quad \forall x \in \mathcal{T}_o$$

where $\ell_o(x)$ is labor input from occupation o, $k(x)$ is capital input, and $a(x)$ represents task-specific capital productivity. Capital is produced from final output at unit cost.

A.1.2. Labor Demand

Given occupational wages $\{w_o\}_{o=1}^{O}$, cost minimization determines the optimal allocation of tasks between labor and capital. For each occupation o, tasks are assigned according to:

$$\mathcal{T}_o^{\ell} = \{x \in \mathcal{T}_o : w_o \leq 1/a(x)\} \quad \text{and} \quad \mathcal{T}_o^{k} = \{x \in \mathcal{T}_o : w_o > 1/a(x)\}$$

where $\mathcal{T}_o^{\ell}$ denotes tasks performed by labor and $\mathcal{T}_o^{k}$ denotes tasks performed by capital.

The equilibrium price of each task equals the unit cost of production:

$$p(x) = \begin{cases} 1/a(x) & \text{if } x \in \mathcal{T}_o^{k} \\ w_o & \text{if } x \in \mathcal{T}_o^{\ell} \end{cases}$$

Task demand follows from the CES structure: $y(x) = y \cdot p(x)^{-\sigma}$. Integrating over all

tasks performed by occupation o yields labor demand:

$$L_o = \int_{x \in \mathcal{T}_o^\ell} \ell_o(x) dx = y \cdot w_o^{-\sigma} \cdot M_{\mathcal{T}_o^\ell}$$

where $M_{\mathcal{T}_o^\ell} = \int_{\mathcal{T}_o^\ell} dx$ is the measure of tasks performed by occupation o.

A.1.3. Reduced-Form Representation

The zero-profit condition implies:

$$1 = \int_{\mathcal{T}} p(x)^{1-\sigma} dx = \int_{\cup_o \mathcal{T}_o^k} a(x)^{\sigma-1} dx + \sum_{o=1}^{O} w_o^{1-\sigma} \cdot M_{\mathcal{T}_o^\ell}$$

Define the share of tasks performed by labor in occupation o as $s_o^\ell = M_{\mathcal{T}_o^\ell} / M_{\mathcal{T}}$, where $M_{\mathcal{T}}$ is the total measure of tasks. Similarly, let $s^k = 1 - \sum_o s_o^\ell$ denote the share of tasks performed by capital, with average capital productivity a^k such that $s^k (a^k)^{\sigma-1} = \int_{\cup_o \mathcal{T}_o^k} a(x)^{\sigma-1} dx / M_{\mathcal{T}}$.

Solving for equilibrium output and substituting out capital yields the reduced-form production function:

$$y = A \left(\sum_{o=1}^{O} \alpha_o^{\frac{1}{\sigma}} L_o^{\frac{\sigma-1}{\sigma}} \right)^{\frac{\sigma}{\sigma-1}}$$

where:

$$A = \left[1 - s^k (a^k)^{\sigma-1} \right]^{-\frac{\sigma}{\sigma-1}} \quad \text{(aggregate productivity)}$$

$$\alpha_o = \frac{s_o^\ell}{1 - s^k (a^k)^{\sigma-1}} \quad \text{(effective labor share of occupation } o\text{)}$$

This reduced form captures the essential features of the task model: α_o represents occupation o's share of labor-performed tasks after accounting for automation. When technology advances increase $a(x)$ for tasks in $\mathcal{T}_o$, more tasks shift from labor to capital, reducing s_o^ℓ and hence α_o. The occupational wage then follows:

$$w_o = \frac{\partial y}{\partial L_o} = y^{\frac{1}{\sigma}} \alpha_o^{\frac{1}{\sigma}} L_o^{-\frac{1}{\sigma}} \tag{A1}$$

This parsimonious representation allows us to analyze the distributional effects of automation and AI through changes in task shares $\{\alpha_o\}$ without explicitly tracking individual task assignments.

A.2. Workers and Labor Supply

A.2.1. Properties of the Correlation Function

The labor supply side of our model builds on a Roy framework with correlated productivity across occupations. Central to our analysis is the correlation function $F : \mathbb{R}_+^O \to \mathbb{R}_+$, which governs the substitution structure between occupations. This function satisfies three key properties:

a. **Homogeneity of degree one:** $F(\lambda x_1, \ldots, \lambda x_O) = \lambda F(x_1, \ldots, x_O)$ for all $\lambda > 0$
b. **Unboundedness:** $\lim_{x_o \to \infty} F(x_1, \ldots, x_O) = \infty$ for any o
c. **Sign-switching property:** Mixed partial derivatives alternate in sign—the n-th order mixed partial is non-negative if n is odd and non-positive if n is even

The sign-switching property ensures that occupations are gross substitutes from workers' perspective, a crucial feature for equilibrium uniqueness. Additionally, $C(u_1, \ldots, u_O) = \exp[-F(-\ln u_1, \ldots, -\ln u_O)]$ forms a max-stable copula, guaranteeing that workers' occupational choices aggregate consistently across the population.[37]

A.2.2. Labor Supply

Workers are heterogeneous in their productivity across occupations. Each worker i draws a productivity vector $\boldsymbol{\epsilon}(i) = \{\epsilon_o(i)\}_{o=1}^O$ from the joint distribution:

$$\Pr[\epsilon_1(i) \le \epsilon_1, \ldots, \epsilon_O(i) \le \epsilon_O] = \exp\left[-F\left(A_1\epsilon_1^{-\theta}, \ldots, A_O\epsilon_O^{-\theta}\right)\right]$$

where $A_o > 0$ captures average productivity in occupation o and $\theta > 0$ governs the dispersion of productivity across workers. The marginal distributions are Fréchet: $\Pr[\epsilon_o(i) \le \epsilon] = \exp(-A_o\epsilon^{-\theta})$.

Workers choose occupations to maximize utility. A worker with productivity vector $\boldsymbol{\epsilon}(i)$ receives utility $u_o(i) = w_o\epsilon_o(i)$ from working in occupation o, where the productivity term captures both output produced and the inverse of effort cost. The optimal choice is:

$$o^*(i) = \arg\max_o \{w_o\epsilon_o(i)\} \tag{A2}$$

Given this optimization, the fraction of workers choosing occupation o is:

$$\pi_o = \Pr[w_o\epsilon_o(i) = \max_{o'} w_{o'}\epsilon_{o'}(i)] = \frac{A_o w_o^\theta F_o(A_1 w_1^\theta, \ldots, A_O w_O^\theta)}{F(A_1 w_1^\theta, \ldots, A_O w_O^\theta)} \tag{A3}$$

where $F_o = \partial F/\partial x_o$ denotes the partial derivative with respect to the o-th argument.[38]

[37] Max-stability ensures that $C(u_1, \ldots, u_O) = C(u_1^{1/m}, \ldots, u_O^{1/m})^m$ for all $m > 0$ and $(u_1, \ldots, u_O) \in [0,1]^O$. This property is essential for the aggregation of individual choices to yield tractable labor supply functions.

[38] The derivation of employment shares follows from the principle of maximum stability for multivariate

Total labor supply to occupation o is $L_o = \pi_o \bar{L}$, where $\bar{L}$ is the total workforce. The elasticity of labor supply with respect to wages determines how workers reallocate across occupations:

$$\Theta_{oo'} \equiv \frac{\partial \ln L_o}{\partial \ln w_{o'}} = \begin{cases} \theta \left[\left. \frac{x_{o'} F_{oo'}}{F_o} \right|_{x_j = A_j w_j^\theta} - \pi_{o'} \right] & \text{if } o \neq o' \\ \theta \left[\left. \frac{x_o F_{oo}}{F_o} \right|_{x_j = A_j w_j^\theta} + 1 - \pi_o \right] & \text{if } o = o' \end{cases} \tag{A4}$$

where $x_o = A_o w_o^\theta$ for notational convenience. The derivation of these elasticities from the employment share equation is provided in Section C.2.

The cross-elasticities $\Theta_{oo'}$ for $o \neq o'$ are negative (reflecting substitution) while own-elasticities Θ_{oo} are positive. Importantly, $\sum_{o'} \Theta_{oo'} = 0$, confirming that proportional wage increases do not affect relative employment—only relative wage changes induce reallocation.[39]

A.3. Proof of Equilibrium Existence and Uniqueness

PROPOSITION A1. *Given the production structure in Section A.1 and labor supply in Section A.2, a unique competitive equilibrium exists.*

PROOF. **Existence:** Define employment shares $\lambda_o = L_o / \bar{L}$ and note that market clearing requires

$$\lambda = \pi(w(\lambda)),$$

where $\pi(\cdot)$ are labor supply shares from (A3) and $w(\cdot)$ are occupational wages from (A1). The mapping $T : \Delta^{O-1} \to \Delta^{O-1}$ defined by $T(\lambda) = \pi(w(\lambda))$ is continuous: (i) $\pi(w)$ is continuous and strictly positive by the properties of the correlation function F, and (ii) $w(\lambda)$ is continuous from the CES production structure. Since T maps the compact convex simplex Δ^{O-1} into itself, Brouwer's fixed-point theorem guarantees at least one equilibrium λ^* and corresponding w^* (unique up to a scalar normalization).

Uniqueness: Two features rule out multiple equilibria.

(i) *Labor supply:* By the sign-switching property of F, the elasticity matrix

$$\Theta_{oo'} = \frac{\partial \ln L_o}{\partial \ln w_{o'}}$$

satisfies $\Theta_{oo} > 0$, $\Theta_{oo'} < 0$ for $o \neq o'$, and $\sum_{o'} \Theta_{oo'} = 0$. Thus, occupations are gross substitutes from the workers' perspective.

extreme value distributions. See Section C.1 for the complete proof.

[39] See Section C.3 for the proof that row sums equal zero using the homogeneity property of F.

(ii) *Labor demand:* From (A1), own-wage elasticities are negative ($\partial \ln w_o / \partial \ln L_o = -1/\sigma < 0$), while cross-elasticities are positive for $o \neq o'$ under $\sigma > 1$, implying that occupations are gross substitutes in production.

Taken together, excess demand in log-space has a Jacobian that is a *P*-matrix (positive diagonal dominance with gross-substitute sign pattern). By the Gale–Nikaidô global univalence theorem (or equivalently Kelso–Crawford/Gul–Stacchetti arguments for gross substitutes), the fixed point λ^* is unique, and so are relative wages w^* once a normalization is imposed.

Conclusion Under $\sigma > 1$ and the sign-switching (gross substitutes) property of F, a competitive equilibrium always exists and is unique in relative wages and employment shares.

□

A.4. Derivation of Wage Incidence in Proposition 2

Starting from the equilibrium conditions:

$$d \ln \boldsymbol{w} = \frac{1}{\sigma} d \ln y \cdot \mathbf{1} - \frac{1}{\sigma} d \ln \boldsymbol{\alpha} - \frac{1}{\sigma} d \ln \boldsymbol{L} \quad \text{(labor demand)}$$
$$d \ln \boldsymbol{L} = \Theta \cdot d \ln \boldsymbol{w} \quad \text{(labor supply)}$$

Substituting the labor supply response into the demand equation:

$$d \ln \boldsymbol{w} = \frac{1}{\sigma} d \ln y \cdot \mathbf{1} - \frac{1}{\sigma} d \ln \boldsymbol{\alpha} - \frac{1}{\sigma} \Theta \cdot d \ln \boldsymbol{w}$$
$$\left(\mathbf{I} + \frac{\Theta}{\sigma} \right) d \ln \boldsymbol{w} = \frac{1}{\sigma} d \ln y \cdot \mathbf{1} - \frac{1}{\sigma} d \ln \boldsymbol{\alpha}$$

Since $\sum_{o'} \Theta_{oo'} = 0$ for all o (see Appendix C.3), the matrix $(\mathbf{I} + \Theta/\sigma)$ is invertible. Solving for wages:

$$d \ln \boldsymbol{w} = \frac{1}{\sigma} d \ln y \cdot \mathbf{1} - \underbrace{\left(\mathbf{I} + \frac{\Theta}{\sigma} \right)^{-1}}_{\equiv \Delta} \cdot \frac{d \ln \boldsymbol{\alpha}}{\sigma}$$

This establishes equation (3) with the pass-through matrix $\Delta = (\mathbf{I} + \Theta/\sigma)^{-1}$.

A.5. Derivation of Mobility Gains

Consider a marginal worker initially in occupation o who transitions to occupation o' following the shock. Before the shock, this worker was indifferent between the two occupations:

$$\ln w_o + \ln \epsilon_o(i) = \ln w_{o'} + \ln \epsilon_{o'}(i)$$

After the shock, the worker strictly prefers o':

$$\ln w_o + d\ln w_o + \ln \epsilon_o(i) < \ln w_{o'} + d\ln w_{o'} + \ln \epsilon_{o'}(i)$$

The equivalent variation (EV) for this marginal switcher satisfies:

$$\ln w_o + d\ln w_o + \ln \epsilon_o(i) + \text{EV}(i) = \ln w_{o'} + d\ln w_{o'} + \ln \epsilon_{o'}(i)$$

Using the initial indifference condition:

$$\text{EV}(i) = d\ln w_{o'} - d\ln w_o$$

For small changes, the share of workers transitioning from o to o' when $d\ln w_{o'} > d\ln w_o$ is:

$$\mu_{oo'} = -\Theta_{oo'}(d\ln w_{o'} - d\ln w_o)$$

Note that $\Theta_{oo'} < 0$ for $o \neq o'$, so $\mu_{oo'} > 0$ when wages rise more in o'.

The average mobility gain for workers initially in occupation o is:

$$\begin{aligned}
\text{Mobility Gain}_o &= \sum_{o': d\ln w_{o'} > d\ln w_o} \mu_{oo'} \cdot \text{EV}_{oo'} \\
&= \sum_{o': d\ln w_{o'} > d\ln w_o} [-\Theta_{oo'}(d\ln w_{o'} - d\ln w_o)] \cdot (d\ln w_{o'} - d\ln w_o) \\
&= -\sum_{o'} \Theta_{oo'}(d\ln w_{o'} - d\ln w_o)^2 \cdot \mathbf{1}_{d\ln w_{o'} > d\ln w_o}
\end{aligned}$$

This establishes equation (5).

A.6. Proof of Proposition 4

We derive the spectral decomposition of wage incidence using the eigendecomposition $\Theta = U\Lambda V$, where $V = U^{-1}$.

Step 1: Decompose the technological shock. Since the eigenvectors $\{\boldsymbol{u}_n\}$ form a basis for $\mathbb{R}^O$, we can write:

$$\frac{d\ln \boldsymbol{\alpha}}{\sigma} = \sum_{n=1}^{O} b_n \boldsymbol{u}_n$$

where the coefficients are $b_n = \boldsymbol{v}_n' \cdot (d\ln \boldsymbol{\alpha}/\sigma)$ with $\boldsymbol{v}_n'$ being the n-th row of V.

Step 2: Apply the eigendecomposition to the pass-through matrix. The pass-through

matrix can be written as:

$$\Delta = \left(\mathbf{I} + \frac{\Theta}{\sigma}\right)^{-1} = \left(\mathbf{I} + \frac{U\Lambda V}{\sigma}\right)^{-1}$$
$$= U\left(\mathbf{I} + \frac{\Lambda}{\sigma}\right)^{-1} V = \sum_{n=1}^{O} \frac{1}{1+\lambda_n/\sigma} \boldsymbol{u}_n \boldsymbol{v}_n'$$

Step 3: Compute the wage response. Substituting into the wage incidence equation:

$$d\ln \boldsymbol{w} = \frac{d\ln y}{\sigma}\mathbf{1} - \Delta \cdot \frac{d\ln \boldsymbol{\alpha}}{\sigma}$$
$$= \frac{d\ln y}{\sigma}\mathbf{1} - \sum_{n=1}^{O} \frac{1}{1+\lambda_n/\sigma} \boldsymbol{u}_n \boldsymbol{v}_n' \cdot \left(\sum_{m=1}^{O} b_m \boldsymbol{u}_m\right)$$
$$= \frac{d\ln y}{\sigma}\mathbf{1} - \sum_{n=1}^{O} \frac{b_n}{1+\lambda_n/\sigma} \boldsymbol{u}_n$$

The last equality uses the orthogonality property $\boldsymbol{v}_n' \cdot \boldsymbol{u}_m = \delta_{nm}$.

This completes the proof, showing that each eigenshock $\boldsymbol{u}_n$ passes through to wages with a dampening factor $(1+\lambda_n/\sigma)^{-1}$.

A.7. Proof of Proposition 5

We derive the joint productivity distribution from the skill-specific distributions and the max operator.

Step 1: Skill-specific productivity. For each skill s, productivity follows a correlated Fréchet distribution:

$$\Pr[\epsilon_1^s(i) \le \epsilon_1^s, \ldots, \epsilon_O^s(i) \le \epsilon_O^s] = \exp\left[-\left(\sum_{o=1}^{O} (\epsilon_o^s)^{\frac{-\theta}{1-\rho_s}}\right)^{1-\rho_s}\right]$$

Step 2: Occupational productivity as maximum. Since $\epsilon_o(i) = \max_{s\in\mathcal{S}} A_o^s \cdot \epsilon_o^s(i)$, we have:

$$\Pr[\epsilon_1(i) \le \epsilon_1, \ldots, \epsilon_O(i) \le \epsilon_O] = \Pr\left[\epsilon_o^s(i) \le \frac{\epsilon_o}{A_o^s}, \forall o, \forall s\right]$$
$$= \prod_{s\in\mathcal{S}} \Pr\left[\epsilon_o^s(i) \le \frac{\epsilon_o}{A_o^s}, \forall o\right]$$

where the product follows from independence across skills.

Step 3: Substitute and simplify. Using the skill-specific distribution:

$$= \prod_{s \in \mathcal{S}} \exp\left[-\left(\sum_{o=1}^{O} (A_o^s)^{\frac{\theta}{1-\rho_s}} \epsilon_o^{\frac{-\theta}{1-\rho_s}} \right)^{1-\rho_s} \right]$$
$$= \exp\left[-\sum_{s \in \mathcal{S}} \left(\sum_{o=1}^{O} \left[(A_o^s)^{\theta} \epsilon_o^{-\theta} \right]^{\frac{1}{1-\rho_s}} \right)^{1-\rho_s} \right]$$

Step 4: Define aggregate parameters. Let $A_o = \sum_s (A_o^s)^{\theta}$ and $\omega_o^s = (A_o^s)^{\theta}/A_o$. Then:

$$(A_o^s)^{\theta} \epsilon_o^{-\theta} = \omega_o^s A_o \epsilon_o^{-\theta}$$

Substituting yields the correlation function:

$$F(x_1, \ldots, x_O) = \sum_{s \in \mathcal{S}} \left[\sum_{o=1}^{O} (\omega_o^s x_o)^{\frac{1}{1-\rho_s}} \right]^{1-\rho_s}$$

where $x_o = A_o \epsilon_o^{-\theta}$, completing the proof.

A.8. Proof of Proposition 6

We derive the employment shares and correlated elasticities under the CNCES structure.

Part 1: Employment Shares

From equation (A3), the employment share is:

$$\pi_o = \frac{A_o w_o^{\theta} F_o(x_1, \ldots, x_O)}{F(x_1, \ldots, x_O)}$$

For CNCES, $F(x_1, \ldots, x_O) = \sum_{s \in \mathcal{S}} G_s^{1-\rho_s}$ where $G_s = \sum_{o'} (\omega_{o'}^s x_{o'})^{\frac{1}{1-\rho_s}}$.
The partial derivative is:

$$F_o = \frac{\partial F}{\partial x_o} = \sum_{s \in \mathcal{S}} G_s^{-\rho_s} \omega_o^s (\omega_o^s x_o)^{\frac{\rho_s}{1-\rho_s}}$$

Therefore:

$$\pi_o = \frac{x_o F_o}{\sum_{o'} x_{o'} F_{o'}} = \sum_{s \in \mathcal{S}} \frac{(\omega_o^s x_o)^{\frac{1}{1-\rho_s}}}{G_s} \cdot \frac{G_s^{1-\rho_s}}{F}$$

$$= \sum_{s \in \mathcal{S}} \underbrace{\frac{(\omega_o^s A_o w_o^\theta)^{\frac{1}{1-\rho_s}}}{\sum_{o'} (\omega_{o'}^s A_{o'} w_{o'}^\theta)^{\frac{1}{1-\rho_s}}}}_{\pi_o^{s,W}} \cdot \underbrace{\frac{G_s^{1-\rho_s}}{\sum_{s'} G_{s'}^{1-\rho_{s'}}}}_{\pi^{s,B}}$$

This establishes equation (8) with $\pi_o^s = \pi_o^{s,W} \cdot \pi^{s,B}$.

Part 2: Correlated Elasticities

To derive equation (9), we need the second derivative:

$$F_{oo'} = \frac{\partial^2 F}{\partial x_o \partial x_{o'}} = -\sum_{s \in \mathcal{S}} \frac{\rho_s}{1-\rho_s} G_s^{-\rho_s - 1} \cdot \omega_o^s (\omega_o^s x_o)^{\frac{\rho_s}{1-\rho_s}} \cdot \omega_{o'}^s (\omega_{o'}^s x_{o'})^{\frac{\rho_s}{1-\rho_s}}$$

The ratio becomes:

$$\frac{x_{o'} F_{oo'}}{F_o} = -\sum_{s \in \mathcal{S}} \frac{\rho_s}{1-\rho_s} \cdot \underbrace{\frac{(\omega_{o'}^s x_{o'})^{\frac{1}{1-\rho_s}}}{G_s}}_{\mu_{o'}^s} \cdot \underbrace{\frac{G_s^{-\rho_s} \omega_o^s (\omega_o^s x_o)^{\frac{\rho_s}{1-\rho_s}}}{F_o}}_{\gamma_o^s}$$

Substituting $x_o = A_o w_o^\theta$ and noting that: - $\mu_{o'}^s = \pi_{o'}^{s,W}$ (within-skill share) - $\gamma_o^s = \pi_o^s / \pi_o$ (skill s's contribution to occupation o) - $\pi_o^s = \pi_o^{s,W} \cdot \pi^{s,B}$

We obtain:

$$\theta \frac{x_{o'} F_{oo'}}{F_o}\bigg|_{x_j = A_j w_j^\theta} = -\theta \sum_{s \in \mathcal{S}} \frac{\rho_s}{1-\rho_s} \cdot \pi_o^{s,W} \pi_{o'}^{s,W} \cdot \frac{\pi^{s,B}}{\pi_o}$$

This completes the proof of equation (9).

A.9. Proof of Proposition 7 (Hat Algebra)

The proof demonstrates how observed employment shares serve as sufficient statistics for predicting counterfactual changes without requiring wage or productivity levels.

Step 1: Express employment shares in terms of the correlation function.

Given wages $\boldsymbol{w}_t$ and group-specific productivity $\{A_t^g\}_{g \in G}$, employment shares are:

$$\pi_{o,t}^g = \frac{A_{o,t}^g w_{o,t}^\theta F_o(A_{1,t}^g w_{1,t}^\theta, \ldots, A_{O,t}^g w_{O,t}^\theta)}{F(A_{1,t}^g w_{1,t}^\theta, \ldots, A_{O,t}^g w_{O,t}^\theta)}$$

Step 2: Define correlation-adjusted shares.

Let the correlation-adjusted employment share be:

$$\tilde{\pi}^g_{o,t} = \frac{A^g_{o,t} w^\theta_{o,t}}{F(A^g_{1,t} w^\theta_{1,t}, \ldots, A^g_{O,t} w^\theta_{O,t})}$$

Since F_o is homogeneous of degree zero, we obtain:

$$\pi^g_{o,t} = \tilde{\pi}^g_{o,t} F_o(\tilde{\pi}^g_{1,t}, \ldots, \tilde{\pi}^g_{O,t})$$

This establishes a one-to-one mapping between observed shares $\{\pi^g_{o,t}\}$ and adjusted shares $\{\tilde{\pi}^g_{o,t}\}$.

Step 3: Derive the evolution of adjusted shares.

For wage changes from t to $t+1$, the ratio of adjusted shares is:

$$\frac{\tilde{\pi}^g_{o,t+1}}{\tilde{\pi}^g_{o,t}} = \frac{(w_{o,t+1}/w_{o,t})^\theta}{F(A^g_{1,t} w^\theta_{1,t+1}, \ldots, A^g_{O,t} w^\theta_{O,t+1}) / F(A^g_{1,t} w^\theta_{1,t}, \ldots, A^g_{O,t} w^\theta_{O,t})}$$

Using the homogeneity property of F, the denominator simplifies to:

$$\frac{F(A^g_{1,t} w^\theta_{1,t+1}, \ldots, A^g_{O,t} w^\theta_{O,t+1})}{F(A^g_{1,t} w^\theta_{1,t}, \ldots, A^g_{O,t} w^\theta_{O,t})} = F(\{\hat{w}^\theta_{o,t+1} \tilde{\pi}^g_{o,t}\}_{o \in O})$$

where $\hat{w}_{o,t+1} = w_{o,t+1}/w_{o,t}$ denotes the relative wage change.

Step 4: Obtain the counterfactual algorithm.

The adjusted shares evolve according to:

$$\tilde{\pi}^g_{o,t+1} = \frac{\tilde{\pi}^g_{o,t} \hat{w}^\theta_{o,t+1}}{F(\{\hat{w}^\theta_{o',t+1} \tilde{\pi}^g_{o',t}\}_{o' \in O})}$$

Finally, recover the counterfactual employment shares:

$$\pi^g_{o,t+1} = \tilde{\pi}^g_{o,t+1} F_o(\tilde{\pi}^g_{1,t+1}, \ldots, \tilde{\pi}^g_{O,t+1})$$

This completes the proof and provides an algorithm to compute counterfactual employment shares using only observed shares and relative wage changes, without requiring knowledge of productivity levels or absolute wages. □

A.10. Dynamic Model with Forward-Looking Workers

This appendix extends the static framework to incorporate forward-looking occupational choice with adjustment frictions. The dynamic model enables analysis of transition paths

and the timing of labor market responses to technological shocks.

A.11. Workers' Dynamic Problem

Setup. Consider a continuum of hand-to-mouth workers distributed across O occupations. Workers maximize expected lifetime utility over consumption $c_t(i)$ and labor effort $\ell_t(i)$:

$$U\left(\{c_t(i), \ell_t(i)\}_{t=0}^{\infty}\right) = \sum_{t=0}^{\infty} \beta^t [\ln c_t(i) - \ln \ell_t(i)]$$

where $\beta \in (0,1)$ is the discount factor.

Productivity draws. Each period, workers draw productivity vectors

$$\boldsymbol{\epsilon}_t(i) = (\epsilon_{1,t}(i), \ldots, \epsilon_{O,t}(i))$$

from the same multivariate Fréchet distribution as in the static model:

$$\Pr[\epsilon_{1,t}(i) \le \epsilon_1, \ldots, \epsilon_{O,t}(i) \le \epsilon_O] = \exp\left[-F(A_{1,t}\epsilon_1^{-\theta}, \ldots, A_{O,t}\epsilon_O^{-\theta})\right]$$

where the correlation function F embeds the CNCES structure:

$$F(x_1, \ldots, x_O) = \sum_{s=1}^{S} \left[\sum_{o=1}^{O} (\omega_{so} x_o)^{\frac{1}{1-\rho_s}}\right]^{1-\rho_s}$$

Occupational choice with transition costs. After observing $\boldsymbol{\epsilon}_t(i)$, workers choose occupations subject to transition costs $\tau_{oo'} \ge 0$ (measured in utility units). The instantaneous utility from occupation o' is:

$$u_t(i) = \ln w_{o',t} + \kappa \ln \epsilon_{o',t}(i)$$

where $\kappa > 0$ governs the short-run labor supply elasticity, capturing sluggish adjustment relative to the static model's long-run elasticity θ.

Value function. The Bellman equation for a worker in occupation o with productivity $\boldsymbol{\epsilon}_t$ is:

$$v_{o,t}(\boldsymbol{\epsilon}_t) = \max_{o'} \left\{\ln w_{o',t} + \kappa \ln \epsilon_{o',t} + \beta V_{o',t+1} - \tau_{oo'}\right\}$$

where $V_{o',t+1} = \mathbb{E}_{\boldsymbol{\epsilon}}[v_{o',t+1}(\boldsymbol{\epsilon})]$ is the expected continuation value.

Aggregation. Define the inclusive value:

$$Z_{oo',t} = \exp(\beta V_{o',t+1} + \ln w_{o',t} - \tau_{oo'})$$

Given the Fréchet structure, the expected value simplifies to:

$$V_{o,t} = \ln\left[F(A_{1,t}Z_{o1,t}^{\theta/\kappa}, \ldots, A_{O,t}Z_{oO,t}^{\theta/\kappa})^{\kappa/\theta}\right] + \bar{\gamma}\frac{\kappa}{\theta}$$

where $\bar{\gamma}$ is the Euler-Mascheroni constant.

This formulation nests the static model when $\kappa = \theta$ (no adjustment frictions) and generates gradual transitions when $\kappa < \theta$ (costly adjustment). The correlation structure F preserves the DIDES property: workers transition more easily between skill-similar occupations, but adjustment slows when technological shocks cluster within skill domains.

A.12. Occupation Switching Probabilities

This section derives the transition probabilities between occupations, showing how the correlation structure generates realistic mobility patterns.

Switching probability. The probability that a worker in occupation o switches to o' at time t is:

$$\mu_{oo',t} = \Pr\left[Z_{oo',t}\epsilon_{o',t}^{\kappa} \geq \max_{o''} Z_{oo'',t}\epsilon_{o'',t}^{\kappa}\right]$$

Using the properties of the multivariate Fréchet distribution (see Section C.1), this probability becomes:

$$\mu_{oo',t} = \frac{A_{o',t}Z_{oo',t}^{\theta/\kappa}F_{o'}(A_{1,t}Z_{o1,t}^{\theta/\kappa}, \ldots, A_{O,t}Z_{oO,t}^{\theta/\kappa})}{F(A_{1,t}Z_{o1,t}^{\theta/\kappa}, \ldots, A_{O,t}Z_{oO,t}^{\theta/\kappa})}$$

where $F_{o'} = \partial F/\partial x_{o'}$ denotes the partial derivative.

Correlation-adjusted transition rates. Define the correlation-adjusted transition probability:

$$\tilde{\mu}_{oo',t} = \frac{A_{o',t}Z_{oo',t}^{\theta/\kappa}}{F(A_{1,t}Z_{o1,t}^{\theta/\kappa}, \ldots, A_{O,t}Z_{oO,t}^{\theta/\kappa})}$$

This adjustment isolates the role of correlation from the baseline substitution effect. The observed and adjusted probabilities are related by:

$$\mu_{oo',t} = \tilde{\mu}_{oo',t}F_{o'}(\tilde{\mu}_{o1,t}, \ldots, \tilde{\mu}_{oO,t})$$

This establishes a one-to-one mapping between observed transitions $\{\mu_{oo',t}\}$ and adjusted rates $\{\tilde{\mu}_{oo',t}\}$.

Euler equation for mobility. The evolution of adjusted transition rates satisfies:

$$\ln\frac{\tilde{\mu}_{oo',t}}{\tilde{\mu}_{oo,t}} = \frac{\theta}{\kappa}\ln\frac{w_{o',t}}{w_{o,t}} + \beta\ln\frac{\tilde{\mu}_{oo',t+1}}{\tilde{\mu}_{o'o',t+1}} + (\beta - 1)\tau_{oo'}$$

This Euler equation shows that relative transition rates depend on three factors:

- Current wage differentials (scaled by θ/κ, the short-run elasticity)
- Future option values (captured by next period's staying probabilities)
- Transition costs (discounted by $\beta - 1 < 0$)

The correlation-adjusted formulation enables estimation of θ/κ from observed transitions while accounting for the skill-based clustering that constrains mobility between distant occupations.

A.13. Static Production Equilibrium

This section characterizes the production side of the economy, which remains static within each period while labor allocations adjust dynamically across periods.

Production technology. Taking task assignments as given, output aggregates capital and labor across occupations via CES technology:

$$Y_t = \left[(s_t^k)^{\frac{1}{\sigma}} (y_t^k)^{\frac{\sigma-1}{\sigma}} + \sum_{o=1}^{O} (s_{o,t}^\ell)^{\frac{1}{\sigma}} (y_{o,t}^\ell)^{\frac{\sigma-1}{\sigma}} \right]^{\frac{\sigma}{\sigma-1}}$$

where:

- $y_t^k = a_t^k k_t$ is effective capital input with productivity a_t^k
- $y_{o,t}^\ell = L_{o,t}$ is labor input in occupation o
- $\sigma > 0$ is the elasticity of substitution between inputs
- s_t^k and $s_{o,t}^\ell$ are time-varying task shares for capital and labor

Equilibrium with endogenous capital. Capital adjusts freely within each period. Under the assumption $s_t^k (a_t^k)^{\sigma-1} < 1$ (ensuring finite output), optimal capital demand is:

$$k_t = s_t^k (a_t^k)^\sigma Y_t$$

Substituting this into the production function yields the reduced-form output:

$$Y_t = \left[\frac{\sum_{o=1}^{O} (s_{o,t}^\ell)^{\frac{1}{\sigma}} L_{o,t}^{\frac{\sigma-1}{\sigma}}}{1 - s_t^k (a_t^k)^{\sigma-1}} \right]^{\frac{\sigma}{\sigma-1}}$$

Wage determination. Competitive labor markets equate wages to marginal products:

$$w_{o,t} = \frac{\partial Y_t}{\partial L_{o,t}} = Y_t^{\frac{1}{\sigma}} (s_{o,t}^\ell)^{\frac{1}{\sigma}} L_{o,t}^{-\frac{1}{\sigma}}$$

The task shares $\{s_{o,t}^\ell\}$ capture the distributional effects of technology: when automation or AI displaces labor from tasks in occupation o, the corresponding $s_{o,t}^\ell$ declines, reducing

wages even as aggregate productivity may rise through lower production costs.

A.14. Dynamic Equilibrium

This section defines the dynamic equilibrium, accounting for data limitations and characterizing the conditions for market clearing across time.

Measurement reconciliation. The retrospective design of the March CPS creates a discrepancy between measured job flows and observed employment levels. We account for this by augmenting the employment evolution equation:

$$L_{o,t} = \sum_{o'=1}^{O} \mu_{o'o,t} L_{o',t-1} + \Delta L_{o,t}$$

where $\Delta L_{o,t}$ represents exogenous net inflows/outflows satisfying $\sum_o L_{o,t} = 1$ (normalization) and $\sum_o \Delta L_{o,t} = 0$ (no aggregate employment change).

Model primitives. The economy is characterized by:

- Time-varying fundamentals: $\boldsymbol{A}_t = \{A_{o,t}\}$ (productivity), $\boldsymbol{s}_t = \{s^{\ell}_{o,t}\}$ (task shares), a^k_t (capital productivity)
- Structural parameters: $\tau_{oo'}$ (transition costs), ω_{os} (skill weights), σ (demand elasticity), θ (dispersion), ρ_s (skill correlation), κ (short-run elasticity), β (discount factor)

Definition (Dynamic Equilibrium). A dynamic equilibrium is a sequence $\{\boldsymbol{L}_t, \boldsymbol{w}_t, \mu_t, V_t\}_{t=0}^{\infty}$ satisfying:

a. *Production equilibrium:* Wages equal marginal products and output clears markets:

$$w_{o,t} = Y_t^{\frac{1}{\sigma}} (s^{\ell}_{o,t})^{\frac{1}{\sigma}} L_{o,t}^{-\frac{1}{\sigma}}$$

$$Y_t = \left[\frac{\sum_o (s^{\ell}_{o,t})^{\frac{1}{\sigma}} L_{o,t}^{\frac{\sigma-1}{\sigma}}}{1 - s^k_t (a^k_t)^{\sigma-1}} \right]^{\frac{\sigma}{\sigma-1}}$$

b. *Optimal expectations:* Workers correctly anticipate future values:

$$V_{o,t} = \ln \left[F(A_{1,t} Z_{o1,t}^{\theta/\kappa}, \ldots, A_{O,t} Z_{oO,t}^{\theta/\kappa})^{\kappa/\theta} \right] + \bar{\gamma} \frac{\kappa}{\theta}$$

c. *Optimal mobility:* Transition probabilities satisfy workers' optimization:

$$\mu_{oo',t} = \frac{A_{o',t} Z_{oo',t}^{\theta/\kappa} F_{o'}(A_{1,t} Z_{o1,t}^{\theta/\kappa}, \ldots, A_{O,t} Z_{oO,t}^{\theta/\kappa})}{F(A_{1,t} Z_{o1,t}^{\theta/\kappa}, \ldots, A_{O,t} Z_{oO,t}^{\theta/\kappa})}$$

d. *Labor market clearing:* Employment evolves according to transitions:

$$L_{o,t} = \sum_{o'} \mu_{o'o,t} L_{o',t-1} + \Delta L_{o,t}$$

This equilibrium preserves the DIDES structure: technological shocks that cluster in skill space generate limited mobility (through μ) and force adjustment through wages, creating persistent inequality during transitions.

A.15. System in Changes

This section expresses the dynamic equilibrium in growth rates, facilitating the analysis of transition paths and steady-state convergence.

Notation. Define the growth factor $\dot{x}_{t+1} = x_{t+1}/x_t$ for any variable x. For utility, define $u_{o,t} = \exp(V_{o,t})$ to work with levels rather than logs.

Production in changes. Log-differentiating the wage equation yields:

$$\sigma \ln \dot{w}_{o,t+1} + \ln \dot{L}_{o,t+1} = \ln \dot{Y}_{t+1} + \ln \dot{s}^{\ell}_{o,t+1}$$

This links wage growth to changes in aggregate output, task shares, and employment.

Dynamic system in growth rates. The evolution of correlation-adjusted transition probabilities and expected utilities can be expressed as:

$$\frac{\tilde{\mu}_{oo',t}}{\tilde{\mu}_{oo',t-1}} = \frac{\dot{A}_{o',t} \dot{u}^{\beta\theta/\kappa}_{o',t+1} \dot{w}^{\theta/\kappa}_{o',t}}{F(\{\tilde{\mu}_{oo'',t-1} \dot{A}_{o'',t} \dot{u}^{\beta\theta/\kappa}_{o'',t+1} \dot{w}^{\theta/\kappa}_{o'',t}\}_{o''=1}^{O})} \tag{A5}$$

$$\dot{u}_{o,t+1} = F(\{\tilde{\mu}_{oo'',t} \dot{A}_{o'',t+1} \dot{u}^{\beta\theta/\kappa}_{o'',t+2} \dot{w}^{\theta/\kappa}_{o'',t+1}\}_{o''=1}^{O})^{\kappa/\theta} \tag{A6}$$

The observed transition probabilities follow:

$$\mu_{oo',t} = \tilde{\mu}_{oo',t} F_{o'}(\tilde{\mu}_{o1,t}, \ldots, \tilde{\mu}_{oO,t})$$

with employment evolving according to the transition matrix and exogenous flows.

Interpretation. Equations (A5)–(A6) form a forward-looking system where current mobility depends on future expected utilities. The correlation function F preserves the DIDES structure: when technological shocks cluster (affecting the growth rates $\dot{A}_{o,t}$ and $\dot{s}^{\ell}_{o,t}$ in skill-similar occupations), the denominator in (A5) limits relative mobility adjustments, forcing wage changes to absorb the shock.

See Appendix C.5 for detailed derivations.

A.16. Dynamic Hat Algebra

This section extends the hat algebra to dynamic settings, enabling counterfactual analysis of transition paths under alternative technological scenarios.

Counterfactual notation. For counterfactual fundamentals $\{\hat{\boldsymbol{A}}_t, \hat{\boldsymbol{s}}_t, \hat{a}_t^k\}$, define:

- $\hat{x}_t = \dot{x}'_t/\dot{x}_t$: ratio of counterfactual to baseline growth rates
- $\dot{x}'_t = x'_t/x'_{t-1}$: counterfactual growth rate

Counterfactual equilibrium. The wage response follows from production equilibrium:

$$\hat{w}_{o,t+1} = \left(\frac{\hat{Y}_{t+1} \hat{s}^{\ell}_{o,t+1}}{\hat{L}_{o,t+1}} \right)^{\frac{1}{\sigma}}$$

Counterfactual transition probabilities evolve recursively:

$$\tilde{\mu}'_{oo',t} = \frac{\tilde{\mu}'_{oo',t-1} \dot{\tilde{\mu}}_{oo',t} \hat{A}_{o',t} \hat{u}^{\beta\theta/\kappa}_{o',t+1} \hat{w}^{\theta/\kappa}_{o',t}}{F(\{\tilde{\mu}'_{oo'',t-1} \dot{\tilde{\mu}}_{oo'',t} \hat{A}_{o'',t} \hat{u}^{\beta\theta/\kappa}_{o'',t+1} \hat{w}^{\theta/\kappa}_{o'',t}\}_{o''=1}^{O})}$$

Expected utilities adjust according to:

$$\hat{u}_{o,t+1} = F(\{\tilde{\mu}'_{oo'',t} \dot{\tilde{\mu}}_{oo'',t+1} \hat{A}_{o'',t+1} \hat{u}^{\beta\theta/\kappa}_{o'',t+2} \hat{w}^{\theta/\kappa}_{o'',t+1}\}_{o''=1}^{O})^{\kappa/\theta}$$

with observed transitions $\mu'_{oo',t} = \tilde{\mu}'_{oo',t} F_{o'}(\tilde{\mu}'_{o1,t}, \ldots, \tilde{\mu}'_{oO,t})$ and employment evolution:

$$L'_{o,t} = \sum_{o'} \mu'_{o'o,t} L'_{o',t-1} + \Delta L_{o,t}$$

A.16.1. Initial Conditions

For unexpected shocks at $t = 1$ (with baseline conditions at $t = 0$: $\hat{u}_{o,0} = 1$, $\mu'_{oo',0} = \mu_{oo',0}$, $L'_{o,0} = L_{o,0}$):

$$\tilde{\mu}'_{oo',1} = \frac{\vartheta_{oo',1} \hat{A}_{o',1} \hat{w}^{\theta/\kappa}_{o',1} \hat{u}^{\beta\theta/\kappa}_{o',2}}{F(\{\vartheta_{oo'',1} \hat{A}_{o'',1} \hat{w}^{\theta/\kappa}_{o'',1} \hat{u}^{\beta\theta/\kappa}_{o'',2}\}_{o''=1}^{O})}$$

$$\hat{u}_{o,1} = F(\{\vartheta_{oo',1} \hat{A}_{o',1} \hat{w}^{\theta/\kappa}_{o',1} \hat{u}^{\beta\theta/\kappa}_{o',2}\}_{o'=1}^{O})^{\kappa/\theta}$$

where $\vartheta_{oo',1} = \tilde{\mu}_{oo',1} \hat{u}^{\beta\theta/\kappa}_{o',1}$ captures the initial adjustment.

See Appendix C.5 for detailed derivations.

A.17. Welfare Metrics

This section derives welfare measures that account for both wage changes and mobility gains through the lens of staying probabilities.

Value function decomposition. The recursive value function can be rewritten to highlight the role of staying probabilities:

$$\begin{aligned} V_{o,t} &= \ln w_{o,t} + \beta V_{o,t+1} + \frac{\kappa}{\theta} \ln \left(\frac{F(A_{1,t} Z_{o1,t}^{\theta/\kappa}, \ldots, A_{O,t} Z_{oO,t}^{\theta/\kappa})}{\exp(\beta V_{o,t+1} + \ln w_{o,t})^{\theta/\kappa}} \right) + \bar{\gamma} \frac{\kappa}{\theta} \\ &= \ln(A_{o,t}^{\kappa/\theta} w_{o,t}) + \beta V_{o,t+1} + \frac{\kappa}{\theta} \ln \left(\frac{1}{\tilde{\mu}_{oo,t}} \right) + \bar{\gamma} \frac{\kappa}{\theta} \end{aligned}$$

Iterating forward yields:

$$V_{o,t} = \sum_{s=t}^{\infty} \beta^{s-t} \ln \left[\left(\frac{A_{o,s}}{\tilde{\mu}_{oo,s}} \right)^{\kappa/\theta} w_{o,s} \right] + \frac{\bar{\gamma}\kappa}{\theta(1-\beta)}$$

Equivalent variation. The welfare change from baseline to counterfactual, measured as equivalent variation $\delta_{o,t}$, satisfies:

$$V'_{o,t} = V_{o,t} + \frac{\ln \delta_{o,t}}{1-\beta}$$

This yields:

$$\delta_{o,t} = (1-\beta) \sum_{s=t}^{\infty} \beta^{s-t} \ln \left[\frac{w'_{o,s}}{w_{o,s}} \left(\frac{A'_{o,s}/\tilde{\mu}'_{oo,s}}{A_{o,s}/\tilde{\mu}_{oo,s}} \right)^{\kappa/\theta} \right]$$

Hat algebra representation. Expressed in terms of counterfactual changes:

$$\delta_{o,t} = (1-\beta) \sum_{s=t}^{\infty} \beta^{s-t} \ln \left(\hat{w}_{o,s} \cdot \hat{\tilde{\mu}}_{oo,s}^{-\kappa/\theta} \right)$$

The term $\hat{\tilde{\mu}}_{oo,s}^{-\kappa/\theta}$ captures mobility gains: when technological shocks reduce staying probabilities (workers transition more), this provides partial welfare compensation for wage losses. The

Appendix B. Additional Empirical Results

B.1. Occupation Classification

Our analyses require constructing occupation-level panels for the period 1980–2018. To this end, following Autor et al. (2024), we use a consistent occupation coding scheme (occ1990dd), originally developed by Dorn (2009) and updated through 2018, which yields a balanced panel of 306 consistent, 3-digit occupations. This detailed classification preserves crucial occupational variation and accurately captures the structure of the labor market over the period.

B.2. Occupational Skill Requirements

This appendix details the construction of occupational skill requirements $\{\omega_o^s\}$ from O*NET data, following the methodology of Lise and Postel-Vinay (2020).

Data Source. O*NET version 28.2 provides comprehensive occupational information for 873 occupations. The database contains 277 descriptors organized into nine categories, with ratings derived from two sources: (i) worker surveys for occupation-specific assessments, and (ii) occupational analyst surveys for standardized evaluations. We retain 218 descriptors from five categories—skills, abilities, knowledge, work activities, and work context—as these directly correspond to the theoretical concept of skill requirements. The remaining categories (job interests, work values, work styles, and experience/education requirements) are excluded as they reflect preferences or credentials rather than skill utilization.

Dimension Reduction. Following Lise and Postel-Vinay (2020), we apply PCA with exclusion restrictions to extract three interpretable skill dimensions:

a. **Cognitive skills**: Identified through the mathematics knowledge descriptor
b. **Manual skills**: Identified through the mechanical knowledge descriptor
c. **Interpersonal skills**: Identified through the social perceptiveness descriptor

These exclusion restrictions ensure that each principal component has a clear economic interpretation while maintaining orthogonality—a property that aligns with the model's assumption of independent skill-specific productivity draws. The first three components explain 58% of total variation (cognitive: 35.6%, manual: 15.2%, interpersonal: 6.9%), with the dominance of cognitive and manual dimensions reflecting their primary role in occupational differentiation.

Construction of Skill Requirements. The raw principal component loadings contain negative values, violating the theoretical requirement that $\omega_o^s \geq 0$. We address this through a

two-step procedure:

Step 1: Apply linear transformations to map each occupation's loading on principal component s to the unit interval:

$$r_o^s = \frac{PC_o^s - \min_{o'} PC_{o'}^s}{\max_{o'} PC_{o'}^s - \min_{o'} PC_{o'}^s}$$

This preserves relative distances between occupations in each skill dimension—crucial for maintaining the distance-dependent substitution structure.

Step 2: Convert to variance-weighted shares to obtain the final skill requirements:

$$\omega_o^s = \frac{r_o^s \times \text{Var}_s}{\sum_{s' \in \mathcal{S}} r_o^{s'} \times \text{Var}_{s'}}$$

where Var_s is the proportion of variance explained by component s. This weighting ensures that skills contributing more to occupational variation receive proportionally higher weight in the correlation function F, consistent with their greater role in determining substitution patterns.

Mapping to Occupation Codes. The final step maps O*NET occupation codes to the consistent occ1990dd classification used throughout the analysis, enabling linkage with employment and wage data. The crosswalk covers 306 three-digit occupations, preserving granular variation while maintaining temporal consistency from 1980-2018.

B.3. Measures of Automation and AI Exposure

Existing Measures and Task Evaluation. The literature has developed several measures of occupational exposure to automation, each capturing different aspects of technological vulnerability. These include occupational routine task intensity (Autor and Dorn 2013), the decline in labor share due to the adoption of industrial robots, machines, and software (Acemoglu and Restrepo 2022), and occupational exposure to automation patents (Autor et al. 2024). These measures share a common theoretical foundation rooted in Polanyi's Paradox (Autor 2015): jobs codifiable into well-defined rules or algorithms are more susceptible to automation and are typically classified as routine. Consistent with this framework, numerous studies document that occupations with higher automation exposure have experienced slower wage growth over the past four decades.

In contrast to automation, measuring occupational exposure to artificial intelligence presents unique challenges, as its full economic impact remains unrealized. To address this challenge, recent research has leveraged large language models (LLMs) as predictive tools for assessing economic outcomes. Eloundou et al. (2024) pioneered this approach by evaluating occupational exposure to LLMs through a dual methodology: human annotators

and GPT-4 classified O*NET tasks using an exposure rubric to determine whether LLMs can perform or assist with specific tasks. Their findings highlight the potential of LLMs as general-purpose technologies.

Subsequent validation studies strengthen confidence in this approach. Bick, Blandin, and Deming (2024) and Tomlinson et al. (2025) demonstrate high correlations between LLM task evaluations and ex-post real-world generative AI adoption patterns. Most compelling, Brynjolfsson, Chandar, and Chen (2025) provide causal evidence that LLM exposure measures predict actual labor market outcomes: using high-frequency administrative payroll data, they document that early-career workers (ages 22-25) in the most AI-exposed occupations have experienced a 13% relative decline in employment since widespread AI adoption, with effects concentrated in occupations where AI automates rather than augments human labor.

Our Methodology: ChatGPT Task Evaluation. Building on this validated literature, we adopt a streamlined yet comparable approach leveraging ChatGPT to directly estimate AI and automation exposure. Our methodology employs the O*NET database, which provides detailed descriptions of 19,200 tasks across 862 occupations. Each task undergoes two distinct assessments:

- **AI Exposure**: We query ChatGPT: "Can generative AI (e.g., large language models like ChatGPT) potentially perform this task without human intervention?" This assessment captures the extent to which occupations are exposed to AI-driven technologies.
- **Automation Exposure**: We query ChatGPT: "Can industrial robots, machines, and computers (no AI capability) perform this task without human intervention?" This distinguishes tasks automatable using conventional, rule-based systems from those requiring advanced AI capabilities.

Based on these evaluations, ChatGPT estimates that approximately 6,000 tasks (roughly one-third of the total) can be performed by AI without human intervention—a scale comparable to traditional automation technologies. This classification provides a granular perspective on the differential impacts of AI versus traditional automation across occupations. We then calculate the share of automatable or AI-exposed tasks within each occupation to construct our exposure measures.

Validation Against Existing Measures. To validate our approach, we compare our ChatGPT-based measures with established metrics in the literature. Figure B1 demonstrates that our occupational exposure to generative AI correlates strongly with Eloundou et al. (2024)'s measure, yielding a correlation coefficient of 0.825. This high correlation validates our streamlined methodology while confirming the robustness of LLM-based evaluation approaches.

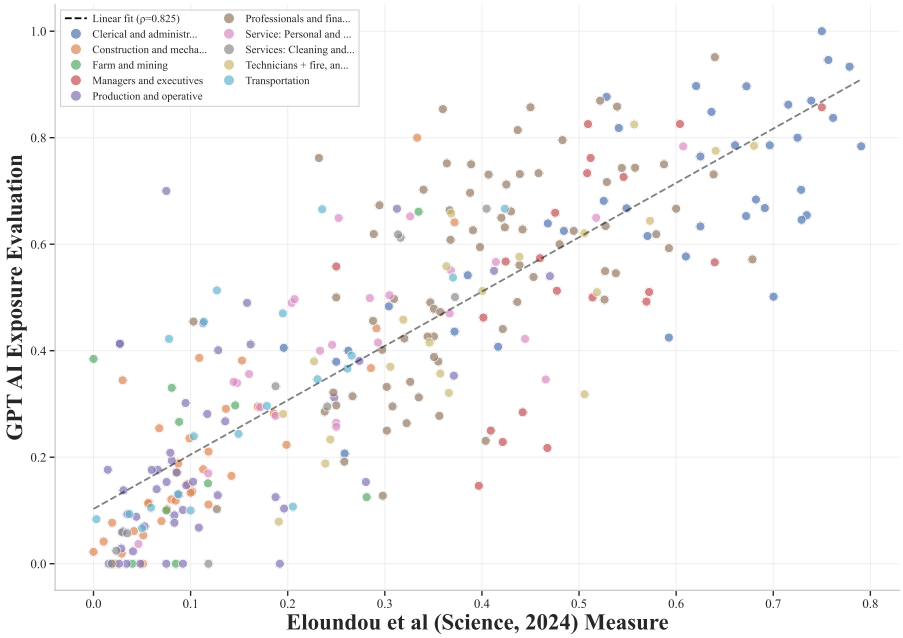

FIGURE B1. Comparison of AI Exposure Measures

This figure compares our ChatGPT AI evaluation scores (y-axis) with the science-based measure from Eloundou et al. (2024) (x-axis). Points represent occupations colored by broad occupational categories. The dashed line shows the linear fit with correlation coefficient ρ = 0.825. The strong positive relationship validates our ChatGPT evaluation methodology against established measures in the literature.

Figure B2 further validates our automation exposure measure by comparing ChatGPT's estimates with existing metrics. Panels (a) and (b) compare our estimates with the automation exposure measure from Acemoglu and Restrepo (2022). Since their measure operates at the demographic-age-education group level rather than the occupational level, we plot exposure against log median wage in 1980. The striking similarity of the two distributions across income levels confirms the validity of our approach. Panel (c) demonstrates a strong correlation between our measure and occupational routine task intensity, while Panel (d) reveals consistent patterns with exposure to automation patents from Autor et al. (2024).

These validation exercises demonstrate that our ChatGPT-based methodology produces measures highly consistent with established approaches while offering the advantage of direct, task-level evaluation for both automation and AI exposure. This validation is crucial for our subsequent analysis of how technological clustering in skill space shapes labor market incidence.

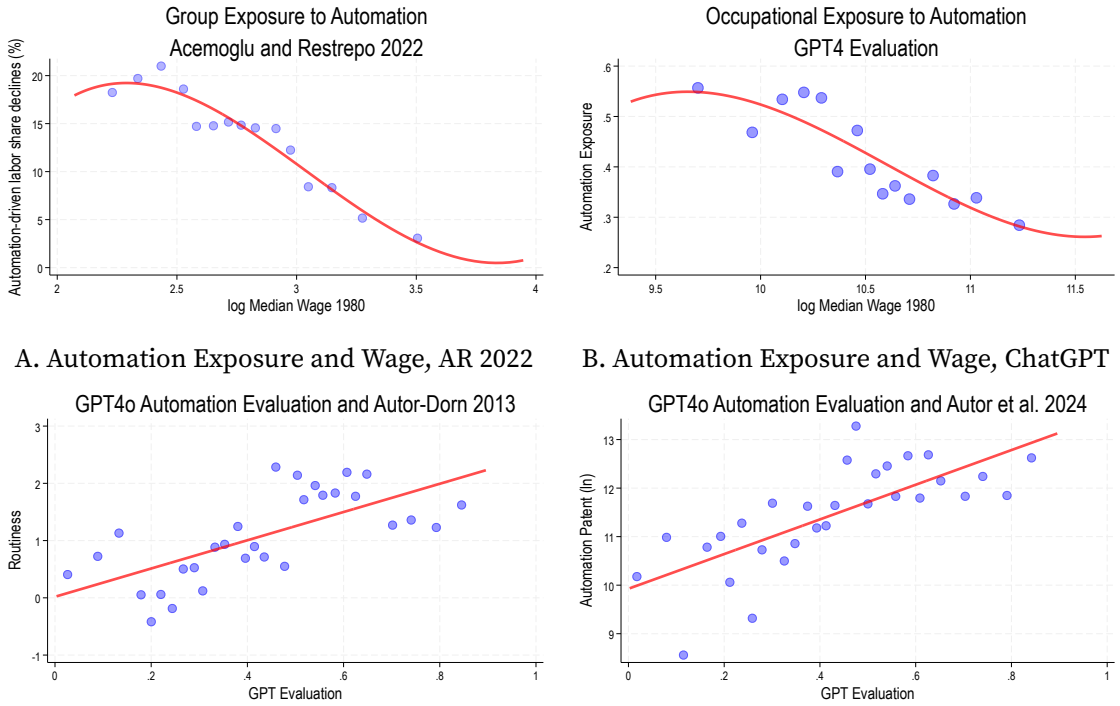

A. Automation Exposure and Wage, AR 2022

B. Automation Exposure and Wage, ChatGPT

C. Routine Task Intensity

D. Automation Patent Exposure

FIGURE B2. Validation of Automation Exposure Measures

This figure compares automation exposure as evaluated by ChatGPT with existing measures using binscatter plots. Panel (a) shows the decline in labor share due to automation from Acemoglu and Restrepo (2022), Panel (b) presents our ChatGPT estimates, Panel (c) compares with routine task intensity from Autor and Dorn (2013), and Panel (d) validates against automation patent exposure from Autor et al. (2024). The consistent patterns across all measures validate our ChatGPT evaluation approach.

B.4. Technological Exposure across Inter-personal Dimension

Figure B3 illustrates how occupational exposure to automation and AI varies with interpersonal skill requirements. Panel (a) shows that occupations requiring greater interpersonal skills tend to be less exposed to automation, aligning with the intuition that social and emotional intelligence—often critical in managerial, negotiation, and caregiving roles—are difficult to codify into rule-based processes. In contrast, Panel (b) reveals that occupations with higher interpersonal skill requirements tend to be more exposed to AI, though with greater variance. This noisier relationship suggests that while AI can assist or complement interpersonal tasks (e.g., customer support or education), full automation remains limited by the complexity of human interaction.

These findings reinforce the distinct nature of AI and automation risks: whereas automation displaces predictable, rule-based tasks, AI is more likely to augment or replace cognitive tasks, including those requiring some degree of human interaction. However, interpersonal-intensive occupations—such as psychologists, teachers, and business exec-

utives—still rely on empathy, persuasion, and social nuance, which remain challenging for AI to fully replicate.

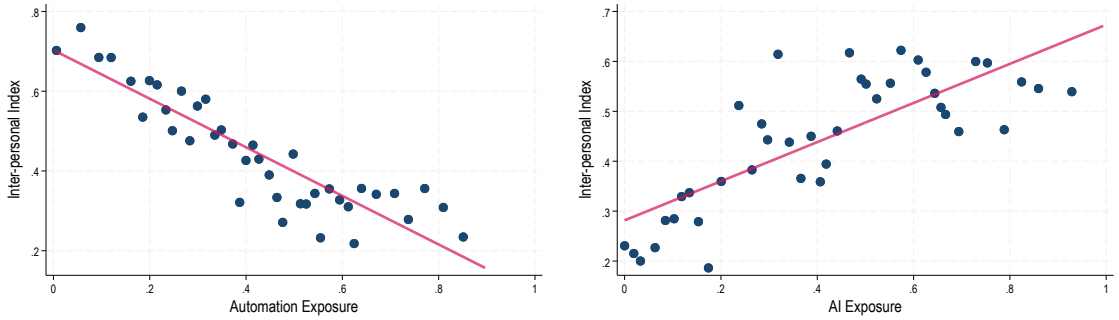

A. Interpersonal vs. Automation Exposure B. Interpersonal vs. AI Exposure

FIGURE B3. Technological Exposures across Interpersonal Skills

This figure illustrates the relationship between occupational interpersonal skill requirements and exposure to automation (Panel (a)) and AI (Panel (b)).

B.5. Wage and Employment Effects of Automation

This section provides additional details on the wage and employment effects of automation exposure. The Panel Study of Income Dynamics (PSID) is a widely used longitudinal dataset that has tracked nearly 9,200 U.S. families since 1968. We leverage its panel structure to estimate relative wage trends by occupation while controlling for selection effects.

Since the main specifications have already been discussed, we now present additional results in Figure B4, which examines wage effects by gender and under different control specifications. Panel A reports the wage effects of automation separately for men and women, showing that the results are nearly identical, with no statistically significant differences. Panel B introduces additional controls, with the blue line accounting for age and age^2 for the blue line and allows for changing return to education for the green line, while the green line further allows for a changing return to education. The results suggest that changes in the return to education explain about a quarter of the wage effects attributed to automation.

However, when estimating elasticities, we prefer the main specification without controlling for changes in the return to education. From a long-run perspective, new workers may adjust their educational and occupational choices in response to shifts in the skill premium.

We now present additional results on the heterogeneous employment effects of automation across demographic groups, which are used to estimate correlation structures. Panel A of Figure B5 displays the average change in log employment shares between 1980 and 2010 by gender for white workers, while Panel B presents the corresponding

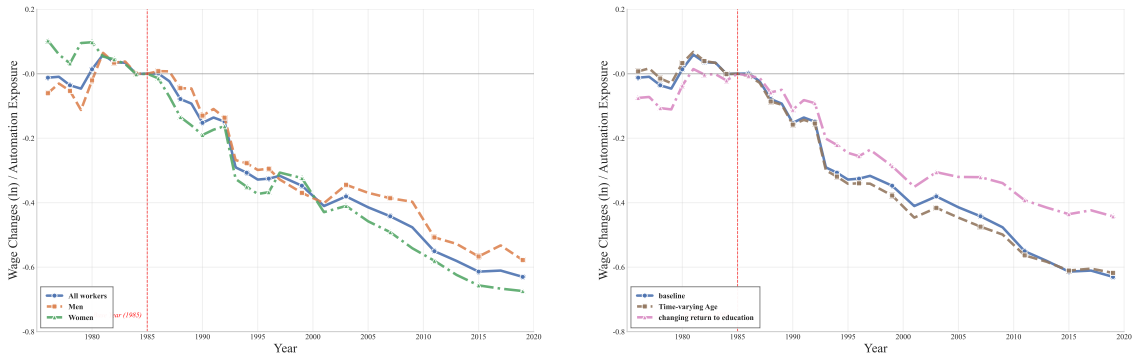

A. Wage Effects by Gender B. Additional Controls

FIGURE B4. Effects of Automation on Wages

Notes: Panel A presents the wage effects of automation separately for men and women, showing no statistically significant differences. Panel B introduces additional controls, where the blue line includes age and age^2, and the green line further accounts for a changing return to education. The latter explains approximately 25% of the wage effects attributed to automation.

employment effects for Black workers. The results indicate that white men are the least responsive to automation. Based on the data, this group was predominantly employed in occupations requiring more manual skills, which, as shown in our estimation results, are less portable across occupations. This pattern is reflected in our estimation procedure, which captures the variation in occupational transitions. As a result, the estimated correlation parameter for manual skills, ρ_{Man}, is relatively small, indicating lower substitutability of manual-intensive jobs.

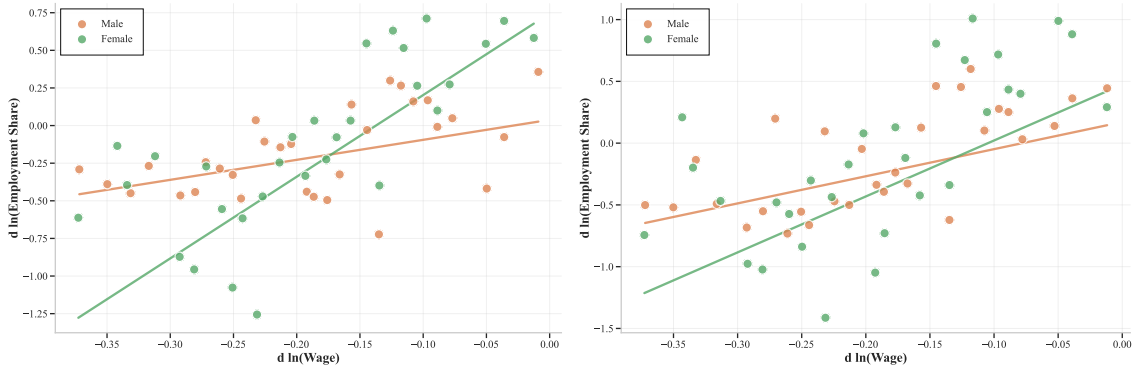

A. White Workers B. Black Workers

FIGURE B5. Heterogeneous Employment Effects by Demographic Groups

Notes: Panel A shows the employment effects of automation for white workers by gender, while Panel B presents the results for Black workers.

The PPML estimator jointly incorporates changes in the employment distribution, naturally weighting employment shares in the estimation process.

B.6. Alternative Nested CES Specifications and Model Comparison

This section demonstrates why standard Nested CES specifications fail to capture realistic substitution patterns, validating our CNCES framework's flexible skill-based approach.

Nested CES Framework. Standard Nested CES partitions occupations into mutually exclusive nests $\mathcal{O} = \bigcup_{n=1}^{N} \mathcal{N}_n$ with $\mathcal{N}_i \cap \mathcal{N}_j = \varnothing$. This generates within-nest elasticity $\theta/(1-\rho_n)$ and cross-nest elasticity θ, assuming each occupation belongs to exactly one nest.[40]

Estimation Results. Table B1 presents PPML estimates for two standard nesting structures using our 1980–2000 automation data.

TABLE B1. Nested CES Estimation Results

	Occupation Categories			**Skill Intensity**		
θ (Cross-nest)	2.67 (0.31)			2.05 (0.28)		
Nest	Low-skill	High-skill	Manuf.	Cognitive	Manual	Interpers.
ρ_n (Within-nest)	0.26 (0.18)	0.00 (–)	0.00 (–)	0.30 (0.15)	0.00 (–)	0.45 (0.20)
Within-nest elasticity	3.61	2.67	2.67	2.93	2.05	3.73

Standard errors in parentheses. Dashes indicate parameters constrained to zero.

Three patterns emerge. First, most within-nest correlations ρ_n are statistically zero: occupations within predefined categories are no closer substitutes than the cross-nest average. Second, cross-nest elasticities (2.05–2.67) approach our CES benchmark of 3.12, indicating rigid nesting provides minimal improvement over independence. Third, these estimates contrast sharply with our CNCES results: $\theta = 1.10$ with substantial correlations ($\rho_{\text{Cog}} = 0.77$, $\rho_{\text{Man}} = 0.48$), revealing two-thirds of substitution occurs within skill dimensions.

Why Nested CES Fails. The failure stems from imposing discrete boundaries on continuous skill requirements. Nested CES assumes $\omega_o^s \in \{0,1\}$—each occupation uses exactly one skill. Our data reveals occupations draw from 2.3 skills on average with continuous intensities $\omega_o^s \in (0,1)$. A financial analyst primarily uses cognitive skills ($\omega_o^{\text{cog}} = 0.75$) but also requires interpersonal abilities ($\omega_o^{\text{int}} = 0.20$). Forcing such occupations into single nests destroys the natural substitution structure.[41]

[40] The productivity distribution is $\Pr[\boldsymbol{\epsilon}(i) \le \boldsymbol{\epsilon}] = \exp\left[-\sum_{n=1}^{N}\left(\sum_{o\in\mathcal{N}_n} \epsilon_o^{\frac{-\theta}{1-\rho_n}}\right)^{1-\rho_n}\right]$.

[41] Mathematically, CNCES nests standard Nested CES when $\omega_o^s \in \{0,1\}$, reducing to $F(x_1,\ldots,x_O) = \sum_s \left[\sum_{o:\omega_o^s=1} x_o^{\frac{1}{1-\rho_s}}\right]^{1-\rho_s}$.

These results confirm that flexible skill-based distances—not arbitrary categorical boundaries—determine occupational substitutability and shape technological incidence.

B.7. The Network Topology of AI Exposure

To complement our analysis of automation exposure in the main text, this section examines how AI exposure maps onto the occupational substitution network using 2018 data, when AI capabilities had become more clearly defined.

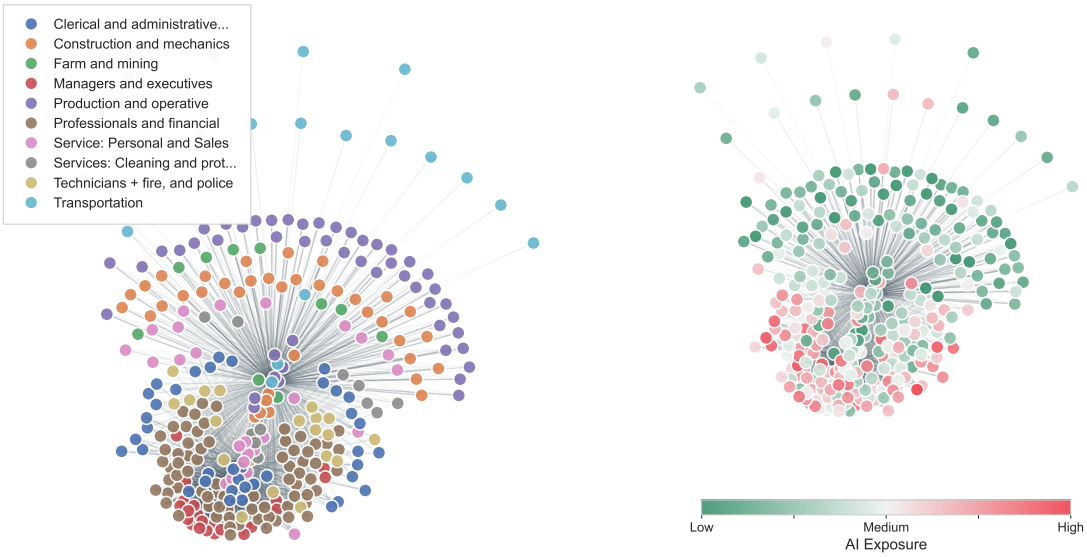

FIGURE B6. The Network Structure of Occupational Substitutability and AI Exposure, 2018

This figure presents the occupational substitution network for 2018, following the same methodology as Figure 3. Edges represent substitutability between occupation pairs based on estimated cross-wage elasticities, with darker lines indicating stronger substitution relationships. The left panel shows occupational clustering by broad categories, while the right panel maps AI exposure using a green gradient (darker green indicates higher AI exposure). The concentration of AI exposure in professional and cognitive-intensive occupations contrasts with the automation pattern, yet exhibits similar clustering within skill-adjacent occupations.

Figure B6 demonstrates that our parsimonious skill-based framework remains robust over time, continuing to generate natural occupational clusters that align with economic intuition. Despite nearly four decades of technological change and labor market evolution between 1980 and 2018, the fundamental structure persists: occupations group according to their cognitive, manual, and interpersonal skill requirements. The professional cluster remains cohesive, production occupations maintain their tight interconnections, and service occupations continue to form distinct sub-clusters based on their specific skill combinations.

The stability of this network structure validates our modeling choice to characterize occupations by their location in a three-dimensional skill space. The 2018 network shows

some evolution—certain connections have strengthened while others have weakened—but the overall topology remains remarkably consistent. This persistence suggests that the skill-based organization of work represents a fundamental feature of the labor market rather than a temporary configuration. Our CNCES framework, by incorporating these skill dimensions through the correlation structure, captures this enduring architecture.

The right panel reveals how AI exposure maps onto the occupational network, providing a striking contrast to automation. AI exposure (shown in darker green) concentrates in the professional and financial cluster, with particularly high intensity among occupations requiring advanced cognitive skills such as financial analysts, market researchers, and technical writers. This concentration extends to adjacent clerical and administrative occupations that share cognitive skill requirements. The spatial pattern of AI exposure—clustering in cognitive-intensive occupations at the opposite end of the network from automation's manual-intensive targets—emerges naturally from AI's capacity to perform tasks involving pattern recognition, language processing, and analytical reasoning.

Notably, both automation and AI exhibit the clustering pattern predicted by our framework: technological shocks concentrate within skill-adjacent occupations rather than dispersing randomly across the network. This parallel structure, despite affecting different segments of the labor market, underscores a fundamental insight of our model. When technologies target specific skills, they necessarily affect clusters of related occupations. The network visualization makes this abstract concept concrete, showing how our three-skill parameterization successfully captures the complex substitution patterns that govern labor market adjustment to technological change.

B.8. Gender-Specific Spectral Decomposition

The spectral decomposition reveals striking gender differences in how technological shocks interact with occupational structure, reflecting distinct employment distributions across skill space.

Automation's Gender-Differentiated Impact. Figure B7 reveals that automation constrains male workers more severely than female workers. For men (Panel A), automation concentrates 31% of variance on the smallest eigenvalue (1.95), compared to 27% at eigenvalue 2.15 for women (Panel B). This difference reflects occupational segregation: men dominate production and operative occupations where automation clusters, while women's employment disperses across service, clerical, and professional occupations.

The eigenvalue difference—1.95 versus 2.15—implies substantially different adjustment capacities. Male workers face effective elasticity of approximately 1.9, while female workers retain elasticity near 2.3. This 20% difference in mobility translates directly to

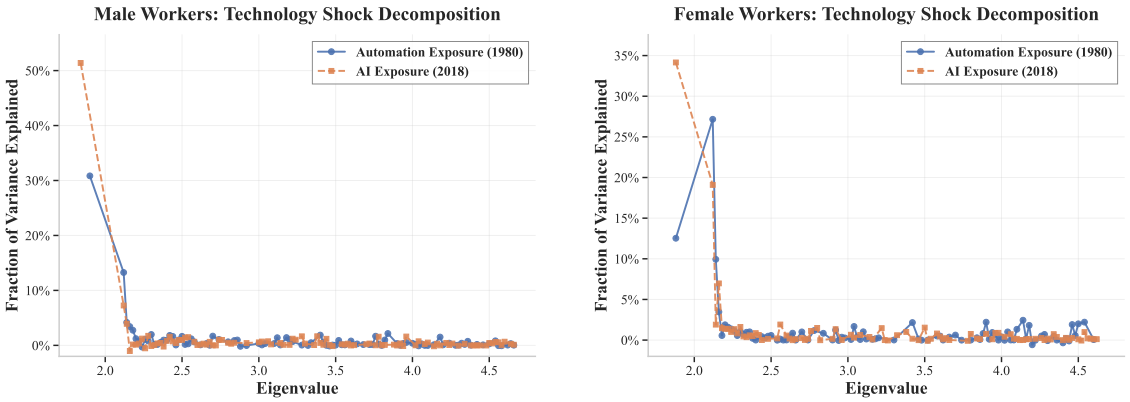

A. Male Workers B. Female Workers

FIGURE B7. Technology Shock Decomposition by Gender

Variance decomposition of automation (1980) and AI (2018) exposures into eigenshocks for male and female workers. Gender-specific employment distributions generate distinct substitution structures and eigenvalue patterns.

wage incidence: male production workers experience pass-through rates approaching 45%, while female workers in similar exposure levels face 38% pass-through. The gender gap emerges not from different skill transferability but from employment concentration—men's overrepresentation in manual-intensive occupations creates fewer escape routes when automation strikes.

AI's Convergent Pattern. In contrast, AI exposure shows remarkable similarity across genders. Both panels display extreme concentration on the smallest eigenvalue: 51% for men and 34% for women, both at eigenvalue 1.95. Despite women's higher representation in cognitive-intensive occupations potentially affected by AI, the clustering pattern remains universal. This convergence suggests AI's broad reach across cognitive tasks affects both gender-segregated and integrated occupations equally.

The similar eigenvalue loading implies comparable mobility constraints. Both male and female workers in AI-exposed occupations face effective elasticities around 1.8–2.0, generating pass-through rates of 45–50%. Unlike automation, where occupational segregation provides some insulation for female workers, AI's cognitive focus creates uniform rigidity across gender lines.

Implications for Distributional Analysis. These gender-specific patterns highlight how initial employment distributions shape technological incidence. Automation's concentration in male-dominated manual occupations amplifies its impact on male workers through both direct exposure and constrained mobility. Female workers' diversification across skill clusters—partly reflecting historical exclusion from manufacturing—inadvertently

provides better adjustment options. For AI, the universal nature of cognitive tasks eliminates this protective dispersion, suggesting future technological shocks may generate more uniform gender impacts while maintaining severe clustering effects.

B.9. The Employment Effects of Automation and AI

As discussed in the main text, clustering shocks lead to smaller employment adjustments while exacerbating wage disparities. Panel (a) of Figure B8 illustrates the relationship between changes in log employment shares and relative wage changes for automation. The CES benchmark (dashed line) rotates counterclockwise, overstating employment shifts, particularly for negatively impacted occupations. This suggests that the CES framework underestimates the rigidity in labor reallocation caused by clustering shocks.

Panel (b) presents the same employment effects for AI exposure, revealing a similar pattern. The CES model again overstates employment adjustments, failing to account for the constrained worker mobility induced by the skill-clustering nature of AI-exposed occupations. These findings highlight the importance of incorporating a richer substitution structure, as captured by DIDES, to better reflect labor market frictions in response to technological change.

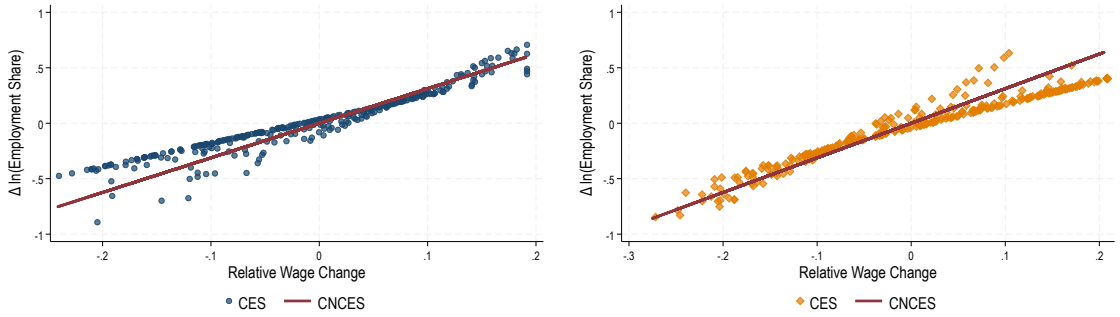

A. Automation B. AI

FIGURE B8. Employment Effects of Technological Shocks

Notes: This figure compares employment effects of automation (Panel a) and AI (Panel b) against the CES benchmark. The CES framework overestimates employment adjustments, particularly in negatively impacted occupations, due to its failure to account for clustering shocks that restrict labor mobility.

B.10. Construct Job Transition with CPS

Our estimation strategy hinges on observing aggregate job flows across occupations. To construct our occupation-level panel for the period 1980–2018, we rely on individual-level data from the US Census Bureau's March Current Population Survey (CPS). Each March CPS provides detailed information on respondents' current occupation as well as the

occupation in which they spent most of the previous calendar year. We restrict our sample to individuals aged 25–64 who are employed full-time and have worked at least 26 weeks in the preceding year, thereby ensuring the reliability of our occupational transition estimates. We also exclude observations with extreme or inconsistent income values to mitigate measurement error. Using these data, we construct annual job flow rates for occupations.

Employing a consistent occupation coding scheme, we generate a balanced panel of 306 three-digit occupations. Given the sparsity of observed transitions at this detailed level, we further aggregate these occupations into 15 clusters using a k-means algorithm based on occupational skill requirements. This intuitive clustering groups together occupations with similar skill profiles, ensuring robust estimates of aggregate job flows and facilitating subsequent analyses.

Furthermore, as noted by Artuç, Chaudhuri, and McLaren (2010), the retrospective design of the March CPS captures job transitions over a period shorter than a full year—respondents report the longest-held job from the previous calendar year, typically reflecting employment around mid-year. To correct for this timing bias, we annualize the observed job transition probabilities using the transformation [42]

$$\mu_t^{\text{ANN}} = \mu_t^2.$$

[42] This approach ensures that no annual job-to-job flows are missing.

Appendix C. Additional Materials

C.1. Derivation of Employment Shares

This appendix derives the closed-form expression for occupational employment shares under the multivariate Fréchet productivity distribution.

PROPOSITION C1. *Given the joint productivity distribution:*

$$\Pr[\epsilon_1(i) \leq \epsilon_1, \ldots, \epsilon_O(i) \leq \epsilon_O] = \exp\left[-F\left(A_1\epsilon_1^{-\theta}, \ldots, A_O\epsilon_O^{-\theta}\right)\right]$$

the share of workers choosing occupation o is:

$$\pi_o = \frac{A_o w_o^\theta F_o(A_1 w_1^\theta, \ldots, A_O w_O^\theta)}{F(A_1 w_1^\theta, \ldots, A_O w_O^\theta)}$$

PROOF. We derive the probability that a worker chooses occupation o, which occurs when $w_o\epsilon_o(i) \geq w_{o'}\epsilon_{o'}(i)$ for all $o' \neq o$.

First, consider the joint probability that occupation o yields utility less than t and is optimal:

$$\begin{aligned}
&\Pr[w_o\epsilon_o(i) < t \text{ and } w_o\epsilon_o(i) = \max_{o'} w_{o'}\epsilon_{o'}(i)] \\
&= \Pr[w_o\epsilon_o(i) < t \text{ and } w_o\epsilon_o(i) \geq w_{o'}\epsilon_{o'}(i), \forall o' \neq o]
\end{aligned}$$

This equals the probability that all occupational utilities are below t, with occupation o being the highest. Using the law of total probability:

$$= \int_0^t \frac{\partial}{\partial z} \Pr[w_{o'}\epsilon_{o'} \leq z, \forall o'] \Big|_z \, dz$$

Substituting the joint distribution and differentiating:

$$\begin{aligned}
&= \int_0^t \frac{\partial}{\partial z} \exp\left[-F\left(A_1 w_1^\theta z^{-\theta}, \ldots, A_O w_O^\theta z^{-\theta}\right)\right] dz \\
&= \int_0^t A_o w_o^\theta F_o\left(A_1 w_1^\theta z^{-\theta}, \ldots, A_O w_O^\theta z^{-\theta}\right) \\
&\quad \times \exp\left[-F\left(A_1 w_1^\theta z^{-\theta}, \ldots, A_O w_O^\theta z^{-\theta}\right)\right] \theta z^{-\theta-1} dz
\end{aligned}$$

Using the homogeneity of degree one property of F:

$$F\left(A_1 w_1^\theta z^{-\theta}, \ldots, A_O w_O^\theta z^{-\theta}\right) = z^{-\theta} F\left(A_1 w_1^\theta, \ldots, A_O w_O^\theta\right)$$

Since F_o is homogeneous of degree zero (as the derivative of a degree-one homoge-

neous function):

$$F_o\left(A_1 w_1^\theta z^{-\theta}, \ldots, A_O w_O^\theta z^{-\theta}\right) = F_o\left(A_1 w_1^\theta, \ldots, A_O w_O^\theta\right)$$

Substituting these properties:

$$\begin{aligned}
&= \int_0^t A_o w_o^\theta F_o(A_1 w_1^\theta, \ldots, A_O w_O^\theta) \exp\left[-F(A_1 w_1^\theta, \ldots, A_O w_O^\theta) z^{-\theta}\right] \theta z^{-\theta-1} dz \\
&= \frac{A_o w_o^\theta F_o(A_1 w_1^\theta, \ldots, A_O w_O^\theta)}{F(A_1 w_1^\theta, \ldots, A_O w_O^\theta)} \\
&\quad \times \int_0^t \exp\left[-F(A_1 w_1^\theta, \ldots, A_O w_O^\theta) z^{-\theta}\right] F(A_1 w_1^\theta, \ldots, A_O w_O^\theta) \theta z^{-\theta-1} dz
\end{aligned}$$

The integral evaluates to:

$$\int_0^t \exp[-\Lambda z^{-\theta}] \Lambda \theta z^{-\theta-1} dz = 1 - \exp[-\Lambda t^{-\theta}]$$

where $\Lambda = F(A_1 w_1^\theta, \ldots, A_O w_O^\theta)$.

Therefore:

$$\Pr[w_o \epsilon_o(i) < t \text{ and optimal}] = \frac{A_o w_o^\theta F_o(A_1 w_1^\theta, \ldots, A_O w_O^\theta)}{F(A_1 w_1^\theta, \ldots, A_O w_O^\theta)} \left(1 - \exp[-\Lambda t^{-\theta}]\right)$$

Taking the limit as $t \to \infty$:

$$\begin{aligned}
\pi_o &= \lim_{t \to \infty} \Pr[w_o \epsilon_o(i) < t \text{ and } w_o \epsilon_o(i) = \max_{o'} w_{o'} \epsilon_{o'}(i)] \\
&= \frac{A_o w_o^\theta F_o(A_1 w_1^\theta, \ldots, A_O w_O^\theta)}{F(A_1 w_1^\theta, \ldots, A_O w_O^\theta)}
\end{aligned}$$

This completes the proof. □

Remark: This result crucially depends on the max-stability property of the multivariate Fréchet distribution and the homogeneity properties of the correlation function F. The employment share expression shows that occupation o's share depends on its productivity-weighted wage ($A_o w_o^\theta$), scaled by how the correlation function responds to changes in that occupation's attractiveness (F_o/F).

C.2. Derivation of Labor Supply Elasticities

This section derives the labor supply elasticity matrix Θ from the employment share equation (A3).

Starting from the employment share:

$$\pi_o = \frac{A_o w_o^\theta F_o(A_1 w_1^\theta, \ldots, A_O w_O^\theta)}{F(A_1 w_1^\theta, \ldots, A_O w_O^\theta)}$$

Let $x_o = A_o w_o^\theta$ and define the wage index $W = F(x_1, \ldots, x_O)^{1/\theta}$. The elasticity with respect to relative wages is:

$$\begin{aligned}\frac{\partial \ln \pi_o}{\partial \ln(w_{o'}/W)} &= \frac{\partial}{\partial \ln(w_{o'}/W)} \ln\left[\frac{x_o F_o(x_1, \ldots, x_O)}{F(x_1, \ldots, x_O)}\right] \\ &= \frac{\partial}{\partial \ln(w_{o'}/W)} \ln\left[\left(\frac{w_o}{W}\right)^\theta F_o\left(\frac{x_1}{W^\theta}, \ldots, \frac{x_O}{W^\theta}\right)\right]\end{aligned}$$

Using the fact that F is homogeneous of degree one (hence F_o is homogeneous of degree zero):

$$\frac{\partial \ln \pi_o}{\partial \ln(w_{o'}/W)} = \begin{cases} \theta \frac{x_{o'} F_{oo'}}{F_o} & \text{if } o' \neq o \\ \theta \frac{x_o F_{oo}}{F_o} + \theta & \text{if } o' = o \end{cases}$$

To obtain the elasticity with respect to absolute wages, we use:

$$\frac{\partial \ln \pi_o}{\partial \ln w_{o'}} = \frac{\partial \ln \pi_o}{\partial \ln(w_{o'}/W)} \cdot \frac{\partial \ln(w_{o'}/W)}{\partial \ln w_{o'}} + \frac{\partial \ln \pi_o}{\partial \ln W} \cdot \frac{\partial \ln W}{\partial \ln w_{o'}}$$

Since $\frac{\partial \ln(w_{o'}/W)}{\partial \ln w_{o'}} = 1 - \frac{\partial \ln W}{\partial \ln w_{o'}}$ and $\frac{\partial \ln W}{\partial \ln w_{o'}} = \pi_{o'}$:

$$\begin{aligned}\frac{\partial \ln \pi_o}{\partial \ln w_{o'}} &= \theta \frac{x_{o'} F_{oo'}}{F_o} - \theta \pi_{o'} \quad \text{for } o' \neq o \\ \frac{\partial \ln \pi_o}{\partial \ln w_o} &= \theta \frac{x_o F_{oo}}{F_o} + \theta - \theta \pi_o = \theta \frac{x_o F_{oo}}{F_o} + \theta(1 - \pi_o)\end{aligned}$$

Since $L_o = \pi_o \bar{L}$, the labor supply elasticity is:

$$\Theta_{oo'} = \frac{\partial \ln L_o}{\partial \ln w_{o'}} = \frac{\partial \ln \pi_o}{\partial \ln w_{o'}} = \begin{cases} \theta \left[\left. \frac{x_{o'} F_{oo'}}{F_o} \right|_{x_j = A_j w_j^\theta} - \pi_{o'} \right] & \text{if } o \neq o' \\ \theta \left[\left. \frac{x_o F_{oo}}{F_o} \right|_{x_j = A_j w_j^\theta} + 1 - \pi_o \right] & \text{if } o = o' \end{cases}$$

This completes the derivation of the labor supply elasticity matrix in equation (A4).

C.3. Zero Row Sum Property of the Elasticity Matrix

A crucial property of the labor supply elasticity matrix Θ is that its row sums equal zero, implying that uniform wage changes do not affect relative employment. This result follows directly from the homogeneity of degree one property of the correlation function F.

PROPOSITION C2. *For the elasticity matrix Θ defined in equation* (A4)*, we have:*

$$\sum_{o'=1}^{O} \Theta_{oo'} = 0 \quad \textit{for all } o$$

PROOF. Starting from the definition of employment shares in equation (A3):

$$\pi_o = \frac{A_o w_o^\theta F_o(A_1 w_1^\theta, \ldots, A_O w_O^\theta)}{F(A_1 w_1^\theta, \ldots, A_O w_O^\theta)}$$

Let $x_o = A_o w_o^\theta$ for notational simplicity. The sum of elasticities for row o is:

$$\begin{aligned}
\sum_{o'=1}^{O} \Theta_{oo'} &= \sum_{o'=1}^{O} \frac{\partial \ln \pi_o}{\partial \ln w_{o'}} \\
&= \sum_{o'=1}^{O} \theta \frac{\partial \ln \pi_o}{\partial \ln x_{o'}} \\
&= \theta \sum_{o'=1}^{O} \left[\frac{x_{o'} F_{oo'}}{F_o} - \pi_{o'} \right] + \theta \cdot \mathbf{1}_{o=o'} \\
&= \frac{\theta}{F_o} \sum_{o'=1}^{O} x_{o'} F_{oo'} + \theta(1 - \pi_o) - \theta \sum_{o' \neq o} \pi_{o'}
\end{aligned}$$

Since $\sum_{o'=1}^{O} \pi_{o'} = 1$, we have $1 - \pi_o = \sum_{o' \neq o} \pi_{o'}$, which simplifies the expression to:

$$\sum_{o'=1}^{O} \Theta_{oo'} = \frac{\theta}{F_o} \sum_{o'=1}^{O} x_{o'} F_{oo'}$$

Now we invoke Euler's theorem for homogeneous functions. Since F is homogeneous of degree one, its partial derivative F_o is homogeneous of degree zero. By Euler's theorem applied to F_o:

$$\sum_{o'=1}^{O} x_{o'} \frac{\partial F_o}{\partial x_{o'}} = 0 \cdot F_o = 0$$

But $\frac{\partial F_o}{\partial x_{o'}} = F_{oo'}$ by definition, therefore:

$$\sum_{o'=1}^{O} x_{o'} F_{oo'} = 0$$

This immediately implies:

$$\sum_{o'=1}^{O} \Theta_{oo'} = \frac{\theta}{F_o} \cdot 0 = 0$$

□

This zero row sum property has important economic implications. It ensures that proportional wage increases—such as those resulting from aggregate productivity growth—do not induce occupational reallocation. Only relative wage changes, such as those caused by asymmetric technological shocks, trigger worker mobility across occupations. This property is essential for the model's consistency and ensures that the labor market responds only to distributional shocks rather than level effects.

C.4. Proof of Eigenvalue Properties

This section proves the eigenvalue properties of the labor supply elasticity matrix Θ stated in Lemma 1.

PROOF. We establish each property in turn.

Part 1: Existence of zero eigenvalue with uniform eigenvector.

From Section C.3, we know that $\sum_{o'} \Theta_{oo'} = 0$ for all o. This implies:

$$\Theta \cdot \mathbf{1} = \mathbf{0}$$

where $\mathbf{1} = [1, 1, \ldots, 1]'$. Therefore, $\lambda = 0$ is an eigenvalue with right eigenvector $\boldsymbol{u}_1 = \mathbf{1}/\sqrt{O}$ (normalized).

Part 2: Non-negativity of all eigenvalues.

The matrix Θ has the structure:

$$\Theta_{oo'} = \begin{cases} \theta\left[\frac{x_o F_{oo}}{F_o} + 1 - \pi_o\right] > 0 & \text{if } o = o' \\ \theta\left[\frac{x_{o'} F_{oo'}}{F_o} - \pi_{o'}\right] < 0 & \text{if } o \neq o' \end{cases}$$

The sign-switching property of F ensures $F_{oo'} \leq 0$ for $o \neq o'$, making Θ a matrix with positive diagonal and negative off-diagonal elements. Additionally, the diagonal dominance condition holds:

$$\Theta_{oo} = -\sum_{o' \neq o} \Theta_{oo'} > 0$$

By the Gershgorin circle theorem, all eigenvalues lie in the union of discs:

$$\lambda \in \bigcup_{o} \left\{ z \in \mathbb{C} : |z - \Theta_{oo}| \leq \sum_{o' \neq o} |\Theta_{oo'}| \right\}$$

Since $\Theta_{oo} = \sum_{o' \neq o} |\Theta_{oo'}|$ (from the zero row sum), each disc is centered at a positive point with radius equal to the center. Therefore, all discs lie in the right half-plane: $\text{Re}(\lambda) \geq 0$.

For a real matrix with real eigenvalues (which Θ has due to its economic interpretation), this implies $\lambda \geq 0$.

Part 3: Uniqueness of zero eigenvalue.

Suppose $\lambda = 0$ has geometric multiplicity greater than 1. Then there exists a non-uniform vector $\boldsymbol{x} \neq c\mathbf{1}$ such that $\Theta\boldsymbol{x} = \mathbf{0}$.

Without loss of generality, normalize $\boldsymbol{x}$ so that $\max_o x_o = 1$ and $\min_o x_o < 1$. Let $o^* = \arg\max_o x_o$. Then:

$$0 = (\Theta\boldsymbol{x})_{o^*} = \Theta_{o^*o^*} + \sum_{o' \neq o^*} \Theta_{o^*o'} x_{o'}$$

Since $x_{o'} < x_{o^*} = 1$ for at least one o' and $\Theta_{o^*o'} < 0$ for all $o' \neq o^*$:

$$\sum_{o' \neq o^*} \Theta_{o^*o'} x_{o'} > \sum_{o' \neq o^*} \Theta_{o^*o'} = -\Theta_{o^*o^*}$$

This gives $(\Theta\boldsymbol{x})_{o^*} > 0$, contradicting $\Theta\boldsymbol{x} = \mathbf{0}$. Therefore, the zero eigenvalue has geometric (and algebraic) multiplicity 1.

□

C.5. Additional Derivations for Dynamic Model

C.5.1. Derivation of System in Changes (Section A.15)

This section provides detailed derivations for the dynamic system expressed in growth rates.

Production equilibrium in changes. Log-differentiating the wage equation yields:

$$\sigma \ln \dot{w}_{o,t+1} + \ln \dot{L}_{o,t+1} = \ln \dot{Y}_{t+1} + \ln \dot{s}^{\ell}_{o,t+1}$$

This implies wages adjust according to:

$$\dot{\boldsymbol{w}}_{t+1} = \dot{w}(\dot{\boldsymbol{L}}_{t+1}, \dot{\boldsymbol{\Psi}}_{t+1})$$

where $\dot{\boldsymbol{\Psi}}_{t+1}$ represents changes in fundamentals.

Evolution of adjusted mobility. Starting from the definition:

$$\tilde{\mu}_{oo',t} = \frac{A_{o',t} Z^{\theta/\kappa}_{oo',t}}{F(A_{1,t} Z^{\theta/\kappa}_{o1,t}, \ldots, A_{O,t} Z^{\theta/\kappa}_{oO,t})}$$

Taking the ratio across time:

$$\frac{\tilde{\mu}_{oo',t}}{\tilde{\mu}_{oo',t-1}} = \frac{A_{o',t}Z_{oo',t}^{\theta/\kappa}/A_{o',t-1}Z_{oo',t-1}^{\theta/\kappa}}{F(A_{1,t}Z_{o1,t}^{\theta/\kappa},\ldots)/F(A_{1,t-1}Z_{o1,t-1}^{\theta/\kappa},\ldots)}$$

Using $Z_{oo',t} = \exp(\beta V_{o',t+1} + \ln w_{o',t} - \tau_{oo'})$ and $\dot{u}_{o,t} = \exp(V_{o,t} - V_{o,t-1})$:

$$\frac{\tilde{\mu}_{oo',t}}{\tilde{\mu}_{oo',t-1}} = \frac{\dot{A}_{o',t}\dot{u}_{o',t+1}^{\beta\theta/\kappa}\dot{w}_{o',t}^{\theta/\kappa}}{F(\{A_{o'',t}Z_{oo'',t}^{\theta/\kappa}/F_{t-1}\}_{o''=1}^{O})}$$

where $F_{t-1} = F(A_{1,t-1}Z_{o1,t-1}^{\theta/\kappa},\ldots,A_{O,t-1}Z_{oO,t-1}^{\theta/\kappa})$.
Using the homogeneity of F and noting that $A_{o'',t}Z_{oo'',t}^{\theta/\kappa}/F_{t-1} = \tilde{\mu}_{oo'',t-1}\dot{A}_{o'',t}\dot{u}_{o'',t+1}^{\beta\theta/\kappa}\dot{w}_{o'',t}^{\theta/\kappa}$:

$$\boxed{\frac{\tilde{\mu}_{oo',t}}{\tilde{\mu}_{oo',t-1}} = \frac{\dot{A}_{o',t}\dot{u}_{o',t+1}^{\beta\theta/\kappa}\dot{w}_{o',t}^{\theta/\kappa}}{F(\{\tilde{\mu}_{oo'',t-1}\dot{A}_{o'',t}\dot{u}_{o'',t+1}^{\beta\theta/\kappa}\dot{w}_{o'',t}^{\theta/\kappa}\}_{o''=1}^{O})}}$$

Evolution of expected utility. From the value function:

$$V_{o,t} = \frac{\kappa}{\theta}\ln F(A_{1,t}Z_{o1,t}^{\theta/\kappa},\ldots,A_{O,t}Z_{oO,t}^{\theta/\kappa}) + \bar{\gamma}\frac{\kappa}{\theta}$$

The change in value is:

$$V_{o,t+1} - V_{o,t} = \frac{\kappa}{\theta}\ln\frac{F(A_{1,t+1}Z_{o1,t+1}^{\theta/\kappa},\ldots)}{F(A_{1,t}Z_{o1,t}^{\theta/\kappa},\ldots)}$$

Using homogeneity to factor out $F(A_{1,t}Z_{o1,t}^{\theta/\kappa},\ldots)$:

$$V_{o,t+1} - V_{o,t} = \frac{\kappa}{\theta}\ln F\left(\left\{\frac{A_{o'',t+1}Z_{oo'',t+1}^{\theta/\kappa}}{F(A_{1,t}Z_{o1,t}^{\theta/\kappa},\ldots)}\right\}_{o''=1}^{O}\right)$$

Substituting $A_{o'',t+1}Z_{oo'',t+1}^{\theta/\kappa} = A_{o'',t}Z_{oo'',t}^{\theta/\kappa}\dot{A}_{o'',t+1}\dot{Z}_{oo'',t+1}^{\theta/\kappa}$ and recognizing that $A_{o'',t}Z_{oo'',t}^{\theta/\kappa}/F_t = \tilde{\mu}_{oo'',t}$:

$$\boxed{\dot{u}_{o,t+1} = F(\{\tilde{\mu}_{oo'',t}\dot{A}_{o'',t+1}\dot{u}_{o'',t+2}^{\beta\theta/\kappa}\dot{w}_{o'',t+1}^{\theta/\kappa}\}_{o''=1}^{O})^{\kappa/\theta}}$$

Labor market clearing. Employment evolves through transitions:

$$L_{o,t} = \sum_{o'} \mu_{o'o,t} L_{o',t-1}$$

where observed transitions relate to adjusted rates via:

$$\mu_{oo',t} = \tilde{\mu}_{oo',t} F_{o'}(\tilde{\mu}_{o1,t}, \ldots, \tilde{\mu}_{oO,t})$$

These equations form a complete system characterizing the dynamic equilibrium in growth rates, preserving the DIDES structure through the correlation function F.

C.5.2. Derivation of Dynamic Hat Algebra (Section A.16)

This section derives the counterfactual evolution equations for the dynamic model.

Counterfactual wage determination.. From the production equilibrium, counterfactual wages relate to baseline wages through:

$$\hat{w}_{o,t+1} = \frac{\dot{w}'_{o,t+1}}{\dot{w}_{o,t+1}} = \left(\frac{\hat{Y}_{t+1} \hat{s}^{\ell}_{o,t+1}}{\hat{L}_{o,t+1}} \right)^{\frac{1}{\sigma}}$$

where hats denote ratios of counterfactual to baseline growth rates.

Evolution of counterfactual transition probabilities.. Starting from the ratio of counterfactual to baseline growth rates:

$$\frac{\tilde{\mu}'_{oo',t}}{\tilde{\mu}'_{oo',t-1}} = \frac{\dot{\tilde{\mu}}_{oo',t} \hat{A}_{o',t} \hat{u}^{\beta\theta/\kappa}_{o',t+1} \hat{w}^{\theta/\kappa}_{o',t}}{\text{[Denominator]}}$$

The denominator requires careful manipulation. Using the ratio of counterfactual to baseline correlation functions:

$$\text{[Denominator]} = \frac{F(\{\tilde{\mu}'_{oo'',t-1} \dot{A}'_{o'',t} \dot{u}'^{\beta\theta/\kappa}_{o'',t+1} \dot{w}'^{\theta/\kappa}_{o'',t}\}_{o''})}{F(\{\tilde{\mu}_{oo'',t-1} \dot{A}_{o'',t} \dot{u}^{\beta\theta/\kappa}_{o'',t+1} \dot{w}^{\theta/\kappa}_{o'',t}\}_{o''})}$$

Recognizing that counterfactual growth rates equal baseline growth times hat values, and using homogeneity of F:

$$= F\left(\left\{ \frac{\tilde{\mu}'_{oo'',t-1}}{\tilde{\mu}_{oo'',t-1}} \cdot \tilde{\mu}_{oo'',t} \cdot \hat{A}_{o'',t} \hat{u}^{\beta\theta/\kappa}_{o'',t+1} \hat{w}^{\theta/\kappa}_{o'',t} \right\}_{o''} \right)$$

Therefore, the recursive formula is:

$$\boxed{\tilde{\mu}'_{oo',t} = \frac{\tilde{\mu}'_{oo',t-1}\dot{\tilde{\mu}}_{oo',t}\hat{A}_{o',t}\hat{u}^{\beta\theta/\kappa}_{o',t+1}\hat{w}^{\theta/\kappa}_{o',t}}{F(\{\tilde{\mu}'_{oo'',t-1}\dot{\tilde{\mu}}_{oo'',t}\hat{A}_{o'',t}\hat{u}^{\beta\theta/\kappa}_{o'',t+1}\hat{w}^{\theta/\kappa}_{o'',t}\}_{o''=1}^{O})}}$$

Evolution of counterfactual expected utility.. Following similar steps for the utility growth rates:

$$\begin{aligned}\hat{u}_{o,t+1} &= \frac{\dot{u}'_{o,t+1}}{\dot{u}_{o,t+1}} \\ &= \frac{F(\{\tilde{\mu}'_{oo'',t}\dot{A}'_{o'',t+1}\dot{u}'^{\beta\theta/\kappa}_{o'',t+2}\dot{w}'^{\theta/\kappa}_{o'',t+1}\}_{o''})^{\kappa/\theta}}{F(\{\tilde{\mu}_{oo'',t}\dot{A}_{o'',t+1}\dot{u}^{\beta\theta/\kappa}_{o'',t+2}\dot{w}^{\theta/\kappa}_{o'',t+1}\}_{o''})^{\kappa/\theta}}\end{aligned}$$

Using the same homogeneity argument:

$$\boxed{\hat{u}_{o,t+1} = F(\{\tilde{\mu}'_{oo'',t}\dot{\tilde{\mu}}_{oo'',t+1}\hat{A}_{o'',t+1}\hat{u}^{\beta\theta/\kappa}_{o'',t+2}\hat{w}^{\theta/\kappa}_{o'',t+1}\}_{o''=1}^{O})^{\kappa/\theta}}$$

Observed transitions and employment evolution.. The observed counterfactual transitions incorporate correlation effects:

$$\mu'_{oo',t} = \tilde{\mu}'_{oo',t}F_{o'}(\tilde{\mu}'_{o1,t}, \ldots, \tilde{\mu}'_{oO,t})$$

Employment evolves through the transition matrix plus exogenous flows:

$$L'_{o,t} = \sum_{o'} \mu'_{o'o,t}L'_{o',t-1} + \Delta L_{o,t}$$

These equations provide a complete characterization of counterfactual dynamics, preserving the DIDES structure through the correlation function F while enabling analysis of alternative technological scenarios.

C.5.3. Initial Dynamics with Unexpected Shocks

For unexpected shocks at $t = 1$, the economy begins at baseline equilibrium with $\hat{u}_{o,0} = 1$, $\mu'_{oo',0} = \mu_{oo',0}$, and $L'_{o,0} = L_{o,0}$.

Deriving the initial utility adjustment.. The baseline expected utility at $t = 0$ is:

$$u_{o,0} = F(\{A_{o',0}Z^{\theta/\kappa}_{oo',0}\}_{o'=1}^{O})^{\kappa/\theta}$$

Since initial conditions are identical ($A'_{o',0} = A_{o',0}$, $w'_{o',0} = w_{o',0}$), we can rewrite using counterfactual notation:

$$u_{o,0} = F\left(\left\{\frac{A_{o',0}}{A'_{o',0}} \cdot \frac{Z_{oo',0}}{Z'_{oo',0}} \cdot A'_{o',0} Z'^{\theta/\kappa}_{oo',0}\right\}_{o'=1}^{O}\right)^{\kappa/\theta}$$

Since the ratios equal unity at $t = 0$:

$$u_{o,0} = F(\{A'_{o',0} Z'^{\theta/\kappa}_{oo',0}\}_{o'=1}^{O})^{\kappa/\theta}$$

After the shock, counterfactual utility at $t = 1$ is:

$$u'_{o,1} = F(\{A'_{o',1} Z'^{\theta/\kappa}_{oo',1}\}_{o'=1}^{O})^{\kappa/\theta}$$

Taking the ratio and using homogeneity of F:

$$\begin{aligned}\frac{u'_{o,1}}{u_{o,0}} &= \frac{F(\{A'_{o',1} Z'^{\theta/\kappa}_{oo',1}\}_{o'})^{\kappa/\theta}}{F(\{A'_{o',0} Z'^{\theta/\kappa}_{oo',0}\}_{o'})^{\kappa/\theta}} \\ &= F\left(\left\{\frac{A'_{o',1} Z'^{\theta/\kappa}_{oo',1}}{F(\{A'_{o'',0} Z'^{\theta/\kappa}_{oo'',0}\}_{o''})}\right\}_{o'=1}^{O}\right)^{\kappa/\theta}\end{aligned}$$

Connecting to baseline transition probabilities.. Note that at $t = 0$:

$$\begin{aligned}\tilde{\mu}_{oo',0} &= \frac{A_{o',0} Z^{\theta/\kappa}_{oo',0}}{F(\{A_{o'',0} Z^{\theta/\kappa}_{oo'',0}\}_{o''})} \\ &= \frac{\frac{A_{o',0} Z^{\theta/\kappa}_{oo',0}}{A'_{o',0} Z'^{\theta/\kappa}_{oo',0}} \cdot A'_{o',0} Z'^{\theta/\kappa}_{oo',0}}{F\left(\left\{\frac{A_{o'',0} Z^{\theta/\kappa}_{oo'',0}}{A'_{o'',0} Z'^{\theta/\kappa}_{oo'',0}} \cdot A'_{o'',0} Z'^{\theta/\kappa}_{oo'',0}\right\}_{o''}\right)}\end{aligned}$$

Since initial conditions are identical, the ratios equal unity, yielding:

$$\tilde{\mu}_{oo',0} = \frac{A'_{o',0} Z'^{\theta/\kappa}_{oo',0}}{F(\{A'_{o'',0} Z'^{\theta/\kappa}_{oo'',0}\}_{o''})}$$

Combining this with the utility ratio:

$$\frac{u'_{o,1}}{u_{o,0}} = F\left(\left\{\tilde{\mu}_{oo',0} \cdot \frac{A'_{o',1}Z'^{\theta/\kappa}_{oo',1}}{A'_{o',0}Z'^{\theta/\kappa}_{oo',0}}\right\}_{o'=1}^{O}\right)^{\kappa/\theta}$$
$$= F\left(\left\{\tilde{\mu}_{oo',0} \cdot \dot{A}'_{o',1}\dot{Z}'^{\theta/\kappa}_{oo',1}\right\}_{o'=1}^{O}\right)^{\kappa/\theta}$$

Since $Z_{oo',t} = \exp(\beta V_{o',t+1} + \ln w_{o',t} - \tau_{oo'})$:

$$\dot{u}'_{o,1} = F(\{\tilde{\mu}_{oo',0}\dot{A}'_{o',1}\dot{w}'^{\theta/\kappa}_{o',1}\dot{u}'^{\beta\theta/\kappa}_{o',2}\}_{o'=1}^{O})^{\kappa/\theta}$$

Computing the initial hat values.. The baseline utility growth follows:

$$\dot{u}_{o,1} = F(\{\tilde{\mu}_{oo',0}\dot{A}_{o',1}\dot{w}^{\theta/\kappa}_{o',1}\dot{u}^{\beta\theta/\kappa}_{o',2}\}_{o'=1}^{O})^{\kappa/\theta}$$

The hat value is:

$$\hat{u}_{o,1} = \frac{\dot{u}'_{o,1}}{\dot{u}_{o,1}}$$
$$= F\left(\left\{\frac{\tilde{\mu}_{oo',0}\dot{A}'_{o',1}\dot{w}'^{\theta/\kappa}_{o',1}\dot{u}'^{\beta\theta/\kappa}_{o',2}}{F(\{\tilde{\mu}_{oo'',0}\dot{A}_{o'',1}\dot{w}^{\theta/\kappa}_{o'',1}\dot{u}^{\beta\theta/\kappa}_{o'',2}\}_{o''})}\right\}_{o'=1}^{O}\right)^{\kappa/\theta}$$

Recognizing that $\dot{A}'_{o',1}/\dot{A}_{o',1} = \hat{A}_{o',1}$ and similarly for other variables:

$$\hat{u}_{o,1} = F\left(\left\{\tilde{\mu}_{oo',1} \cdot \hat{A}_{o',1}\hat{w}^{\theta/\kappa}_{o',1}\hat{u}^{\beta\theta/\kappa}_{o',2} \cdot \frac{u'_{o',1}/u_{o',1}}{u'_{o',1}/u_{o',1}}\right\}_{o'=1}^{O}\right)^{\kappa/\theta}$$

Note that $u'_{o',1}/u_{o',1} = (u'_{o',1}/u_{o',0}) \cdot (u_{o',0}/u_{o',1}) = \dot{u}'_{o',1}/\dot{u}_{o',1} = \hat{u}_{o',1}$.
Defining $\vartheta_{oo',1} = \tilde{\mu}_{oo',1}\hat{u}^{\beta\theta/\kappa}_{o',1}$:

$$\boxed{\hat{u}_{o,1} = F(\{\vartheta_{oo',1}\hat{A}_{o',1}\hat{w}^{\theta/\kappa}_{o',1}\hat{u}^{\beta\theta/\kappa}_{o',2}\}_{o'=1}^{O})^{\kappa/\theta}}$$

Initial transition probabilities.. Following parallel derivation for transition probabilities, starting from:

$$\frac{\tilde{\mu}'_{oo',1}}{\tilde{\mu}_{oo',1}} = \frac{A'_{o',1}Z'^{\theta/\kappa}_{oo',1}/A_{o',1}Z^{\theta/\kappa}_{oo',1}}{F(\{A'_{o'',1}Z'^{\theta/\kappa}_{oo'',1}\}_{o''})/F(\{A_{o'',1}Z^{\theta/\kappa}_{oo'',1}\}_{o''})}$$

After similar manipulations:

$$\tilde{\mu}'_{oo',1} = \frac{\vartheta_{oo',1}\hat{A}_{o',1}\hat{w}_{o',1}^{\theta/\kappa}\hat{u}_{o',2}^{\beta\theta/\kappa}}{F(\{\vartheta_{oo'',1}\hat{A}_{o'',1}\hat{w}_{o'',1}^{\theta/\kappa}\hat{u}_{o'',2}^{\beta\theta/\kappa}\}_{o''=1}^{O})}$$

The adjustment factor $\vartheta_{oo',1}$ captures the combined effect of the initial shock and forward-looking expectations, encoding how unexpected changes propagate through the DIDES structure.